DRAFT

Characterization of the San Andres-Glorieta Aquifer

AT HOMESTAKE MINING COMPANY SUPERFUND SITE

Grants, New Mexico

May 3, 2021

CHARACTERIZATION OF THE SAN ANDRES-GLORETA AQUIFER AT HOMESTAKE MINING COMPANY SUPERFUND SITE GRANTS, NEW MEXICO

MAY 2021

TABLE OF CONTENTS

TABLE OF CONTENTS (continued)

TABLES

FIGURES

APPENDICES

ACRONYMS AND ABBREVIATIONS

ABI	Acoustic Televiewer
AGI	Advanced Geosciences Inc.
CEC	Cation Exchange Capacity
COPC	Chemical of Potential Concern
CSM	Conceptual Site Model
CPS	counts per second
DEM	Digital Elevation Model
DO	Dissolved Oxygen
EC	Electrical Conductivity
EPA	Environmental Protection Agency
ER	electrical resistivity
ERT	Electrical Resistivity Tomography
FRes	Fluid Resistivity
FTemp	Fluid Temperature
FS	Feasibility Study
gpd/ft	gallons per day per foot
GPS	global positioning system
HDR	HDR Engineering, Inc.
HMC	Homestake Mining Company of California
HPFM	Heat-pulse flowmeter
LTP	Large Tailing Pile
msl	mean sea level
NMOSE	New Mexico Office of the State Engineer

NRC	Nuclear Regulatory Commission
OBI	Optical Televiewer
ORP	Oxygen Reduction Potential
QC	Quality Control
RPD	relative percent difference
SAG	San Andres-Glorieta
SMC	San Mateo Creek
STP	Small Tailing Pile
TDS	Total dissolved solids
TI	Technical Impracticability
TIER	Technical Impracticability Evaluation Report
USCS	Unified Soil Classification System
USEPA	United States Environmental Protection Agency
USGS	U.S. Geological Survey
USNRC	U.S. Nuclear Regulatory Commission
XRD	X-ray Diffraction

1 INTRODUCTION

1.1 Background

This summary report describes the physical and geochemical characteristics of the San Andres-Glorieta (SAG) Aquifer in the area where it subcrops at the base of the alluvial aquifer hydraulically downgradient the Homestake Mining Company Superfund Site (Site), Near Milan, New Mexico. The scope of work is summarized in a Workplan submitted and approved by the United States Environmental Protection Agency (USEPA) (HDR, 2020b). This information will be used to update the Conceptual Site Model (CSM) and the groundwater flow and solute transport model.

The Site is located approximately 5.5 miles north of Milan, in Cibola County, New Mexico. Homestake Mining Company of California (HMC) opened and began operating the mill facility in 1958 under two partnerships. Beginning in 1981, HMC became both the sole owner and operator. In 2001, HMC merged with Barrick Gold Corporation. Currently, HMC is a wholly owned indirect subsidiary of Barrick Gold Corporation and owns the Homestake Facility.

The Site is a former uranium mill located in the San Mateo Creek Basin in Cibola County, New Mexico. The mill operated from 1958 to 1990. Milling operations produced two on-Site tailing piles: the Small Tailing Pile (STP) and the Large Tailing Pile (LTP). Both tailing piles have influenced groundwater quality in the alluvial aquifer and shallow bedrock aquifer units immediately below and downgradient from the Site. The Site was placed on USEPA's Superfund National Priorities List in September 1983 at the request of the State of New Mexico due to elevated selenium concentrations in the alluvial aquifer near the Site. HMC has been conducting active groundwater remediation at the Site since 1977.

Groundwater impacted by contaminants of potential concern (COPCs), including uranium, selenium, and molybdenum, by milling operations at the Site has been documented with groundwater sampling to have migrated to the west through the San Mateo alluvial aquifer. Initial groundwater flow and solute transport modeling included in the Technical Impracticability Evaluation Report (TIER) and the Feasibility Study (FS) show uranium in groundwater in the San Mateo aquifer will merge with groundwater in the Rio San Jose alluvial aquifer which flows to the south (HDR, 2020a). Regional geologic mapping shows the San Andres-Glorieta (SAG) aquifer directly underlies the Rio San Jose alluvial aquifer roughly 3 miles west of the Site. Initial groundwater flow and solute transport modeling presented in the TIER also shows groundwater from the alluvium could enter the SAG aquifer where the SAG is in direct contact with the alluvial aquifer.

1.2 Purpose

The purpose of this work is to characterize the physical and geochemical properties of the SAG aquifer and to further evaluate the hydraulic connection between the SAG and the alluvial aquifer. This information will be used to update the CSM and the groundwater flow and solute transport model.

2 SITE CHARACTORISTICS

2.1 Geology

The Site is in the southeastern portion of the Colorado Plateau physiographic province, on the south flank of the San Juan Basin. Figure 2-1 presents a portion of the geologic map of the Grants quadrangle (Dillinger 1990). The region experienced structural deformation (regional folding and block uplift) associated with the Zuni Uplift from the Late Cretaceous through the Eocene during the Laramide Orogeny (Cooley et al. 1969). This uplift formed the Zuni Mountains, which consist of a northwest-trending monoclinal fold approximately 75 miles long and 30 miles wide to the southwest of Grants composed of Precambrian crystalline basement rocks overlain by Permian to Jurassic sedimentary rocks (Langman et al. 2012).

2.1.1 Alluvium

Quaternary alluvium consists of fluvial deposits (e.g. meandering stream and flood over bank deposits) eroded from localized andesite and basalt flows and surrounding bedrock; some of which were ore-bearing rock. As a result, the alluvium contains naturally occurring uranium, as well as selenium and molybdenum, which are typically present in uranium deposits (HMC 2012).

The lithology types and stratigraphic placement observed in the borehole logs (primarily clays and sands with varying silt and/or gravel) are consistent with a fluvial depositional environment (e.g. meandering stream and flood over bank deposits). Sand beds generally range from five to 20 feet thick. Clay and silt beds typically range from two to 10 feet thick. Clasts range from rounded to sub-angular grains, though the majority are sub-rounded, indicating that sediments were transported a moderate distance from their source (Novak-Szabo et al. 2018). This type of depositional environment results in the presence of a higher permeability channel and channel lag deposits positioned directly adjacent to fine-grained, low permeability over bank deposits.

2.1.2 Bedrock

Bedrock at the Site consist of the Chinle Formation (Late Triassic), San Andres Limestone (Early Permian), and Glorietta Sandstone and Dolostone (Early Permian). The Chinle Formation is composed of laterally continuous sandstone units separated by thick sections of low permeability shale. The Site is located on the eastern flank of a fold, where bedrock dips approximately three to 10 degrees to the north-northeast into the San Juan Basin (Kelley 1967).

More recent faulting associated with the Rio Grande Rift resulted in the large northeast-striking San Mateo normal fault located northeast of the Site and two small-scale normal faults southwest of the Site referred to as the West Fault and the East Fault **Figure 2-2**. The dip of these two faults is nearly vertical and the offset in the Chinle Formation results in the juxtaposition of permeable sandstones with impermeable mudstones and siltstones across the two faults near the Site. Displacement along the East Fault is minimal immediately south of the Felice Acres subdivision and sandstone units are not vertically offset (HMC and Hydro-Engineering 2010).

During the Tertiary (Neogene) volcanic activity associated with the Mount Taylor volcanic field resulted in widely scattered andesite and basalt flows (Kelley 1967). An erosional period followed the volcanism and created the valley forms observed in the San Mateo Creek (SMC) Basin, eroding the surface up to 150 to 200 feet below the current land surface (Langman et al. 2012). This erosional period exposed Cretaceous and Permian bedrock formations, which outcrop in progressively older (northeast to southwest) trending bands to the west and southwest of the milling operations and tailings piles. Erosion of the dipping formations produced a pronounced angular unconformity between bedrock strata and Quaternary valley fill, resulting in sedimentary units within the underlying Chinle and San Andres Formations abruptly truncating at the base of the alluvium.

2.2 Hydrogeology

The hydrogeological framework at the Site consists of a hydraulically unconfined, buried valley alluvial aquifer overlying and in hydraulic connection with discrete bedrock aquifer units within the Chinle Formation and the San Andres and Glorietta Formations.

Though the Chinle Formation is largely comprised of shale, there are three water-bearing units within the Chinle, referred to as the Upper, Middle and Lower Chinle aquifers. The Upper and Middle Chinle aquifers are both largely composed of sandstone, and the Lower Chinle aquifer, which consists of a zone of enhanced water yield within the shale formation. The Chinle aquifers are under semi-confined conditions where they subcrop beneath the alluvial aquifer and confined conditions further downdip.

Groundwater is hydraulically connected between the San Andres and Glorietta Formations forming the San Andres - Glorietta Aquifer (SAG). This aquifer predominantly consists of limestone with sandstone and shale layers.

2.2.1 Alluvial Aquifer System

The unconfined alluvial aquifer at the Site is laterally bound by areas of higher bedrock elevation. The extent of the aquifer is shown on **Figure 2-3**. As a result of these bedrock highs, the alluvial aquifer has been subdivided into three distinct but connected alluvial systems, referred to as the San Mateo, Rio Lobo, and Rio San Jose alluvial systems. The San Mateo alluvial system covers the majority of the Site area, extending northeast, south and southwest of the Site, eventually joining with the Rio Lobo and more extensive Rio San Jose alluvial systems.

2.2.1.1 San Mateo Aquifer

The San Mateo aquifer occurs as a north-south trending buried valley aquifer extending through the Site. Groundwater flow in the San Mateo aquifer is generally north to the south, upgradient of the LTP, and to the southwest in the area of the LTP. An artificial hydraulic barrier that is part of the current remediation system creates a zone on the southern and western sides of the LTP area where the natural gradient is artificially interrupted by a combination of collection and injection operations.

An area of high bedrock southwest and downgradient of the LTP results in a splitting of the San Mateo alluvial aquifer downgradient of the LTP. The portion to the west of the LTP

confluences with the Rio San Jose aquifer. The portion to the south of the LTP confluences with the Rio Lobo aquifer and eventually confluences with the Rio San Jose aquifer. This is shown on **Figure 2-3**.

The San Mateo aquifer generally behaves as an unconfined aquifer with specific yields ranging from 0.038 to 0.28. A specific yield of 0.1 represents the alluvial aquifer at the Site (HMC 2019d). Hydraulic conductivity values are relatively high, ranging from approximately 10 to more than 200 ft/day **Figure 2-4**. The water table ranges between from 40 to 60 feet below the ground surface, with elevations ranging from 6,428 to 6,550 feet above msl during the fall 2019 monitoring event.

2.2.1.2 Rio Lobo Aquifer

The Rio Lobo aquifer is typically a sandy material with minor clay and silt layers. Based on a 1995 investigation, it was determined that saturated portions of the Rio Lobo aquifer were likely confined to narrow sections where the alluvium was deposited within incised channels, or that a subcrop of bedrock drained the Rio Lobo aquifer upgradient of the confluence with the San Mateo Aquifer. Water quality differences between well ND and borehole BK3 and other background wells indicated that the confluence of the Rio Lobo and San Mateo aquifers may be in the vicinity of well ND (HMC 2019b). Groundwater flow direction is shown on **Figure 2-3**.

2.2.1.3 Rio San Jose Aquifer

Rio San Jose aquifer is generally composed of sand and gravel with a wide range of transmissivity. Groundwater in the Rio San Jose aquifer flows southeast from the Bluewater site and merges with San Mateo aquifer. The combined flow continues southeast toward Milan (DOE 2014). Groundwater flow direction is shown on **Figure 2-3.**

2.2.1.4 Alluvium Geochemistry and Minerology

Geochemical and mineralogical investigations of the alluvium from 2018 and 2019 showed arkosic sandstone markers of eroded upstream materials (Arcadis 2018). These were transported through fluvial processes during gradational channel filling during the Quaternary period and deposited on the eroded Chinle Formation bedrock surface. The 2018 and 2019 studies showed significant local heterogeneity in lithology, soil chemistry, and mineralogy associated with the variable fine- and coarse-grained alluvial sediments. The highest uranium concentration encountered in the 2018 and 2019 investigations was in the unsaturated zone, indicating that uranium in alluvial soils is naturally occurring due to transport and deposition of naturally uranium-rich materials throughout geologic time, not from uranium-bearing groundwater.

Gradual declines in dissolved uranium were observed from west to east in the wells installed during the 2018 and 2019 investigation, consistent with observed changes in major ion and trace element chemistry. Groundwater is more oxidizing in the west, producing conditions favorable for uranium mobilization. Groundwater is more reducing in the east due to lower transmissivity and high organic carbon content producing conditions less favorable for uranium mobilization. Uranium leaching analyses yielded soluble uranium from all sediment samples collected during the 2018 and 2019 investigation (Arcadis 2018).

2.2.2 Bedrock Aquifers

2.2.2.1 Chinle Aquifers

The Chinle aquifer system is made up of three water bearing zones within the Chinle Formation, referred to as the Upper, Middle and Lower aquifers. The aquifers subcrop beneath the alluvial aquifers providing hydraulic connection between the units.

2.2.2.1.1 Upper Chinle Aquifer

The Upper Chinle aquifer is a northeast-dipping, confined aquifer composed of a laterally continuous sandstone. Structural elevation contours of the top of the Upper Chinle aquifer indicate minor variations in the steepness of the northeasterly dip, particularly in the area immediately south of the LTP. The aquifer is hydraulically bounded from other Chinle aquifers by competent overlying and underlying shale that has been structurally offset by the West and East Faults. The average thickness of the sandstone is approximately 35 feet (HMC 2012).

The Upper Chinle aquifer subcrops at the base of the alluvium on both sides of the East Fault, most notably at the base of the western side of the LTP. However, the sandstone subcrop does not occur west of the West Fault, rather, the subcrop was offset farther north as a result of the most recent high-angle normal faulting and northeast-dipping bed surface.

The water quality of the Upper Chinle aquifer is influenced by the water quality of the San Mateo aquifer as a result of the alluvial aquifers discharging to the Upper Chinle east of the East Fault and in the vicinity near and north of the LTP (HMC 2012).

Aquifer properties vary significantly within the Upper Chinle aquifer due to the variability of fracturing of the sandstone related to faulting. As a result, a narrow band (several hundred feet wide) of elevated transmissivity exists on both sides of the East Fault. The transmissivity to the west of the East Fault exceeds 10,000 gallons per day per foot (gpd/ft). The transmissivity to the east of the East Fault exceeds 2,000 gpd/ft, but generally ranges between approximately 100 to 2,000 gpd/ft (HMC and Hydro-Engineering, 2010). In contrast, the transmissivity is much lower between the West and East Faults, where the aquifer is not as highly fractured. **Figure 2-5** provides a plan view showing Upper Chinle aquifer transmissivities. The hydraulic conductivity of the Upper Chinle ranges from less than 0.1 ft/day to more than 100 ft/day (HMC and Hydro-Engineering 2010). The saturated thickness of the aquifer ranges from 15 to 65 feet thick with an average thickness of approximately 35 feet near the Site.

Groundwater flow in the Upper Chinle aquifer is greatly influenced by remedial action involving the injection of water into the Upper Chinle and collection of groundwater from a series of extraction wells (**Figure 2-6**). Groundwater at the Site generally flows from areas mounding near the injection wells toward collection wells.

2.2.2.1.2 Middle Chinle Aquifer

The Middle Chinle aquifer is an east to northeast-dipping, confined aquifer composed of laterally continuous sandstone. The Middle Chinle aquifer is similar to the Upper Chinle aquifer and is hydraulically disconnected from other Chinle aquifers by competent overlying

and underlying shale. The Middle Chinle aquifer is generally the thickest of the Chinle aquifers with a saturated thickness ranging from 10 to 80 feet and an average thickness of approximately 44 feet near the Site (HMC 2012).

The Middle Chinle aquifer subcrops at the base of the alluvium. The Middle Chinle is hydraulic connected to the overlying San Mateo aquifer on the west side of the West Fault and between the West and East Faults at an isolated location in an alluvial channel south of the Felice Acres subdivision (HMC 2012).

Transmissivity of the Middle Chinle aquifer varies significantly (HMC and Hydro-Engineering 2010). East of the East Fault, the transmissivity ranges from 100 to 500 gpd/ft. Between the East and West Fault and west of the West fault, the transmissivity can be as high as 5,000 gpd/ft (**Figure 2-7**).

Middle Chinle hydraulic head in areas outside of the two faults is significantly different from the head between the two faults, which demonstrates that the groundwater is not hydraulically connected across fault boundaries (**Figure 2-8**). The West Fault represents a significant barrier to groundwater flow within the Middle Chinle aquifer, with up to 110 feet of hydraulic head difference across the fault in the area west of the LTP.

Pumping of Middle Chinle South Collection wells near the south end of South Felice Acres developed a depression in the Middle Chinle potentiometric surface that extends nearly 500 feet to the northeast and southwest of well Y7 and intercepting much of the groundwater flow beneath Broadview Acres and South Felice Acres.

Groundwater flow west of the West Fault is historically to the southwest and upward where groundwater flows from the Middle Chinle to the San Mateo aquifer. This prevents uranium in the San Mateo aquifer from affecting the water quality of the Middle Chinle aquifer on the west side of the West Fault. The injection of water in the San Mateo temporarily reversed the vertical hydraulic gradient in the northern portion of Section 27 during 2006 through 2014. This situation was corrected in 2016 by moving the injection of water in the San Mateo.

Groundwater between the East and West Fault and Groundwater east of the East Fault is recharged by the San Mateo aquifer. The injection of fresh water into wells CW14 (north of Broadview Acres) and CW30 (west of Felice Acres) has created groundwater mounds. These mounds cause the ground water to flow both north and south from these two wells.

2.2.2.1.3 Lower Chinle Aquifer

The Lower Chinle aquifer is the deepest water bearing unit within the Chinle Formation and is generally located approximately 200 feet above the geologic contact with the SAG. The Lower Chinle aquifer is hydraulically isolated from the overlying Middle Chinle aquifer and underlying SAG regional aquifer. In contrast with the overlying Chinle aquifers, the Lower Chinle aquifer is composed of shale (HMC and Hydro-Engineering 2010).

The Lower Chinle aquifer subcrops at the base of the San Mateo aquifer on either side of the West Fault. Direct hydraulic connectivity with the overlying San Mateo aquifer exists in the area between the West and East Faults southwest of the Felice Acres subdivision and

immediately west of the Valley Verde and Pleasant Valley subdivisions on the west side of the West Fault.

The hydraulic properties of the Lower Chinle aquifer are highly variable and largely depend on secondary permeability within the shale. The ability of the Lower Chinle aquifer to produce water is much lower and less consistent than overlying Upper and Middle Chinle aquifers. Hydraulic conductivity ranges from 0.1 to more than 50 ft/day (HMC and Hydro-Engineering 2010). The transmissivity of the aquifer is generally higher than 100 gpd/ft (750 ft^2/day) near subcrop locations (HMC and Hydro-Engineering 2010). However, selected areas near subcrop locations exceed 1,000 gpd/ft (**Figure 2-9**).

Groundwater flow in the Lower Chinle is shown on **Figure 2-10**. Groundwater elevations for the aquifer ranged from 6,420 to 6,488 feet above msl during the fall 2019 annual monitoring event (HMC and Hydro-Engineering 2019). Groundwater flow west of the West Fault in the Lower Chinle is mainly to the northeast. Groundwater flow between the two faults is to the northeast in the area of the tailings. Groundwater flow is to the northwest in the southern portion of the Lower Chinle aquifer between the faults. The northwesterly flow direction in this area indicates that the Lower Chinle water moves across the West Fault in the area west of Broadview Acres.

2.2.2.2 San Andres-Glorieta Aquifer

The SAG aquifer consists of the San Andres Limestone and Glorietta Sandstone with a total thickness that exceeds 200 feet (HMC and Hydro-Engineering, 2010). Similar to the Chinle aquifers, the aquifer is mildly folded and dips to the east and northeast as a result of regional tectonic deformation. A plan view map of the Site showing well locations, groundwater elevations and inferred contours from 2019 measurements is provided on **Figure 2-11**. The aquifer has been used by HMC as the source of unimpacted clean water for hydraulic containment of the San Mateo and Chinle aquifers.

Groundwater elevations near the Site ranged from 6,417 to 6,420 feet above msl during 2019. Flow direction is to the east-southeast. The water level elevations measured during 2014 show a very flat (0.00086 ft/ft) piezometric surface. The U.S. Geological Survey (USGS) suggested an average transmissivity of 374,000 gpd/ft (Frenzel 1992).

3 FIELD INVESTIGATION

3.1 Alluvial Aquifer

3.1.1 Drilling and Lithologic Sampling

Cascade Drilling, LP (Cascade) of Phoenix, Arizona (licensed in the State of New Mexico) drilled three boreholes through the alluvial formation using a truck mounted roto-sonic drill rig (**Figure 3-1**). Boreholes were drilled as close as possible to planned locations with slight adjustments to site conditions within tens of feet during rig set up. Locations were marked by HMC and confirmed with global positioning system (GPS) unit by the HDR geologist. The upper five feet of each borehole was hand cleared to confirm the absence of underground utilities.

Cascade collected alluvial samples continuously from each borehole, contained them in plastic liners, and labeled them for examination and characterization by an HDR geologist. HDR characterized the material using the Unified Soil Classification System (USCS) generally using terms described in ASTM D2488-09a: Standard Practice for Description and Identification of Soils (Visual-Manual Procedure), where applicable. HDR identified material colors using the Munsell Color System.

The material collected from each borehole included an upper layer of silts and sands, a basalt layer, and a lower layer of silts, sands, and clays. Each alluvial borehole was terminated in bedrock. The bedrock formations were identified based on the color of the material, the structure of the material, and its reactivity to hydrochloric acid. Boring logs are located in **Appendix A**.

3.1.2 Piezometer Installation

Cascade installed a 4-inch PVC piezometer (OB1, OB2, and OB3) in each borehole to monitor water levels within the Rio San Jose aquifer. The screen intervals were placed based on the location of saturated alluvial sand (i.e., well screens were not placed in saturated silts and clays) in each borehole.

OB1 was screen in light colored sandy material immediately beneath a deep clay layer but above bedrock. During the drilling of SAG2, the field team noticed that the color of the sandy material below the clay was red consistent with the color of the underlying Chinle Formation. This caused us to go back to the soil samples collected from OB1 and test the light-colored sandy material with hydrochloric acid. The acid test showed the light-colored sandy material reacted to the acid indicating it is calcium carbonate based and the San Andres Limestone. Therefore, OB1 was screened in the weather unconsolidated portion of the San Andres Limestone.

OB2 and OB3 were initially located on private property to the east of OB1; however, access to the property was not granted. OB2 and OB3 were re-located to the south of OB1 to characterize the groundwater flow direction in the Rio San Jose aquifer. OB2 and OB3 were drilled at the locations shown on **Figure 3-1**. OB2 and OB3 were screened in saturated alluvial sand below basalt. Soil samples collected from this layer were tested with acid to confirm placement in the alluvium (Rio San Jose aquifer). Well construction logs are located in **Appendix B**.

3.2 Bedrock/SAG Aquifer

3.2.1 Bedrock Casing Installation

SAG1 and SAG2 are considered artesian wells located within the Bluewater Underground Water Basin and were subject to conditions of approval set by the New Mexico Office of the State Engineer (NMOSE), including installation of an artesian well casing (**Figure 3.-2**). HDR and HMC provided NMOSE with photographs of the 6-inch black steel well casing for their inspection prior to well construction activities.

Cascade drilled and reamed each borehole to 10 inches in diameter; four inches greater than the diameter of the surface casing. Cascade set the 6-inch diameter black steel surface casings into competent rock. Surface casings were set roughly 10 feet into competent

bedrock. Because of the undulating surface of bedrock, this equates to a depth of 135 feet at SAG1 and to 161 feet at SAG2.

The annular space was filled and sealed using Type II Portland cement grout with a density between 15.4 and 15.5 pounds per gallon as approved by NMOSE. Cascade ensured that the cement grout was within the range specified using a standard calibrated mud balance. NMOSE permitted Adam Arguello to act as an authorized representative to witness the grouting process. The density of each batch of cement grout was documented and approved by Mr. Arguello. Cascade placed the cement grout into the annular space via tremie pipe.

The surface casing seal and compressive strength of the cement grout sealant were tested at SAG1 and SAG2 following the its installation. Bentonite was temporarily added to the bottom of each casing to seal it to the formation. Each casing was sealed and pressurized with 300 PSI of water; the casings held the pressure for 15 minutes as required by NMOSE. The bentonite was removed during subsequent coring.

3.2.2 Bedrock Coring

Cascade cored bedrock at SAG1 and SAG2 using a track mounted LF 70 core drill. The rig used a dual tube PQ core-barrel producing a 3.375-inch core and 4.875-inch diameter borehole. Cascade cored the boreholes continuously from the bottom of the surface casing, through the SAG to the final depth of 500 feet below ground surface each.

Core samples were placed in cardboard core boxes and labeled for examination and characterization by an HDR geologist. HDR characterized bedrock material using terminology generally provided in ASTM D2113 - 14: Standard Practice for Rock Core Drilling and Sampling of Rock for Site Exploration. HDR identified material colors using the Munsell Color System. Items including material descriptions, recovery lengths, rock quality designation lengths, and run times were recorded. Boring logs are in **Appendix A**. Core photos are located in **Appendix C**. Several challenges were experienced during the completion of SAG1 and SAG2. Most of the challenges were related to obstructions or collapsing boreholes. SAG1 and SAG2 were completed as per below:

SAG1

- Cored to 500 feet bgs;
- An obstruction was detected at 204 during the borehole geophysics;
- Cascade mobilized back to Site to clear the borehole several times to 500 ft bgs;
- The borehole continued to be obstructed at 215 ft bgs;
- 5-inch black steel casing was hung to 260 ft bgs and secured (welded to 6-inch casing) at the surface in consultation with the NMOSE;
  - 5-inch black steel casing not not grouted inside the 6-inch steel casing
- Borehole geophysics was completed through the 5-inch casing to the bottom of the borehole.
- FLUTe™ transmissivity profile was completed through the 5-inch casing to the bottom of the borehole; and
- FLUTe™ multi-port well was installed to 484 ft bgs.

SAG2

- Cored to 500 feet bgs;
- An obstruction was detected in the Glorieta at 440 ft bgs during the borehole geophysics;
- An additional obstruction was detected at during the FLUTe™ transmissivity profile at 377 ft bgs, just above the contact between the Glorieta and San Andres;
- FLUTe™ transmissivity profile was completed to 377 ft bgs;
- The FLUTe™ liner was removed;
- Cascade mobilized back to Site and cleared the borehole several times to 500 ft bgs;
- After clearing, the borehole initially stayed open to 500 feet, bgs;
- During the re-installation of the FLUTe™ liner the well was obstructed at 377 ft bgs;
- FLUTe™ multi-port well was installed to 377 ft bgs.

Borehole geophysics, FLUTe™ transmissivity profiling, and FLUTe™ multi-port well installation are described in Section 3.2.3 below.

3.2.2.1 Rock Core Physical Property Analyses

Twenty rock core samples (10 from each borehole) were collected and analyzed of physical properties including porosity, bulk density, percent moisture, and specific gravity by Golder Associates. Five samples were co-located with geochemical samples (five samples each from SAG1 and SAG2) and five additional sample biased to the SAG were collected from each borehole spatially distributed throughout the SAG.

Physical property samples were collected at the same time geochemical samples were collected. Samples were wrapped in foil, plastic wrap, and sealed in zipper lock bags to limit moisture loss. The rock core physical property samples were shipped under Chain of Custody to Golder Associates lab in Mississauga, Ontario. The lab split each sample (20 samples), analyzing two samples from each sample shipped, for a total of 40 analyses. A sample and results summary of the aquifer materials collected for physical property analyses is presented in **Table 3-1.** The physical property analytical reporting is found in **Appendix D**.

One of the key parameters for the CSM is the (primary) porosity of the bedrock. A summary of the porosity values are provided below.

- The porosity of the Chinle ranged from 7 to 11 percent.
- The porosity of the San Andres Limestone ranged from 3 to 34 percent.
- The porosity of the Glorietta Sandstone ranged from 11 to 15 percent.

3.2.3 FLUTe™ Transmissivity Profiling

The FLUTe™ blank flexible liner is driven down the borehole of SAG-1 and SAG-2 by the excess head of water inside the liner above the water table in the formation. That driving head inside the liner is the driving pressure forcing the water from the hole. The driving pressure beneath the liner is uniform throughout the borehole and maintained relatively constant during the measurement.

The data recorded during the liner installation include: liner depth, time, driving head, and tension on the liner. The liner tension is also controlled to be relatively constant as is the driving head inside the liner. The liner velocity per unit driving head as a function of the liner depth in the hole is calculated from the data.

As a liner is everted into the borehole, the liner descends like a perfectly fitting piston and forces the water from the borehole into the formation. When the liner starts down the hole, all the flow paths in the borehole are available for the displacement of the water. The entire transmissivity of the borehole is available for the acceptance of the water displaced by the liner.

The liner velocity down the borehole is controlled by the transmissivity of the borehole beneath the liner and the excess head in the liner. As the liner starts its descent in the borehole, the velocity is relatively high and then the velocity quickly reduces to a moderate rate equal to the flow of the water from the hole. Thereafter, there is a relatively constant driving pressure in the borehole and a steady state radial outward flow of the water from the hole as the liner descends.

However, as the liner descends, it sequentially covers and seals the flow paths in the borehole from the top down. Each time a flow path is sealed by the descending everting liner, the remaining transmissivity of the borehole is decreased by the sealed flow paths. The drop in transmissivity causes a drop in the liner velocity as each flow path is sealed. The drop in velocity provides a direct measurement of the flow that was stopped when the flow path was sealed.

Hence, a step change in velocity occurs at the location of the flow path, and the magnitude of the step change is a direct measure of the flow capacity of that sealed flow path. As the liner passes through an extended region of flow (e.g., a highly fractured region) the velocity graph shows a relatively continuous decline in velocity. A transmissivity profile is calculated from the velocity profile.

The change in liner velocity, dv, multiplied by the cross section of the borehole, Az, is defined as the flow, Qr, that was terminated when the interval of the borehole, dz, was sealed by the liner. Assuming a 1D radial flow into the borehole wall at a flow rate, Qr, over the interval, dz, and a hole wall area, Ar = 2 π ro dz, we get:

$$Qr = dv\ Az = 2\ \pi\ dz\ C\ dH / \ln (r/r_o)$$

Where C is the conductivity of the interval, dH is the driving head in the borehole, r_o is the hole radius, and r is the range to the ambient pressure in the formation. Since $\ln(r/ r_o)$ is

such a slowly varying function with r, even if r is not known, it is usually assumed to be a constant. From this equation, the transmissivity, T= dz C, is calculated or the conductivity C for the interval dz. Both are relevant to the interval dz over which the velocity change occurs. Since the velocity change is calculated for each time step, typically every 2 seconds, the length dz is the distance traversed by the liner descent in that time step. Therefore, when the liner is traveling fast the spatial resolution is less than when the liner is traveling slowly **(Appendix E)**.

3.2.3.1 FLUTe™ Transmissivity Profile Results

The results of the FLUTe™ transmissivity profile for SAG1 and SAG2 are presented as **Figures 3-3 and 3-4**. The FLUTe™ transmissivity profile for SAG1 shows three high transmissivity zones below 350 feet bgs. These groundwater flow zones are in the Glorietta Formation. There may also be some lower transmissive zone above 350 feet bgs. These high transmissive zones likely create a moderate level of uncertainty with respect to the accuracy of the measured transmissive values in these high transmissive zones and likely masked the methods ability to detect lower transmissive zones.

The FLUTe™ transmissivity profile for SAG2 shows high transmissive zones above 150 feet bgs and below 350 feet bgs. The FLUTe™ transmissivity profile for SAG2 also shows a few lower transmissive zones from 200 to 300 feet bgs. Similar to SAG1, the high transmissive zones in SAG2 likely create some uncertainty with respect to the accuracy of the measured transmissive values in these high transmissive zones and likely masked the methods ability to see and accurately measure the transmissivity of any potential lower transmissive zones.

3.2.3.2 Fracture Aperture, Hydraulic Conductivity, and Porosity

The transmissivity of a fracture can be calculated using the Cubic Law if the flow is assumed to be laminar and one adopts the analogy of parallel planar plates to represent the fracture surfaces (Witherspoon et al, 1979). This equation can also be used to calculate the aperture of a fracture with a measured transmissivity.

$$T_f = K_f (2b) = \frac{\rho g (2b)^3}{12\mu}$$

The FLUTe™ transmissivity profile data was used to calculate the aperture of each fracture detected during the FLUTe™ hydraulic conductivity profile. These results are shown on **Figures 3-5 and 3-6** and summarized below.

SAG1

The aperture calculations from the FLUTe™ transmissivity profile show there are numerous transmissive fractures from 358 to 437 ft bgs in the SAG1 borehole. The physical size of the transmissive fractures ranges from 19 to 504 microns with a geometric mean of 58 microns. The transmissivity of the borehole is approximately 9,000 gpd/ft with a bulk hydraulic conductivity of 5 ft/day. The bedrock has a fracture porosity of roughly 0.0005 or 0.05%

SAG2

The aperture calculations from the FLUTe™ transmissivity profile show there are numerous transmissive fractures from 141 to 374 ft bgs in the SAG2 borehole. The physical size of the transmissive fractures ranges from 13 to 780 microns with a geometric mean of 152 microns. The transmissivity of the borehole is approximately 5,700 gpd/ft with a bulk hydraulic conductivity of 3.7 ft/day. The bedrock has an average fracture porosity of roughly 0.0003 or 0.03%.

3.2.4 Borehole Geophysical Logging

Borehole geophysical logging was completed on SAG2 on January 8th and SAG1 on January, 13th and 27th, 2021 to assist in determining bedrock lithological boundaries, depth of discrete water-bearing fractures, the strike and dip of joints, fractures and bedding features, the flow within the borehole, and to provide information for the installation of multi-port wells. Borehole geophysical logging was completed by Jet West Geophysical Services of Farmington, New Mexico.

The suite of borehole geophysical techniques used at each borehole include; fluid temperature (FTemp), fluid resistivity (FRes), three arm mechanical caliper (caliper), natural gamma ray (gamma), heat-pulse flowmeter (HPFM), acoustic televiewer (ABI), and optical televiewer (OBI). Log depths were referenced to ground surface adjacent to the boreholes steel casing. The geophysical logging winch contains an optical depth encoder, to maintain depth measurements accurate within approximately + 0.2 feet throughout a borehole. Borehole logging of SAG1 was combined as one log but was completed during two mobilizations because borehole wall calving prevented logging below 204 feet on January 13th. The second log on January 27th was completed after 5-inch steel casing was installed to stabilize the borehole to 260 feet bgs. Geophysical logs are described below and presented in **Appendix F**.

3.2.4.1 Gamma Log

The gamma log provides a measurement recorded in counts per second (CPS), that is proportional to the natural radioactivity of the formation. Actual counts depend upon the detector size and efficiency but are often normalized in API units. The borehole wall penetration depth of investigation for the gamma log is typically 10 to 12 inches. This log is used principally for lithologic identification and stratigraphic correlation. The gamma-emitting radioisotopes that naturally occur in geologic materials are Potassium 40 and nuclides in the Uranium 238 and Thorium 232 decay series. Potassium 40 occurs with all potassium minerals, including potassium feldspars. Uranium 238 is typically associated with dark shales and uranium mineralization. Thorium 232 is typically associated with biotite, sphene, zircon and other heavy minerals.

Gamma log shows higher levels of natural radioactivity from the bottom of the surface casing to 230 feet bgs than the portion below 230 feet bgs in SAG1. Lower natural radioactivity was recorded from 230 to roughly 400 feet bgs where the natural radioactivity increases from 400 to 484 feet bgs. Gamma log shows higher levels of natural radioactivity from the bottom of the surface casing to 230 feet bgs than the portion below 230 feet bgs in SAG2. Lower natural radioactivity was recorded from 230 to roughly 440 feet bgs. Gamma log

shows relatively consistent levels of baseline natural radioactivity with local increases corresponding with fractures shown on the caliper log potentially due to fractures partially filled with clay.

3.2.4.2 Fluid Temperature and Fluid Resistivity

Fluid temperature, fluid resistivity, caliper, and gamma were completed on SAG1 on January 8th. The HPFM was not conducted in SAG1 on January 8th after it was determined the borehole was obstructed and unstable. After the borehole obstruction was cleared and borehole stabilized by Cascade, HPFM data was obtained on January 27th. These logs have been combined into one log. The geophysical logs for SAG1 and SAG2 are provided in **Appendix F.**

Fluid temperature and fluid resistivity data were recorded while lowering the probe at approximately three to five feet per minute. Geothermal gradients in the near surface earth are usually dominated by conduction and are generally linear increasing with depth due to the relative constancy of the thermal conductivity of earth materials. Convective heat flow within the borehole fluid is caused by formation fluid entering or leaving the borehole at some permeable interval. Therefore, deviations from the linear thermal gradient can be attributed to fluid movement. Slope changes in both the temperature and fluid resistivity logs may be indicative of fluid flow between the formation and the borehole.

Temperature log from SAG1 shows a constant increase in temperature to the bottom of the borehole not indicative of effects from individual fractures. Temperature log from SAG2 shows a constant increase in temperature to 380 feet bgs not indicative of effects from individual fractures. The temperature significantly increases from 380 to 484 feet bgs. Large inflections at the very bottom of a borehole may represent only accumulated sediments with temperature or electrical properties that contrast with the water column.

Fluid resistivity log from SAG1 shows moderate values from 140 to 310 feet bgs indicative of low groundwater flow and then higher values from 310 to 400 feet bgs indicative of potentially higher flows from 310 to 400 feet bgs. The fluid resistivity values reduce from 400 to 484 feet bgs indicative of low groundwater flow. Fluid resistivity log from SAG2 shows higher values from 160 to 380 feet bgs indicative of potentially higher flows. The fluid resistivity values reduce from 380 to 484 feet bgs indicative of low groundwater flow.

3.2.4.3 Heat-Pulse Flow Meter Logs

Heat-pulse flowmeter data were obtained at specific depths inferred from field plots of the caliper, fluid temperature, fluid resistivity, and acoustic televiewer logs. Flowmeter data were recorded under ambient conditions in both down and up runs within each borehole. Subsequent attempts to repeat the logging under pumping induced conditions with a Grundfos Redi-Flo2 were not successful because induced pumping was unable overcome the ambient flow conditions within the boreholes.

Heat Pulse flow meter data for SAG1 shows moderate flow in or out of the borehole from 140 to 300 feet bgs and higher flow in or out of the borehole from 300 to 400 feet bgs and then moderate flow in or out of the borehole from 400 to 484 feet bgs. Heat Pulse flow meter data for SAG2 shows high flow in or out of the borehole from 160 to 240 feet bgs,

moderate flows in or out of the borehole from 240 to 380 feet bgs, and lower flow in or out of the borehole from 380 to 484 feet bgs. Heat-Pulse Flow Meter Logs for SAG1 and SAG2 are provided in **Appendix F.**

3.2.4.4 Caliper Log

The caliper log represents the average borehole diameter determined by the extension of spring-loaded arms of a three-arm caliper probe. One important application of the caliper measurement is to identify intervals where rough borehole walls or washouts have the potential to introduced errors or other measurements where log response is affected by borehole enlargement or "rugosity". Caliper logs may show diameter increases in cavities and, depending on drilling techniques used, in weathered zones. The caliper log is often a useful indicator of fracturing. However, the log anomalies do not directly represent the true in-situ fracture size or geometry. Instead, they represent areas of borehole wall breakage associated with the mechanical weakening at the borehole-fracture intersection. Caliper logs for SAG1 and SAG2 are provided in **Appendix F.**

Inflections to the right in the caliper log show borehole enlargements, for example where the drill bit passed through a bedrock fracture. SAG1 caliper log shows large enlargements at 300, 335, and 480 feet bgs. SAG2 caliper log shows large enlargements from 320 to 335 feet bgs and 430 to 440 feet bgs.

3.2.4.5 Acoustic and Optical Televiewer

Borehole televiewer logging was used to obtain oriented images of borehole walls. Optical televiewer (OBI) imaging was performed by recording magnetically oriented images at 0.007-foot depth increments, with pixels at one-degree arc segments for each 360-degree scan around the borehole wall, while logging downward at a speed of approximately 3.5 to 4 feet per minute. ABI images were recorded at 0.01-foot depth intervals, with one pixel for each 1.25-degree arc-segment around the borehole wall, at a logging speed of approximately three feet per minute. Analysis of the OBI and ABI logs allow void and joint data to be presented in terms of depth, aperture, direction of dip (with respect to North), dip angle, and strike.

These televiewer-interpretations are observed planar-feature depths, down-dip compass direction for each planar feature (note that these are perpendicular to the strike direction, and are referenced to magnetic north), dip angles with respect to horizontal, and estimated feature aperture.

Acoustic televiewer data are presented via two columns (ABI40 “travel time" and “amplitude"), where each column represents a cylindrical image sliced down the north edge and laid flat on the printed page. Magnetic north is at the left edge of each column, and the images progress through east, south, west, and back to north at the right-hand edge.

Optical televiewer images are presented in a similar manner, in a single column labeled “OBI40 image". Magnetic north is also at the left edge of this image column, and the image progresses through east, south, west, and back to north at the right edge.

Acoustic televiewer logs were evaluated using WellCAD’s image-processing module, to measure planar-feature dip angles and down-dip azimuths. All interpreted down-dip

azimuths are referenced to magnetic north. The tadpole plots graphically display the depth, orientation, and category of the bedrock structures interpreted from the televiewer images. The orientations of bedrock structures are graphically displayed on the tadpole plots by a tadpole consisting of a circle, the head, and a line, the tail. The position of the head, left to right on the tadpole plot, gives the dip angle of the bedrock structure. The left side of the track indicates a dip angle of 0º and the right side of the track indicates a dip angle of 90º from horizontal. The position of the tail gives the dip azimuth of the fracture and can be read like a compass. The tail pointing directly up is 0º, north. We note that dip azimuth is perpendicular to strike as the term commonly used by geologists. Features that are clearly represented on both the ABI travel-time and amplitude plots are and visible on the OBI image plots are considered “open". Features represented only (or mostly) on the ABI amplitude plots are likely to have smaller apertures (or possibly represent bedding planes, or tight or mineral-filled joints), and are therefore judged relatively “less open”.

Red tadpoles and corresponding red sine-curve lines superimposed on the ABI plots designate features with dip azimuths within 45º of north, purple tadpoles and corresponding purple sine-curve lines superimposed on the ABI plots designate features with dip azimuths within 45º of east, blue tadpoles and corresponding blue sine-curve lines superimposed on the ABI plots designate features with dip azimuths within 45º of south, and green tadpoles and corresponding green sine-curve lines superimposed on the ABI plots designate features with dip azimuths within 45º of west. Geophysical tadpole plots identifying fracture orientation are provided in **Appendix F**. The transmissive nature of the features identified on the ABI and OBI plots cannot be determined from these televiewer methods however discrete fracture transmissivities were discernable with the FLUTe™ liner tests, discussed in Section 3.2.3.

3.2.5 FLUTe™ Multi-Port Well Design

Each FLUTe™ multi-port well was designed using the FLUTe™ transmissivity profile and the borehole geophysics data. The following rationale was used to select the FLUTe™ port locations and depths.

SAG 1

- Port No 1 was selected to be from 258 to 263 feet bgs targeting a weathered and fractured zone just below the grouted 5-inch steel sleeve casing.
- Port No. 2 was selected to be from 310 to 315 feet bgs targeting a few fractures at the midpoint of the San Andres Formation.
- Port No. 3 was selected to be from 362 to 367 feet bgs targeting a weathered and fractured zone at the contact between the San Andres and Glorieta Formations.
- Port No. 4 was selected to be from 392 to 397 feet bgs targeting a transmissive fracture zone in the top half of the Glorieta Formation.
- Port No. 5 was selected to be from 415 to 420 feet bgs targeting a transmissive fracture zone at the midpoint of the Glorieta.

SAG 2

- Port No. 1 was selected to be from 164 to 169 feet bgs targeting a weathered and fractured zone within the Chinle just below the steel surface casing.
- Port No. 2 was selected to be from 205 to 210 feet bgs targeting a transmissive fracture zone in the top of San Andres containing limestone.
- Port No. 3 was selected to be from 260 to 265 feet bgs targeting a transmissive fracture zone near the midpoint of the San Andres containing sandstone.
- Port No. 4 was selected to be from 315 to 320 feet bgs fracture zone targeting the midpoint of the San Andres containing dolostone.
- Port No. 5 was selected to be from 370 to 375 feet bgs targeting a transmissive weathered and fractured zone at the contact between the San Andres and Glorieta Formations.

3.3 Synoptic Water Levels

Two rounds of water levels were measured from the two newly installed FLUTe™ multiport monitoring wells, SAG1 and SAG2. Depths to water were measured from the top of the FLUTe™ multi-port well, fitting by FLUTe™ personnel on February 18, 2021 and by Homestake personnel on February 26, 2021. These two rounds of depth to water measurements can be found on **Table 3-2**.

Water levels measured on February 18, 2021 at SAG1 show a slight upward vertical gradient of 0.002 feet/ft between the top of Port 1 and bottom of Port 3 (258-367 ft bgs) and slight downward gradient of 0.004 feet/ft between top of Port 3 and bottom of Port 5 (262-420 ft bgs). While water levels measured at SAG2 show a slight downward vertical gradient of 0.007 feet/ft between the top of Port 1 and bottom of Port 2 (164-210 ft bgs) there is a fairly significant downward gradient of 0.431 feet/ft between the top Port 2 and bottom Port 3 (205-265 ft bgs),a slightly less but still significant downward gradient of 0.154 feet/ft between the top Port 3 and bottom Port 4 (260-320 ft bgs) and a very slight upward gradient of 0.002 feet/ft between the top of Port 4 and the bottom of Port 5.

Water levels measured on February 22, 2021 at SAG1 show a slight steady downward gradient of 0.002 feet/ft from the top of Port 1 to the bottom of Port 5 (258-420 ft bgs). While water levels measured at SAG2 show a significant downward gradient of 0.576 feet/ft between the top of Port 1 and bottom of Port 2 (164-210 ft bgs), continuing with less of a downward gradient of 0.119 feet/ft between the top Port 2 and bottom Port 3 (205-265 ft bgs),a slight upward gradient of 0.002 feet/ft between the top Port 3 and bottom Port 4 (260-320 ft bgs) and a very slight downward of 0.001 feet/ft between the top of Port 4 and the bottom of Port 5.

3.4 Geochemical, Mineralogical, and Water Quality Assessments

Select samples of aquifer solids from the Chinle Shale, San Andres Limestone, and Glorietta Sandstone were characterized for their major mineralogical and geochemical characteristics. In addition, groundwater samples were collected from wells installed in the SAG-1 and SAG-2 borings. This information provides a baseline assessment of

geochemical conditions within the aquifer and will be used to support future chemical transport assessments for the SAG aquifer.

3.4.1 Aquifer Solids Characterization

Characterization methods for the aquifer solids were based on basic understanding of the aquifer mineralogy as described in previous reports (Gordon, 1961; USGS, 1972; Brown and Caldwell, 2018). These methods (**Table 3-3**) provide complete geochemical and mineralogical characterization of the various lithologies while also evaluating chemical conditions within the aquifer as related to constituent transport and were developed in accordance with USNRC guidelines for subsurface geochemical characterization at Title II Former Uranium Milling Sites (USNRC, 2003). Geochemical testing was conducted by ACZ Laboratories, Inc. (Steamboat Springs, CO) **(Appendix G)** and mineralogical testing by DCM Science Laboratory (Wheat Ridge, CO) **(Appendix H)**. Regional geological and site-specific sample descriptions (**Table 3-4**) are discussed below with respect to characterization objectives and testing procedures for the Chinle Shale, San Andres Limestone, and Glorietta Sandstone samples:

Chinle Shale: The Chinle Formation overlying the San Andres Limestone was targeted for sampling and has been reported as friable and calcareous mudstone containing clayey and silty sandstone lenses, with weak to strong cementation and ranging in color from grayish-red to light-green and gray (Gordon, 1961). The Chinle Shale intervals selected for analysis from SAG-1 and SAG-2 were described as a weathered, reddish-brown to gray, soft, thinly-bedded and fractured siltstone (**Table 3-4**). Two samples of Chinle Shale (one per boring) were characterized for total metals, sulfur plus carbon forms, and cation exchange capacity (CEC) (**Table 3-5**).

San Andres Limestone: The San Andres Limestone is comprised of an upper limestone unit (60 to 100 ft thick), a middle calcareous sandstone unit (15 to 30 ft thick), and a lower dolomitic limestone unit (20 to 40 ft thick) (Gordon, 1961). The San Andres Limestone intervals selected for analysis from SAG-1 and SAG-2 were classified as moderately fractured and weathered sandstone, dolomite, or limestone (**Table 3-4**). Four samples of San Andres Limestone (two from each boring) were analyzed for total metals and sulfur plus carbon forms. Two samples (one per boring) were analyzed for mineralogical composition using X-ray diffraction (XRD) and a single sample was examined using optical mineralogy (**Table 3-6**). Because cation exchange would not be expected to operate as a significant control on chemical properties or constituent transport in a predominantly carbonate (limestone) aquifer, the San Andres Limestone samples were not characterized for CEC.

Glorieta Sandstone: The Glorieta Sandstone has been described as a well-sorted, medium-grained sandstone, white to light gray in color with limonite flecks (Gordon, 1961). The upper strata tends to be firmly cemented with silica while the lower strata is soft and friable. Calcite cementation may also be present. Vertical fractures are filled with calcite and quartz, often with pyrite. The Glorieta Sandstone intervals selected for analysis from SAG-1 and SAG-2 are classified as a weathered, fractured, and fine-grained sandstone (**Table 3-4**). Four samples of Glorieta Sandstone (two from each boring) were analyzed for total metals, sulfur

plus carbon forms, and CEC. Two samples (one per boring) were analyzed for mineralogical composition using XRD and a single sample was evaluated using optical mineralogy (**Table 3-6**).

3.4.1.1 Mineralogical Results

Bulk XRD analysis was conducted on two samples from the San Andres Limestone and two samples from the Glorieta Sandstone (**Tables 3-**6and **3-7**). Samples from the San Andres Limestone consisted primarily of calcite and/or dolomite (97%), with a small amount of quartz (1%) and < 5% unaccounted (**Table 3-6**). Samples from the Glorieta Sandstone contained much lower carbonate mineral content (6 to 16%) and consisted primarily of quartz (62 to 82%) with lesser amounts of kaolinite and potassium feldspar. Optical microscopy results for these sample were very consistent with respect to major mineral constituents. Microscopy also revealed the presence of minor constituents which could not be detected using XRD. These include pyrite in association with relatively minor Fe oxides in both the San Andres Limestone and Glorieta Sandstone (**Table 3-7**).

3.4.1.2 Major Trace Element Concentrations

The total metals results for all lithologies (**Table 3-8**) indicate the elemental compositions are dominated by Aluminum (Al), Iron (Fe), Magnesium (Mg), Manganese (Mn), Calcium (Ca), Potassium (K), Sodium (Na), and Silica (Si). The relative abundance of these eight elements are shown on **Figure 3-7**. Because Method 3050B does not result in complete dissolution of all silicates (primarily quartz), the Si content was estimated by using the XRD quartz content for the San Andres Limestone and Glorieta Sandstone samples, and from the average Si content of shale (Fleischer and Parker, 1967) for the Chinle Shale samples. The Chinle Shale contains the highest proportion of Fe, Al, and K and with high Si content, consistent with silts and clays containing iron oxides as observed to occur in the form of reddish-colored, oxidized and weathered siltstone at SAG-1 and SAG-2 (**Table 3-8**). The concentrations of major elements (Ca, Mg, Na, K, Fe, and Al, **Table 3-9**) are generally low in the Chinle Shale compared to typical clays and shales (**Table 3-9**). The San Andres Limestone is dominated by Ca and Mg due to the predominant limestone and dolomite mineralogy (**Tables 3-**8and **3-9**). The Glorieta Sandstone samples were also enriched in Ca and Mg, but with relatively higher proportions Al, Fe, K, and Si as would be expected for a sandstone lithology containing quartz, aluminosilicates, and Fe oxides (**Tables 3-8** and **3-9**). Major element concentrations in the Glorieta Sandstone are generally lower compared to typical sandstones (**Table 3-9**).

Trace element concentrations (e.g., Uranium (U), Vanadium (V), Selenium (Se), Molybdenum (Mo), Boron (B)) were variable both within and across rock types although generally higher concentrations of U, V, and B occur in both the Chinle Shale and San Andres Limestone compared to the underlying Glorietta Sandstone (**Figure 3-8**). Molybdenum concentrations were reported as <2 mg/kg in all rock types, consistent with typical values for these rock types (**Table 3-8**). Measurable B was only present in the Chinle Shale samples (**Table 3-8**); higher B concentrations are expected for clays and shales compared to other rock types, although the B concentrations are lower overall compared to typical values (**Table 3-9**). Both U and Se concentrations were lower in the Chinle Shale

relative to typical clays and shales, but those in the remaining samples were consistent with those for a carbonate-rich sandstone or carbonate rock (**Tables 3-**8and **3-9**). Vanadium concentration trends are consistent with those for typical rocks, but with overall lower concentrations (**Figure 3-8**, **Table 3-9**).

3.4.1.3 Carbon, Sulfur, and Cation Exchange Capacity

Total carbon and sulfur content provide an overall indication of inorganic carbonate, detrital organic matter, and/or sulfide minerals (e.g. pyrite). The relative abundance of organic carbon and sulfur forms can also be used to infer whether conditions are relatively oxidizing or reducing, which are important aspects related to transport of dissolved constituents. The total carbon contents are comprised primarily of inorganic carbon (carbonate), with only minor organic carbon, and are highest in the San Andres Limestone samples as would be expected for carbonate rocks. However, due to the more weathered nature of the overlying Chinle Shale, both their total carbon and total sulfur contents were below detection (**Table 3-10**). The total sulfur content of the San Andres Limestone samples consisted of either sulfate-sulfur or sulfide-sulfur (pyrite), while the sulfur content of the Glorietta Sandstone is largely dominated by sulfide-sulfur. The presence of organic carbon and pyrite in a number of samples may tend to impart reducing conditions within the San Andres Limestone and Glorietta Sandstone aquifers, depending of the relative rates of oxygen depletion versus oxygen replenishment from surface recharge.

The CEC of the aquifer materials provides a baseline indication of the potential reactivity of clay minerals with groundwater (**Table 3-10**). The CEC values for the Chinle Shale and Glorietta Sandstone samples are low (1.46 to 7.4 meq/100 g) and would be equivalent to a typical sandy soil containing clay with a low intrinsic CEC, such as kaolinite. Therefore, cation exchange would not be expected to exert significant controls on groundwater chemistry, nor expected to play a major role in attenuation of dissolved constituents with transport through the aquifers.

3.4.2 Groundwater Quality Characterization

Groundwater samples were collected from Wells SAG-1 and SAG-2 in February of 2021 using FLUTe^{TM} groundwater sampling procedures **(Appendix E)** in conjunction with a flow cell to obtain representative samples. Five samples were collected from each well at various depths (**Table 3.-11**). Field parameters included temperature, pH, dissolved oxygen (DO), electrical conductivity (EC), oxidation-reduction potential (ORP) expressed as Eh, and ferrous iron (Fe as Fe2+). All samples were appropriately filtered and/or preserved as required in the field and analyzed for a complete suite of major cations, major anions, nutrients, metals, and radionuclides by ACZ Laboratories, Inc. (Steamboat Springs, CO) **(Appendix I)**.

All groundwater results are reported in **Table 3-11_** which includes the sampling depths, field parameters and laboratory parameters for SAG-1 and SAG-2. All constituents were below detection in the field blank and the relative percent difference (RPD) between the primary sample SAG2-1 and its duplicate (0999) was below 20% for all analytes except for the radionuclides. The major ion results indicate that the groundwater is a calcium-sulfate type water (**Figure 3-9**) with a tendency toward higher proportions of calcium and sulfate

relative to magnesium and bicarbonate with depth. The total dissolved solids (TDS) concentrations ranged from 860 to 1960 mg/L with increasing trends at depth (**Table 3-11**). The concentrations of uranium, selenium, molybdenum, and vanadium are orders of magnitude lower than might occur in an arid, near-surface alluvial aquifer system.

A notable observation at both SAG-1 and SAG-2 (although more pronounced at SAG-2) is the presence of a redox profile, where conditions become more reducing with depth. The shallower samples from SAG-2 tend to have higher DO and lower ferrous Fe compared to those at depth (**Figures 3-10** and **3-11**). The inverse relationship between both DO and ferrous Fe (**Figure 3-12)** illustrates that higher ferrous Fe is associated with low DO concentrations. Both low DO and measurable ferrous Fe are indicators of reducing conditions, where the higher ferrous Fe concentrations correspond to the lowest redox potential values (**Figure 3-13**). The redox profiles are also apparent in the distribution of dissolved nitrogen species, where the oxidized form of nitrogen (nitrate-N) is below detection at depth, but the reduced form (ammonia-N) dominates (**Figure 3-14 and Figure 3-15**).

3.5 Geophysical Survey

HDR mobilized a crew and equipment to the site and completed the Electrical Resistivity Tomography (ERT) survey between December 10 and December 18, 2020. Three ERT transect lines were completed, collecting data over approximately 15,550 linear feet. The ERT lines were aligned roughly parallel and perpendicular to bedrock strike of the SAG and co-located with existing and recently drilled borings/wells. The ERT transect lines and boring/well locations are shown on **Figure 3-16**. A Trimble Catalyst with RTX correction service was used to record the ERT lines and borings/wells with an accuracy of approximately 4-inches. The ERT surveys were conducted according to proposed methodologies; however, a slight change to the line locations and lengths were made due to site access and a third line was added N-S, approximately in-line with several historic wells.

3.5.1 ERT Data Acquisition and Processing

An Advanced Geoscienses Inc. (AGI) SuperSting 112 electrode resistivity system was used to complete the ERT survey. Electrodes were places at 20-foot intervals along each line segment to allow for a total length per segment of approximately 2,220 feet. This length provided sufficient depth penetration of the ERT signal to characterize the geology to approximately 400-feet below land surface. Several line segments were needed to produce these long lines as shown in **Figure 3-16**. Each line segment was overlapped more than 250-ft to ensure continuous data recording without large gaps at depth. Equipment checks were run including a contact resistance check between each electrode as part of each line's setup. This resistance check is key in producing quality data by checking for electrodes with poor soil coupling and/or electrode contact. In dry areas with rocky and sandy soils, it is often necessary to add water around electrodes to help improve electrical continuity between the electrode and the soil. A suitable layer of surface soil was present for most of the electrode locations along the survey lines and in areas crossing rocky terrain (including basalt outcrops) water or salt water-soaked cloth was used to improve high contact

resistances. Contact resistances were able to reach acceptable levels in all cases by adjusting or adding water to the electrodes.

Data were processed using AGI's Earth Imager2D software specialized for resistivity tomography processing. Data collection included use of the dipole-dipole and strong gradient arrays and therefor combining the two array types was a key element of the processing workflow. The general processing workflow included:

1. Extracting (X,Y,Z) coordinates and elevation from collected GPS data at each electrode location;
2. removal of data spikes;
3. inversion modeling settings with a max number of iterations;
4. applying a damping factor, and then;
5. final smoothing of plotted, parameters set to match previous ERT data processing at the mill site.

The number of model iterations varied based on data convergence, and in general were less than six iterations. As part of the processing data quality control (QC), the RMS error percentage is calculated for each ERT segment. Between the eight segments that make up the 3 lines, the lowest RMS was 7.8% and the highest model was 15.2%. These are very good error percentages and these data represent consistent and well-fitting models for this arid environment. Final models were produced using a contour software package from Golden Software, Surfer16. The final data plots were further smoothed by using a linear variogram and typical resistivity logarithmic scales. The cell sizes used during the final model gridding were 10-ft horizontally and 1-ft vertically to better enhance the horizontal nature of the lithology. Then a Gaussian filter of 41 by 5, horizontal/vertical cells was applied to the combined line segments that make up the final longer line plots. This filter removed high frequency noise associated with overlapping data zones, the horizontal biased nature of the filter helps image the natural stratification of the subsurface while removing near vertical distortions often found in resistivity data. **Figures 3-17 through 3-19** present the final processed ERT profiles for the three transects shown on **Figure 3-16**. Initial data inversions of individual line segments are included in **Appendix G**.

3.5.2 ERT Data Interpretation and Boring Correlation

Data plots for each of the three ERT lines are presented on **Figures 3-17through 3-19** with generalized boring logs overlaid on the data. The basic geologic sequence found in the deeper borings show:

- Alluvium (silty, sandy, some clay and gravels);
- Basalt;
- Alluvium (silty, sandy, some clay and gravels);
- Chinle Formation; and
- San Andres/Glorieta Formation.

Typically, these rock types would be more resistive than silty/clayey soils and the ERT profiles would exhibit resistivities that are increasing with depth without the presence of water. Water was observed in the two deeper borings at or less than 130-feet below ground surface.

The resistivity data reinforces the interpretation of the SAG aquifer since the values are lower than expected for these same formations, implying the presence of water. To further evaluate the resistivity interpretation, the ERT data can be compared to the geophysical well logging performed at SAG1 and SAG2. The long and short normal geophysical logs match very closely to the values seen in the ERT model and show a similar relatively low resistances throughout the SAG depth imaged in the resistivity profiles.

The following is a list of general resistivity ranges for the more prominent geologic layers:

1. Alluvium near surface soils – 20 to 500 ohm-m
2. Basalt – 300 to 30,000 ohm-m
3. Chinle – 50 to 2,000 ohm-m
4. Top of the SAG – 50 to 500 ohm-m
5. Lower SAG – mostly 1 to 250 ohm-m with isolated areas as high as 600 ohm-m

The resistivity lines were collected in relatively straight profiles to improved data quality. Therefore, many of the borings are located some distance off the lines including a few that are more than a hundred feet away from the lines. This offset may have some bearing on the resistivity ranges noted above. Furthermore, the interpretation lines shown to represent the breaks in geology noted in the borings often cross contour lines. However, the overall shape and trends of the contours were used to guide the interpreted top of the Chinle and the top of the SAG (for example). In the interpretation more weight was given to connecting lithology from the boring logs as well as remaining in a reasonable range of resistivities for the geology. See dashed interpreted formation contacts include on **Figures 3-17 through 3-19**.

3.5.3 ERT Survey Results

Figures 3-17 through 3-19 present the interpreted ERT data profiles. The horizontal axis on these plots are distance along the lines in feet. The vertical axis is elevation above mean sea level in feet and were taken from a digital elevation model (DEM) and GPS positions. Data is plotted with a four times vertical exaggeration. The color scale represents a logarithmic scale of resistivity values in ohm-meters. The boring logs are shown at projected positions along the ERT lines and the offset and approximate offset direction is noted in parenthesis. Also, noted near the top of the profiles are the approximate crossing line locations.

Figure 3-17 shows the ERT data profile and interpretation for ERT Line 1. This line is roughly oriented S-N and has a short data break and zone where overlap was not possible due to crossing a paved road. One full line segment was used to extend data coverage to the south from the road. This segment was added near the end of the field survey once access to the adjacent property was obtained. The data plot shown on this figure, therefore, shows negative distance along the bottom axis representing the extension of this line further south past the original start of the line.

Line 1 was oriented to pass near some of the historic wells located on the site **(Figure 3-16)**. The logs for these are limited to drillers observations and do not reach the SAG aquifer. Most note termination into a shale that most likely corelates to the contact with the lower Chinle (noted siltstone or mudstone on the current boring logs). The interpreted basalt layer boundaries are show as black lines with ticks and the interpreted contact between the

alluvium and Chinle as dashed black lines and interpreted top of the SAG is shown as dashed red lines. This interpretation of the SAG uses information from the other ERT lines as well as boring SAG1, shown on this figure. This boring is the only boring along this line that reaches the aquifer. One challenge in the interpretation of the top of the Chinle and SAG is the occurrence of what appears to be a variable boundary of higher and lower resistivities, producing a peak and valley affect in the resistivity data. Another notable feature along this line is the interpreted crossing of the "West Fault" that is known to trend SW to NE in this area. The interpreted fault crossing is shown on this line as a red shaded box near the projected location of boring OB3. Further evidence of this fault is present in the lack of the Chinle in boring OB2 and an apparent elevation change in the interpreted top of the SAG.

Figure 3-18 shows the ERT profile for ERT Line 2. This line is roughly oriented NW to SE and crosses Line 1 near the SAG1 boring. The line connects between the two deeper boring conducted as part of this study (Borings SAG1 and SAG2). However, the resistivity values at the top of the SAG near boring SAG1 correlates to a higher resistivity than what is observed on the other ERT lines and seen at boring SAG2. It is possible the higher values seen here as the apparent trough of higher resistivity values that extend down from the basalt layer are out of plane effects from adjacent variations in the Chinle. Another noteworthy observation is the apparent weakening of the continuity of the higher resistance basalt layer, starting at about 2,400-ft distance along the line. At approximately the same location of this change in this layer we also see a deeper more resistive boundary extending nearly vertically in the data, between approximately 2,500 to 3,400 feet along the line. As an overall observation from the interpretation of the top of the SAG appears to have very little dip across the line, indicating this line is aligned along strike of the formation.

Figure 3-19 shows the ERT profile for ERT Line 3. This line is roughly oriented W to E and crosses Line 1 and 2 near the SAG1 boring. The line was collected starting near the property boundry to the west then extending near boring SAG1 and continuing east for a total length of over 6500-feet. Similar to Line 2 and just offset from the SAG1 boring there is an apparent trough of higher resistivity values dipping into the interpreted top of the SAG aquifer. Three of these troughs of higher resistivity values are observed near 2,200, 3,000, and 4,500 feet distances along this line. Again, these features could be related to out of plane effects or possible area of lower water content in the Chinle and top of the San Andres formations. Overall, the interpreted top of the SAG is slightly lower to the east and we see lower resistivity values within the SAG east of the boring SAG1.

4 REVISED CSM

The data generated during this SAG Investigation were used to revise the CSM. Based on this data, there four revisions to the CSM. They include:

4.1 Further Refine the Area Where the SAG was in Direct Contact with Alluvium;

The borings drilled during the SAG investigation and the surface geophysics were used to show the area where the SAG directly underlies the alluvium. The surface geophysics were used to show the type of bedrock in contact with the alluvium based on the surface geophysics. These data were used in conjunction with the boring data to show the area where the SAG was in direct contact with the alluvium. The results are shown on **Figure 4-1**. **Figure 4-1** also shows the SAG/Alluvium contact area and the newly revised SAG/Alluvium contact area.

4.2 Assess if the Alluvium is Dry Above the SAG Contact;

Five borings were drilled through the alluvium. Three borings (OB1, OB2, and OB3) were drilled through the alluvium to the top of bedrock for the installation of alluvial wells. Two borings (SAG1 and SAG2) were drilled through the alluvium to install a surface casing into bedrock and then the bedrock was cored through to 440 and 480 feet bgs. The boring logs (**Appendix A**) show the alluvium in each boring was saturated below the basalt. These data show the alluvium is not dry above the contact with the SAG in this portion of the alluvium.

The depth to groundwater was measured in each newly installed wells (OB1, OB2, and OB3) and nearby alluvial wells. These data were converted to water level elevations and contoured to show groundwater flow directions (**Figure 4-2**). These data show groundwater flows from north to south down the Rio San Jose, north of the SAG investigation area. These data also show the groundwater elevation near Well 846 is lower than surrounding wells, including wells to the south of Well 846. Groundwater elevations measured south of Well 846 are higher in elevation showing groundwater is flowing from south to north towards Well 846. These data show the area around Well 846 is likely a groundwater sink or groundwater is collecting in this area and migrating vertically through the alluvium to the underlying bedrock.

These data show a slight adjustment to the CSM whereas the past CSM characterized the Alluvium as dry and all of the groundwater migrating down the alluvium from the north was migrating vertically into the SAG. The CSM remains the same with respect to the alluvial groundwater entering the SAG; however, the CSM adjustment is that the alluvium remains saturated and the rate of groundwater movement is likely a function of the vertical hydraulic conductivity of the fine-grained material between the saturated coarse-grained alluvium and the underlying SAG.

4.3 Characterize the Physical and Water Transmitting Properties of the SAG;

Two borings (SAG1 and SAG2) were drilled 440 and 480 feet bgs into the SAG. A FLUTe™ transmissivity profile was completed in each well to characterize the physical properties of the SAG. A summary of the physical properties of the SAG are shown on **Figures 3-3 through 3-6**.

A summary of the physical and water transmitting properties is provided below:

Item	SAG1	SAG2
Transmissivity (gpd/ft)	9,000	5,700
Rock Thickness (ft)	240	214
Bulk Hydraulic Conductivity (ft/day)	5.0	3.7
Number of Fractures per Borehole	483	124
Aperture Maximum (microns)	504	780
Aperture Minimum (microns)	19	13
Aperture Mean (microns)	58	152
Fracture Porosity (percent)	0.05%	0.03%

FLUTeTM multi-port wells were installed in each boring. Groundwater levels were measured in port and were used to characterize the vertical movement of groundwater in the SAG. The data shows the vertical water levels and gradients vary. Groundwater level measurements show a downward head between all ports in SAG1. Groundwater level measurements show a downward head between the top three ports (164 to 265 feet bgs) in SAG2 and a small variable head between the bottom two ports.

4.4 Characterize the Mineralogy and Groundwater Geochemistry of the SAG.

Trace element concentrations (e.g., U, V, Se, Mo, B) were variable both within and across rock types although generally higher concentrations of U, V, and B occur in both the Chinle Shale and San Andres Limestone compared to the underlying Glorietta Sandstone. Molybdenum concentrations were reported as <2 mg/kg in all rock types, consistent with typical values for these rock types. Both U and Se concentrations were lower in the Chinle Shale relative to typical clays and shales, but those in the remaining samples were consistent with those for a carbonate-rich sandstone or carbonate rock. Vanadium concentration trends are consistent with those for typical rocks, but with overall lower concentrations.

The groundwater sample results show groundwater is a calcium-sulfate type water with higher proportions of calcium and sulfate relative to magnesium and bicarbonate with depth. Groundwater results also show more reducing with depth. The cation exchange capacity (CEC) of the Chinle Shale and Glorietta Sandstone samples are low (1.46 to 7.4 meq/100 g). Therefore, cation exchange would not be expected to exert significant controls on groundwater chemistry, nor expected to play a major role in attenuation of dissolved

constituents with transport through the aquifers. These data will be used with the solute transport modeling to better understand the potential movement of COPCs in the SAG.

5 REFERENCES

Arcadis, 2018, Evaluation of Water Quality in Regard to Site Background Standards at the Grants Reclamation Project, Prepared for Homestake Mining Company. September.

Brown and Caldwell, 2018, San Mateo Creek Basin and HMC Mill Hydrogeologic Site Conceptual Models, January 8th.

Cooley, M.E., J.W. Harshbarger, J.P. Akers, W.F. Hardt, and O.N. Hicks, 1969, Regional Hydrogeology of the Navajo and Hopi Indian Reservations, Arizona, New Mexico, and Utah, United States Geological Survey Professional Paper, 521-A, 68 pages.

Carl E. Keller, John A. Cherry, and Beth L. Parker, 2014, New Method for Continuous Transmissivity Profiling in Fractured Rock, Groundwater, Vol. 52, No. 3, Pp 352–367.

Dillinger, J.K. 1990. Geologic Map of the Grants 30' x 60' Quadrangle, West-Central New Mexico, United States Geological Survey Coal Investigations Map C-118-A.

DOE, 2014, Site Status Report: Groundwater Flow and Contaminant Transport in the Vicinity of the Bluewater, New Mexico, Disposal Site, U.S. Department of Energy, Office of Legacy Management, November.

Fleischer, M. and R.L Parker, 1967, Data of Geochemistry (Sixth Edition). Chapter D. Composition of the Earth's Crust, Geological Survey Professional Paper 440-D, United States Government Printing Office, Washington D.C.

Frenzel, P.F. 1992, Simulation of Ground-Water Flow in the San Andres-Glorieta Aquifer in the Acoma Embayment and Eastern Zuni Uplift, West-Central New Mexico, USGS Water-Resources Investigations Report 91-4099, Albuquerque, NM.

Gordon, E.D., 1961, Geology and Ground-Water Resources of the Grants-Bluewater Area, Valencia County, New Mexico. New Mexico State Engineer Technical Report 20.

HDR, 2020a, Draft Technical Impracticability Evaluation, Homestake Mining Company Superfund Site, Operable Unit #1 – Groundwater remediation, Cibola County New Mexico, November.

HDR, 2020b, Work Plan: Characterization of the San Andres-Glorieta Aquifer at Homestake Mining Company Superfund Site. November 11th.

HMC and Hydro-Engineering, 2010, Ground-Water Hydrology, Restoration and Monitoring at the Grants Reclamation Site for NMED DP-200, Prepared for the New Mexico Environment Department, February.

HMC and Hydro-Engineering, LLC (HE) 2020. 2019 Annual Monitoring Report / Performance Review for Homestake's Grants Project Pursuant to NRC License SUA-1471 and Discharge Plan DP-200. March.

HMC, 2019b, Semi-Annual Environmental Monitoring Report, Reporting Period July – December 2018, U.S. Nuclear Regulatory Commission License SUA-1471, State of New Mexico DP-200, February.

HMC, 2012, Grants Reclamation Project Updated Corrective Action Program (CAP), Prepared for the Nuclear Regulatory Commission, March.

Kelley, V.C., 1967, Tectonics of the Zuni-Defiance Region, New Mexico and Arizona. In: F.D. Trauger (ed.), Guidebook of Defiance-Zuni-Mt. Taylor Region, Arizona and New Mexico, Eighteenth Field Conference, October 19, 20, and 21 1967, Pp. 27-32.

Langman et al., 2012, Geologic framework, regional aquifer properties (1940s–2009), and spring, creek, and seep properties (2009–10) of the upper San Mateo Creek Basin near Mount Taylor, New Mexico, U.S. Geological Survey Scientific Investigations Report, 2012-5019, 96 p.

Novak-Szabo, T., Sipos, A.A., Shaw, S., Bertoni, D., Pozzebon, A., Grottoli, E., Sarti, G., Ciavola, P., Domokos G., and Jerolmack, D.J., 2018, Universal characteristics of particle shape evolution by bedload chipping, Science Advances, 4:1-11.

P. A. Witherspoon, J. S. Y. Wang, K. Iwail, and J. E. Gale, 1979, Validity of Cubic Law for Fluid Flow in a Deformable Rock Fracture, Department of Materials Science and Mineral Engineering, University of California, Berkeley and Lawrence Berkeley Laboratory University of California, Berkeley, California, October 1979.

U.S. Geological Survey (USGS), 1972, Disposal of Uranium-Mill Effluent by Well Injection in the Grants Area, Valencia County, New Mexico, Geological Survey Professional Paper 386-D. U.S. Government Printing Office, Washington, D.C.

U.S. Nuclear Regulatory Commission (USNRC), 2003, Standard Review Plan for the Review of a Reclamation Plan for Mill Tailings Sites Under Title II of the Uranium Mill Tailings Radiation Control Act of 1978, NUREG-1620, USNRC, Washington, DC.

Tables

Table 3-1 Sampling and Analysis Summary for Aquifer Materials Physical Properties

Formation	Borehole Number	Depth, feet	Sample No.	Specific Gravity, measured	Porosity	Water Content %, measured	Wet Density, g/cm³	Dry Density, g/cm³
Chinle	SAG-1	189	1	2.78	0.111	3.40	2.555	2.471
			2	2.78	0.115	3.20	2.539	2.460
	SAG-2	163	1	2.68	0.073	1.40	2.519	2.484
			2	2.68	0.079	1.40	2.502	2.467
San Andres	SAG-1	202	1	2.67	0.065	1.30	2.528	2.496
			2	2.67	0.066	1.40	2.528	2.493
		216	1	2.68	0.049	0.20	2.553	2.547
			2	2.68	0.048	0.20	2.556	2.551
		235.5	1	2.83	0.174	2.40	2.393	2.337
			2	2.83	0.217	2.20	2.263	2.215
		283	1	2.87	0.343	10.30	2.080	1.886
			2	2.87	0.313	13.60	2.240	1.972
	SAG-2	194	1	2.72	0.045	0.80	2.619	2.598
			2	2.72	0.054	1.00	2.600	2.574
		215	1	2.68	0.037	0.20	2.585	2.580
			2	2.68	0.043	1.00	2.590	2.565
		244	1	2.87	0.239	6.70	2.331	2.185
			2	2.87	0.225	7.60	2.394	2.225
		283	1	2.86	0.264	8.40	2.283	2.106
			2	2.86	0.286	10.40	2.255	2.043
		310	1	2.86	0.197	5.50	2.424	2.298
			2	2.86	0.194	4.60	2.410	2.304
		354	1	2.88	0.210	6.20	2.417	2.276
			2	2.88	0.214	6.40	2.407	2.263
Glorieta	SAG-1	318	1	2.65	0.139	3.80	2.367	2.280
			2	2.65	0.143	2.80	2.335	2.271
		354.5	1	2.65	0.126	3.10	2.389	2.317
			2	2.65	0.140	3.40	2.356	2.278
		402	1	2.68	0.146	4.20	2.386	2.289
			2	2.68	0.136	3.00	2.384	2.315
		426	1	2.66	0.116	1.80	2.394	2.352
			2	2.66	0.120	1.30	2.370	2.340
		464	1	2.68	0.117	1.70	2.405	2.365
			2	2.68	0.118	2.00	2.411	2.363
	SAG-2	396	1	2.66	0.157	3.70	2.324	2.241
			2	2.66	0.163	4.00	2.315	2.226
		439.5	1	2.70	0.120	2.00	2.424	2.376
			2	2.70	0.114	2.40	2.450	2.392
		463	1	2.69	0.143	3.00	2.375	2.306
			2	2.69	0.141	3.50	2.392	2.311

Two trials were performed per core specimen.

Water contents determined from tested specimens.

Density and porosity determinations of irregular shape samples - rock; ASTM D 7263 Method A.

Water Content %; ASTM D2216. Analysis by Golder Associates Ltd. Mississauga ON, Canada.

Table 3-2 FLUTe™ multi-level well depth to water measurements

Multiport Well Port	Port Interval	Feb. 18, 2021	Feb. 22, 2021
SAG1: Port 1	258-263	129.44	128.2
SAG1: Port 2	310-315	129.2	128.33
SAG1: Port 3	362-367	129.13	128.37
SAG1: Port 4	392-397	129.29	128.46
SAG1: Port 5	415-420	129.37	128.57
SAG2: Port 1	164-169	99.17	99.07
SAG2: Port 2	205-210	98.85	125.57
SAG2: Port 3	260-265	123.41	132.71
SAG2: Port 4	315-320	132.66	132.61
SAG2: Port 5	370-375	132.55	132.66

.

Table 3-3 Summary of Geochemical and Mineralogical Characterization Methods.

Parameter	Method	Supporting Detail & Objectives
Bulk Plus Clay Mineralogy[1]	X-ray Diffraction	Rapid and semi-quantitative assessment of a wide variety of crystalline mineral constituents to identify the predominant mineral assemblage.
Optical Mineralogy [1]	Petrographic Analysis	Non-destructive technique utilizing thin sections to identify crystalline and amorphous substances within the native textural framework. Provides high spatial resolution of trace minerals to supplement XRD results.
Total Metals[2]	EPA M3050B with M6020B	Provides baseline COC concentrations and quantitative elemental composition of the aquifer materials to complement mineralogical results.
Sulfur Forms[2]	EPA 600/2-78-054 3.2.4 (Sobek)	Determines various forms of sulfur (total-S, sulfate-S, sulfide-S, organic-S) through selective chemical removal of non-sulfide and/or targeted sulfide minerals followed by IR sulfur analysis.
Total Carbonate as $CaCO_3$[2]	ASA No. 9 29-2,2,4	Supplements the total metals analysis to provide quantitative measurement of the mineral carbonate component (requires analysis of total C and total organic C).
Total Organic Carbon[2]	ASA No. 9 29-2,2,4	Organic C may be present as an impurity in geologic materials and in association with trace elements and can create reducing conditions in an aquifer.
Cation Exchange Capacity[2]	USDA No. 60 (19)	Measures the total capacity for retention of positively-charged ions by clay minerals.

[1]DCM Science Laboratory, Inc. (Wheat Ridge, CO). [2]ACZ Laboratories, Inc. (Steamboat Springs, CO). Total metals include Al, B, Ba, Ca, Fe, Mg, Na, K, Li, Mn, Mo, P, Se, Si, Sr, Ti, U, V.

.

Table 3-4 Field Lithologic Descriptions for Selected Intervals.

Formation	Boring	Depth (ft bgs)	Field Lithologic Description
Chinle Shale	SAG-1	189-190	SILTSTONE: silt; very thinly bedded; reddish brown (2.5yr 4/3); slightly weathered; moderately soft; moderately fractured to intensely fractured; ~20° dips, trace vertical fractures; spacing: 3-6"; open; clean to very thin infilling; moderately weathered to intensely weathered fracturing; slightly rough. Sample collected from 189-190 ft.
	SAG-2	163-164	SILTSTONE: dark reddish gray (10r 4/1); fresh; moderately soft; slightly fractured; little to no dip; tight to slightly open; clean infilling; not healed; stepped. Sample collected from 163-164 ft.
San Andres LS	SAG-1	235.5-236.5	LIMESTONE: fine sand; variegated, very pale brown (10yr 7/3), white (10yr 8/1), light brownish gray (10yr 6/2); moderately weathered to intensely weathered; intensely fractured; wide; not healed; rough. Sample collected from 235.5-236.5 ft.
		283-284	DOLOSTONE: white; moderately weathered; moderately fractured; ~20° dips; tight; very thin infilling; infilling: calcite; not healed; bivalve fossils. Sample collected from 283-284 ft.
	SAG-2	215-216	LIMESTONE: gray; slightly weathered; moderately soft; intensely fractured; little to no dip; slightly open; clean infilling; rough. Sample collected from 215-216 ft.
		244-245	DOLOSTONE: very pale brown (10yr 8/2); moderately weathered; moderately hard; intensely fractured; mostly no dip; moderately open to open; clean to very thin infilling; not healed; moderately rough. Sample collected from 244-245 ft.
Glorieta SS	SAG-1	426-427	SANDSTONE: fine sand; laminated; very pale brown (10yr 7/4); moderately weathered; intensely fractured; horizontal and 45° dips, vertical fractures; clean infilling; not healed; rough; crossbedding. Sample collected from 426-427 ft.
		464-465	SANDSTONE: fine sand; laminated; light bluish gray (10b 8/1); moderately weathered; intensely fractured; horizontal and 45° dips, vertical fractures; clean infilling; not healed; rough. Sample collected from 464-465 ft.
	SAG-2	439.5-440.5	SANDSTONE: fine sand; thinly bedded to very thinly bedded; gray (N6); slightly weathered; hard; slightly fractured; little to no dip; tight; clean infilling; fresh fracturing; not healed; slightly rough. Sample collected from 439.5-440.5 ft.
		463-464	SANDSTONE: fine sand; thinly bedded to very thinly bedded; white (5yr 8/1); slightly weathered; hard; moderately fractured; no vertical fractures; tight; clean infilling; fresh fracturing; partly healed; slightly rough. Sample collected from 463-464 ft.

Table 3-5 Sampling and Analysis Summary for the Aquifer Materials Characterization[1].

Formation	Boring	Depth (ft bgs)	XRD Analysis	Optical Mineralogy	Total Metals	Sulfur Forms	Total, Inorganic & Organic Carbon	CEC
Chinle Shale	SAG-1	189-190	----	----	X	X	X	X
	SAG-2	163-164	----	----	X	X	X	X
San Andres LS	SAG-1	235.5-236.5	X	X	X	X	X	----
		283-284	----	----	X	X	X	----
	SAG-2	215-216	----	----	X	X	X	----
		244-245	X	----	X	X	X	----
Glorieta SS	SAG-1	426-427	----	----	X	X	X	X
		464-465	X	X	X	X	X	X
	SAG-2	439.5-440.5	X	----	X	X	X	X
		463-464	----	----	X	X	X	X

[1] Detailed methods descriptions are provided in Table 3.4.1.

.

Table 3-6 XRD Mineralogy Results (% By Weight) for the SALS and GSS Samples.

Boring	SAG-1	SAG-2	SAG-1	SAG-2
Formation	**San Andres LS**	**San Andres LS**	**Glorieta SS**	**Glorieta SS**
Lithology	**Limestone**	**Dolostone**	**Sandstone**	**Sandstone**
Interval (ft)	**235.5-236.5**	**244-245**	**464-465**	**439.5-440.5**
Sample ID	**SAG1-SALS-235.5-236.5**	**SAG2-SALS-244-245**	**SAG1-GSS-464-465**	**SAG2-GSS-439.5-440.5**
ACZ ID	**L63831-02**	**L63799-03**	**L63831-05**	**L63799-04**
Calcite	79	<2[1]	6	3
Dolomite	18	97	10	3
Illite	-----	-----	<2[1]	<2[1]
Kaolinite	-----	-----	12	4
K-Feldspar	-----	-----	8	6
Quartz	1	1	62	82
Pyrite	-----	-----	-----	<2[1]
Unaccounted	<5	<5	-----	<5

[1] May be present.

.

Table 3-7 Thin Section Optical Mineralogy Results.

Boring	**SAG-1**	**SAG-1**
Formation	**San Andres LS**	**Glorieta SS**
Lithology	**Limestone**	**Sandstone**
Interval (ft)	**235.5-236.5**	**464-465**
Sample ID	**SAG1-SALS-235.5-236.5**	**SAG1-GSS-464-465**
ACZ ID	**L63831-02**	**L63831-05**
Major Mineralogy	Calcite – 81% Dolomite – 18% Quartz – 1%	Quartz – 63% Kaolinite – 12% Dolomite – 10% K-Spar – 8% Calcite – 6% Illite – 6%
Trace Mineralogy	Pyrite, Goethite/Hematite, Mn Oxide, Organic Material	Zircon, Rutile, Apatite, Pyrite, Tourmaline, Iron Oxide, Plagioclase
Petrographic Description	Tan colored limestone primarily containing fine to coarse grained sparry calcite with a grain size that varies from 1 µm to 250 µm. Intermixed with calcite is rhomb shaped grains of dolomite up to 50 µm. Quartz is present in low amounts and occurs as liberated angular fragments and small pockets of fibrous chalcedony up to 275 µm in size. Crosscutting larger fragments of sparry calcite are thin seams of dark brown organic material. The organics commonly carry small pyrite framboids up to 15 µm. Iron oxide is present in trace amounts and occurs as small masses and as pseudomorphs after pyrite. Iron oxide is sometimes seen with black opaque patches of Mn oxide.	Carbonate cemented sandstone primarily containing quartz as angular to well rounded grains with measurements that vary significantly from 1 µm up to 300 µm. Plagioclase and potassium feldspar are present in low amounts and occur as angular grains up to 150 µm. XRD indicates low levels of clay in the form of kaolinite and illite, however, clay is not discernible in thin section by light microscopy. Dolomite and calcite occur as fine liberated grains in the size range of 1 µm to 75 µm. Pyrite is present as a trace and occurs as liberated fragments and cubes up to 75 µm with no apparent oxidation. Accessory minerals include zircon, honey colored rutile, brown tourmaline, colorless apatite and iron oxide.

.

Table 3-8 Total Metals Concentrations for the Various Lithologies.

Boring	SAG-1	SAG-2	SAG-1	SAG-1	SAG-2	SAG-2	SAG-1	SAG-1	SAG-2	SAG-2
Formation	Chinle Shale	Chinle Shale	San Andres LS	San Andres LS	San Andres LS	San Andres LS	Glorieta SS	Glorieta SS	Glorieta SS	Glorieta SS
Lithology	Siltstone	Siltstone	Limestone	Dolostone	Limestone	Dolostone	Sandstone	Sandstone	Sandstone	Sandstone
Interval (ft)	189-190	163-164	235.5-236.5	283-284	215-216	244-245	426-427	464-465	439.5-440.5	463-464
Sample ID	SAG1-CS-189-190	SAG2-CS-163-164	SAG1-SALS-235.5-236.5	SAG1-SALS-283-284	SAG2-SALS-215-216	SAG2-SALS-244-245	SAG1-GSS-426-427	SAG1-GSS-464-465	SAG2-GSS-439.5-440.5	SAG2-GSS-463-464
ACZ ID	L63831-01	L63799-01	L63831-02	L63831-03	L63799-02	L63799-03	L63831-04	L63831-05	L63799-04	L63799-05
Aluminum (%)	1.8	0.498	0.0545	0.0119	0.248	0.046	0.256	0.639	0.298	0.418
Barium	191	130	101	38.7	53.7	22.9	288	95.2	60.7	1070
Boron	14.3	6.46	<20	<2	<2	<19.8	<2	<2	<2	<2
Calcium (%)	0.240	0.0592	35.5	13.9	9.81	21.9	2.72	2.70	1.24	1.25
Iron (%)	3.74	0.22	0.413	0.0934	0.4070	0.172	0.169	0.294	0.370	0.296
Lithium	24.1	1.66	5.68	2.33	1.56	4.35	<0.8	2.02	<0.8	1.1
Magnesium (%)	0.604	0.0479	2.64	8.07	0.042	12.6	0.0441	0.746	0.134	0.515
Manganese	187	57.7	561	168	264	406	63.3	181	62.8	99.5
Molybdenum	<2	<2	<2	<2	<2	<2	<2	<2	<2	<2
Phosphorus	642	<10	243	188	126	275	50.1	208	122	145
Potassium (%)	0.0512	0.197	0.0179	0.0028	0.0616	0.0197	0.0810	0.242	0.0981	0.153
Selenium	0.169	0.0632	0.421	0.277	0.133	0.102	<0.05	0.188	0.247	0.0975
Silicon	1,030	1,020	359	245	743	371	781	2,040	519	995
Sodium (%)	0.0112	0.00388	0.00987	0.0172	<0.002	0.0227	<0.002	0.00307	<0.002	0.00206
Strontium	32	10.4	128	63.9	27.7	73.1	13.8	16.7	9	30.8
Titanium	232	286	15.6	7.35	6.27	14.4	8.48	27.7	9.41	9.06
Uranium	0.449	0.819	0.52	0.675	1.01	2.51	0.125	0.26	1.16	0.173
Vanadium	14.6	20.5	12.5	3.14	3.27	12.7	1.72	4.55	1.82	3.23

.

Table 3-9 Selected Elemental Abundance for Various Rock Types[1].

Element	Clays & Shales	Shales	Sandstone	Carbonate Rocks
MAJOR ELEMENTS (weight %)				
Aluminum	10.45	8.0	2.5	0.42
Calcium	2.53	2.21	3.91	30.23
Iron	3.33	4.72	0.98	0.38
Magnesium	1.34	1.5	0.7	4.7
Potassium	2.28	2.66	1.07	0.27
Sodium	0.66	0.96	0.33	0.04
MINOR ELEMENTS (mg/kg)				
Uranium	3.2	3.7	0.45	2.2
Molybdenum	2	2.6	0.2	0.4
Selenium	0.6	0.6	0.05	0.08
Boron	100	100	35	20
Vanadium	130	130	20	20

[1] Fleischer and Parker, 1967.

.

Table 3-10 Carbon (%), Sulfur (%), and CEC Contents for the Various Lithologies.

Boring	SAG-1	SAG-2	SAG-1	SAG-1	SAG-2	SAG-2	SAG-1	SAG-1	SAG-2	SAG-2
Formation	**Chinle Shale**	**Chinle Shale**	**San Andres LS**	**San Andres LS**	**San Andres LS**	**San Andres LS**	**Glorieta SS**	**Glorieta SS**	**Glorieta SS**	**Glorieta SS**
Lithology	**Siltstone**	**Siltstone**	**Limestone**	**Dolostone**	**Limestone**	**Dolostone**	**Sandstone**	**Sandstone**	**Sandstone**	**Sandstone**
Interval (ft)	**189-190**	**163-164**	**235.5-236.5**	**283-284**	**215-216**	**244-245**	**426-427**	**464-465**	**439.5-440.5**	**463-464**
Sample ID	**SAG1-CS-189-190**	**SAG2-CS-163-164**	**SAG1-SALS-235.5-236.5**	**SAG1-SALS-283-284**	**SAG2-SALS-215-216**	**SAG2-SALS-244-245**	**SAG1-GSS-426-427**	**SAG1-GSS-464-465**	**SAG2-GSS-439.5-440.5**	**SAG2-GSS-463-464**
ACZ ID	**L63831-01**	**L63799-01**	**L63831-02**	**L63831-03**	**L63799-02**	**L63799-03**	**L63831-04**	**L63831-05**	**L63799-04**	**L63799-05**
Total Carbon	<0.1	<0.1	12.9	8.8	3.1	14.1	0.8	1.2	0.4	0.6
Total Inorganic Carbon	<0.1	<0.1	12.9	8.7	3.0	14.0	0.8	1	0.4	0.6
Total Organic Carbon	0.1	0.1	<0.1	0.1	0.1	0.1	<0.1	0.2	<0.1	<0.1
Total-Sulfur	<0.01	<0.01	0.03	0.01	0.37	0.02	0.01	0.08	0.37	0.13
Sulfide-Sulfur	<0.01	<0.01	<0.01	<0.01	0.28	<0.01	<0.01	0.07	0.20	0.09
Sulfate-Sulfur	<0.01	<0.01	0.03	0.01	0.07	0.02	0.01	0.01	0.17	0.04
CEC (meq/100g)	7.4	2.76	NM	NM	NM	NM	1.46	3.19	1.51	1.98

Table 3-11 Complete Water Quality Results from Wells SAG-1 and SAG-2 (February, 2021).

SAMPLE ID	SAG1-1	SAG1-2	SAG1-3	SAG1-4	SAG1-5	SAG2-1	SAG2-2	SAG2-3	SAG2-4	SAG2-5	Field Blank	0999	RPD
Depth (ft)	260.5	312.5	364.5	394.5	417.5	166.5	207.5	262.5	317.5	372.5	-------	-------	-------
Depth Below WT (ft)	132.5	184.5	236.5	266.5	289.5	35.5	76.5	131.5	186.5	241.5	-------	-------	-------
Dissolved O_2 (mg/L)	0.15	0.12	0.16	0.11	0.11	2.79	2.2	0.08	0.07	0.14	-------	-------	-------
Eh (mV)	25.4	110.2	98.9	51.7	96.0	291.8	326.1	152.5	44.9	84.7	-------	-------	-------
Fe^{2+} (mg/L)	3.29	0.89	1.0	2.71	1.84	0.16	0.010	1.0	3.26	2.12	-------	-------	-------
EC (uS/cm)	1238	1390	1488	1817	2011	1220	1216	1228	1234	1351	-------	-------	-------
pH (s.u.)	7.43	7.59	7.63	7.48	7.44	7.21	7.26	7.25	7.56	7.49	-------	-------	-------
Temperature (°C)	13.0	13.7	13.8	12.7	12.9	13.1	12.4	12.4	12.9	13.2	-------	-------	-------
Calcium (mg/L)	135	144	170	332	402	176	172	176	153	195	<0.1	175	0.57
Iron (mg/L)	14.9	0.924	1.03	3.46	1.94	<0.06	<0.06	1.2	3.8	2.7	<0.06	<0.06	-------
Magnesium (mg/L)	45.5	47.4	50.5	61.3	63.1	46	45.6	46.5	48.2	48.6	<0.2	45.7	0.65
Manganese (mg/L)	0.821	4.33	7.61	2.13	3.66	0.046	0.053	0.837	1.91	4.48	<0.01	0.045	2.20
Molybdenum (mg/L)	0.0409	0.0292	0.0351	0.00866	0.0112	0.00211	0.00276	0.0107	0.0175	0.0137	<0.0002	0.00194	8.40
Potassium (mg/L)	3.99	4.82	4.87	3.64	3.19	4.1	4.01	4.14	4.43	4.13	<0.2	4.07	0.73
Selenium (mg/L)	0.00023	0.00021	0.00037	0.0002	0.00018	0.00613	0.00582	0.00364	0.0001	0.00015	<0.0001	0.0063	2.74
Sodium (mg/L)	95.7	123	123	74.5	72.8	65.3	63.6	67.8	82.8	66.5	<0.2	64	2.01
Uranium (mg/L)	0.00175	0.00703	0.00537	0.00201	0.00196	0.00705	0.00703	0.0079	0.00486	0.000582	<0.0001	0.00705	0.00
Vanadium (mg/L)	<0.0005	<0.0005	<0.0005	<0.0005	<0.0005	<0.0005	<0.0005	<0.0005	<0.0005	<0.0005	<0.0005	<0.0005	-------
Total Alkalinity (mg $CaCO_3$/L)	205	201	174	148	152	261	266	275	237	214	<2	267	2.27
Bicarbonate (mg $CaCO_3$/L)	205	201	174	148	152	261	266	275	237	214	<2	267	2.27
Dissolved Organic Carbon (mg/L)	24.2	9.4	11.8	7.1	12.7	2.2	3.2	32.1	12.5	7.3	<1	1.9	14.6
Chloride (mg/L)	72.6	94.3	91.4	40.3	40	54	55.6	56.7	61.7	55.6	<0.5	57.3	5.93
Hardness (mg CaCO3/L)	524	555	632	1080	1260	629	617	631	581	687	<0.2	625	0.64
Nitrate+Nitrite-N (mg/L)	<0.02	<0.02	<0.02	<0.02	<0.02	2.31	2.18	0.025	<0.02	<0.02	<0.02	2.35	1.72
Ammonia-N (mg/L)	0.259	0.739	0.579	0.159	0.191	<0.05	<0.05	0.099	0.786	0.216	<0.05	<0.05	-------
Total Dissolved Solids (mg/L)	860	1120	1140	1670	1960	978	984	970	930	1130	<20	988	1.02
Sulfate (mg/L)	399	461	629	1070	1220	408	410	411	436	593	<1	411	0.73
Sulfide (mg S/L)	<0.02	<0.02	<0.02	<0.02	0.026	<0.02	<0.02	<0.02	0.026	<0.02	<0.02	<0.02	-------
Radium-226 (pCi/L)	1 ±0.22	0.17 ±0.24	2.2 ±0.31	0.82 ±0.21	0.44 ±0.19	0.44 ±0.23	0.22 ±0.13	0.3 ±0.17	4.2 ±0.48	1.3	-0.01 ±0.11	0.36 ±0.11	20.0
Radium-228 (pCi/L)	0.33 ±1	0.87 ±0.86	0.62 ±1.1	0.41 ±0.89	-0.2 ±0.84	0.78 ±0.81	0.55 ±0.57	0.44 ±0.99	-0.25 ±0.9	0.67	-0.13 ±0.77	1.4 ±1.1	56.9
Radium-226+228 (pCi/l)	1.33	1.04	2.82	1.23	0.44	1.22	0.77	0.74	4.2	1.97	-------	1.76	36.2
Thorium-230 (pCi/L)	1.55 ±1.1	0.751 ±2.4	1.34 ±2.1	4.01 ±2.4	4.75 ±3.6	1.01 ±0.59	0.554 ±0.55	3.8 ±3.6	2.55 ±2.4	2.81	1.97 ±1.9	0.183 ±0.26	139

Figures

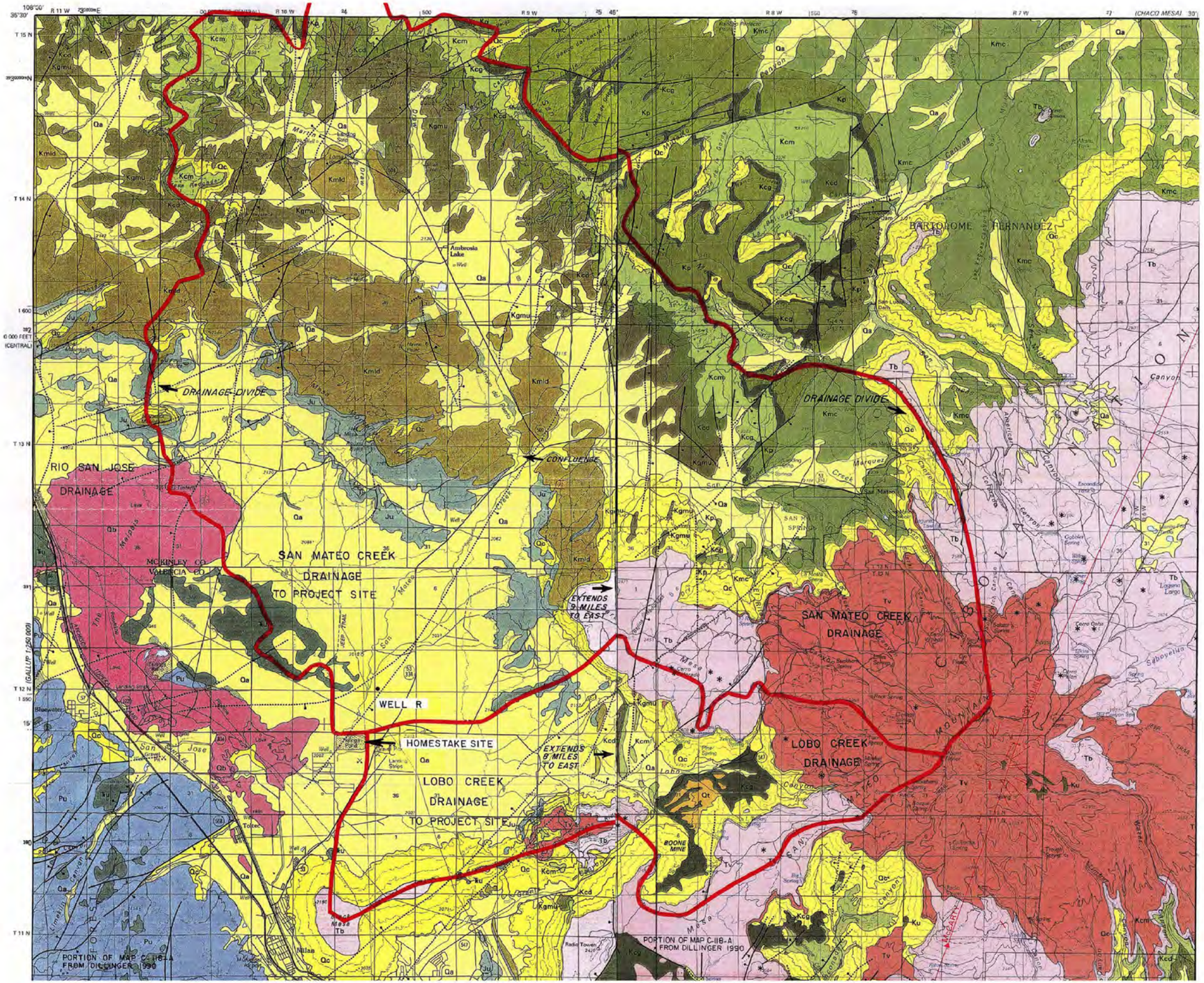

LEGENDS: Correlation of Map Units

Alluvium Colluvium and Terrace Gravel	Qa Qc Qt	Holocene and Pleistocene		QUATERNARY
Basalt Flows	Qb			QUATERNARY OR TERTIARY
	QTb			
	Tb	Pliocene		TERTIARY
Santa Fe Formation	Tv			
	Ts	Pliocene and Miocene		
	UNCONFORMITY			
Cleary Coal Member and Gibson Coal Member	Kmc Kmfc Kp Kcg	Upper Cretaceous		CRETACEOUS
Dilco Coal Member	Kcm			
Gallup Sandstone	Kcd Kg			
Mancos Shale	Kmgmu Kmdu			
Dakota Sandstone	Kdm Kmld			
	UNCONFORMITY			
Morrison Formation Eolian Sandstone Wanakah Formation Entrada Sandstone	Ju			JURASSIC
	UNCONFORMITY			
Chinle Formation Moenkopi Formation	Tu			TRIASSIC
	UNCONFORMITY			
San Andres Limestone Glorieta Sandstone Yeso Formation Abo Formation	Pu	Lower Permian		PERMIAN
	UNCONFORMITY			
Precambrian Granite	pCg			PRECAMBRIAN

Source:
Dillinger, J.K., 1990, Geologic map of the Grants 30' x 60' quadrangle, west-central New Mexico: U.S. Geological Survey, Coal Investigation Map C-118-A, scale 1:100,000.

Adopted from:
Grants Reclamation Project Updated Corrective Action Program, HMC, 2012

HOMESTAKE

BEDROCK GEOLOGY
OVERVIEW MAP
FIGURE 2-1

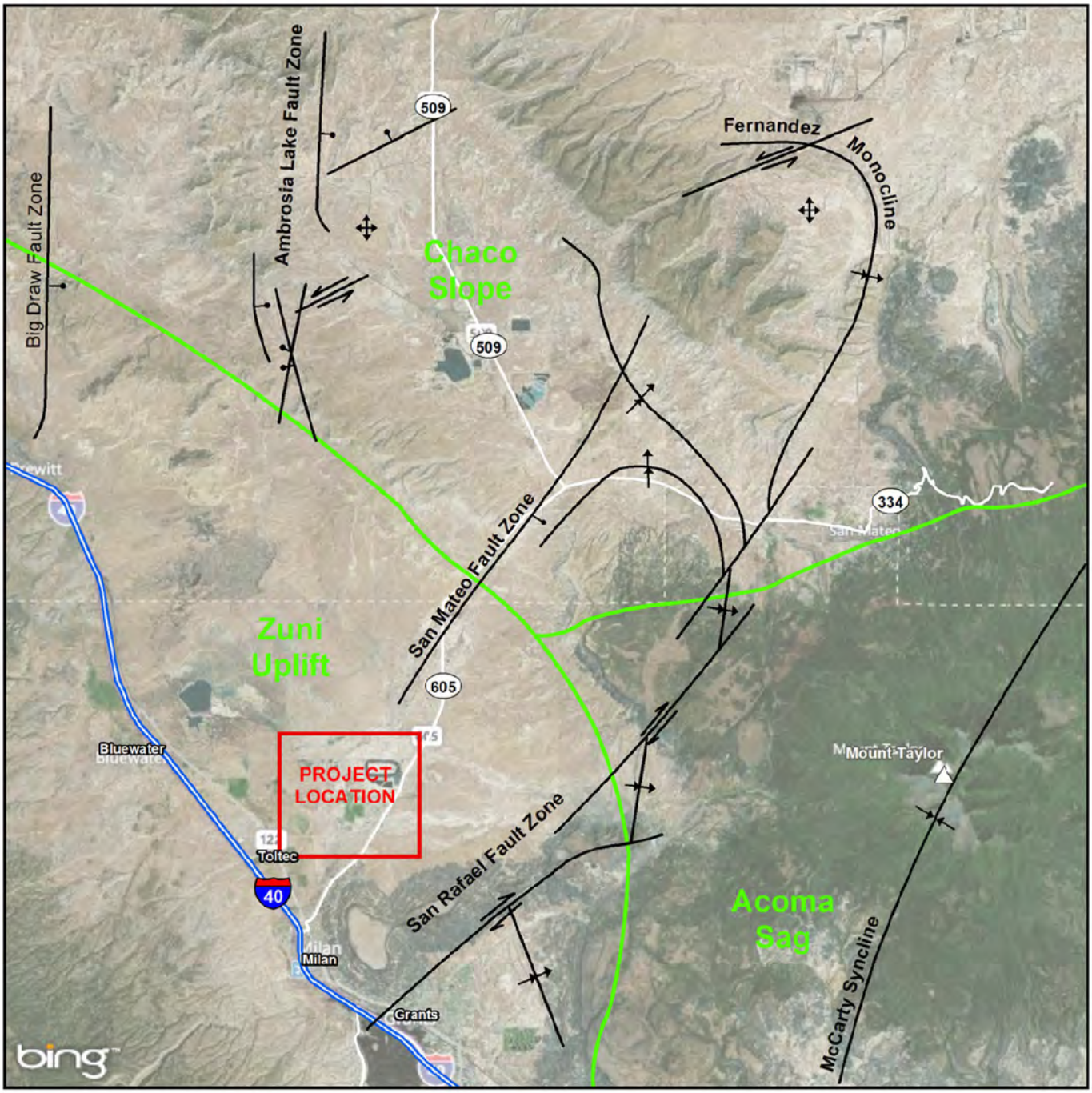

LEGEND:

- Normal Fault
- Strike-Slip (Left-Lateral)
- Strike-Slip (Right-Lateral)
- Monocline
- Syncline
- Dome
- Structural Feature Boundary

N

0 3 6 Miles

Aerial: Bing Maps Hybrid - © 2010 Microsoft Corporation and its data suppliers

Source: Grants Reclamation Project Updated Corrective Action Program, HMC, 2012

Adopted from: Grants Reclamation Project Updated Corrective Action Program, HMC, 2012

PATH: Z:\PROJECTS\PROPOSALS\10\071518_BARRICK_RIF_HOMESTAKEMININGMAP_DOCS\FINAL\SAG_CHAR_REPORT\BARRICK_FIG2_2_PORTRAIT8X11.MXD - USER: HROSADO - DATE: 4/15/2021

HOMESTAKE

REGIONAL STRUCTURAL FEATURES

FIGURE 2-2

COUNTY ROAD 63

COUNTY ROAD 25

LARGE - TAILINGS-PILE

HMC OFFICE

LINED EVAP POND NO. 2

EVAPORATION POND

SMALL TAILINGS

100 ACRE CENTER PIVOT

PLEASANT-VALLEY ESTATES

VALLE VERDE

MURRAY-ACRES

FLOOD IRRIGATION 120 AC FLOOD

BROADVIEW ACRES

FELICE-ACRES

150 ACRE CENTER PIVOT

174 ACRE CENTER PIVOT AND FLOOD IRRIGATION

RALPH CARD ROAD

UNDERBIRD LANE

HWY-122

RAILROAD

HWY-605

19,20 3029

20,21 2928

21,22 2827

22,23 2726

23,24 2625

30,29 3132

29,28 3233

28,27 3334

27,26 3435

26,25 3536

32,33 0504

33,34 4 3

N

LEGEND

- WATER-LEVEL ELEV. CONTOUR
- DATA
- Alluvial Aquifer
- Bedrock High

Source: 2018 Annual Monitoring Report/Performance Review, for Homestake's Grants Project Pursuant to NRC License, SUA1471 and Discharge Plan DP-200, HMC 2019

0 1,800 Feet

ALLUVIAL AQUIFER WATER LEVEL ELEVATIONS

FIGURE 2-3

COUNTY ROAD 63

COUNTY ROAD 25

LARGE - TAILINGS-PILE

HMC OFFICE

LINED EVAP POND NO. 2

COLLECTION POND

SMALL TAILINGS PILE

100 ACRE CENTER PIVOT

PLEASANT-VALLEY ESTATES

MURRAY-ACRES

VALLE VERDE

FLOOD IRRIGATION 120 AC FLOOD

BROADVIEW ACRES

FELICE-ACRES

150 ACRE CENTER PIVOT

174 ACRE CENTER PIVOT AND FLOOD IRRIGATION

THUNDERBIRD LANE

RALPH CARD ROAD

HWY-122

HWY-605

RAILROAD

N

LEGEND

PermeabilityFt_Day

S4 Location and Value

Source: 2018 Annual Monitoring Report/Performance Review, for Homestake's Grants Project Pursuant to NRC License, SUA1471 and Discharge Plan DP-200, HMC 2019

0 1,500 Feet

HYDRAULIC CONDUCTIVITY FOR THE ALLUVIAL AQUIFER, FT/DAY

FIGURE 2-4

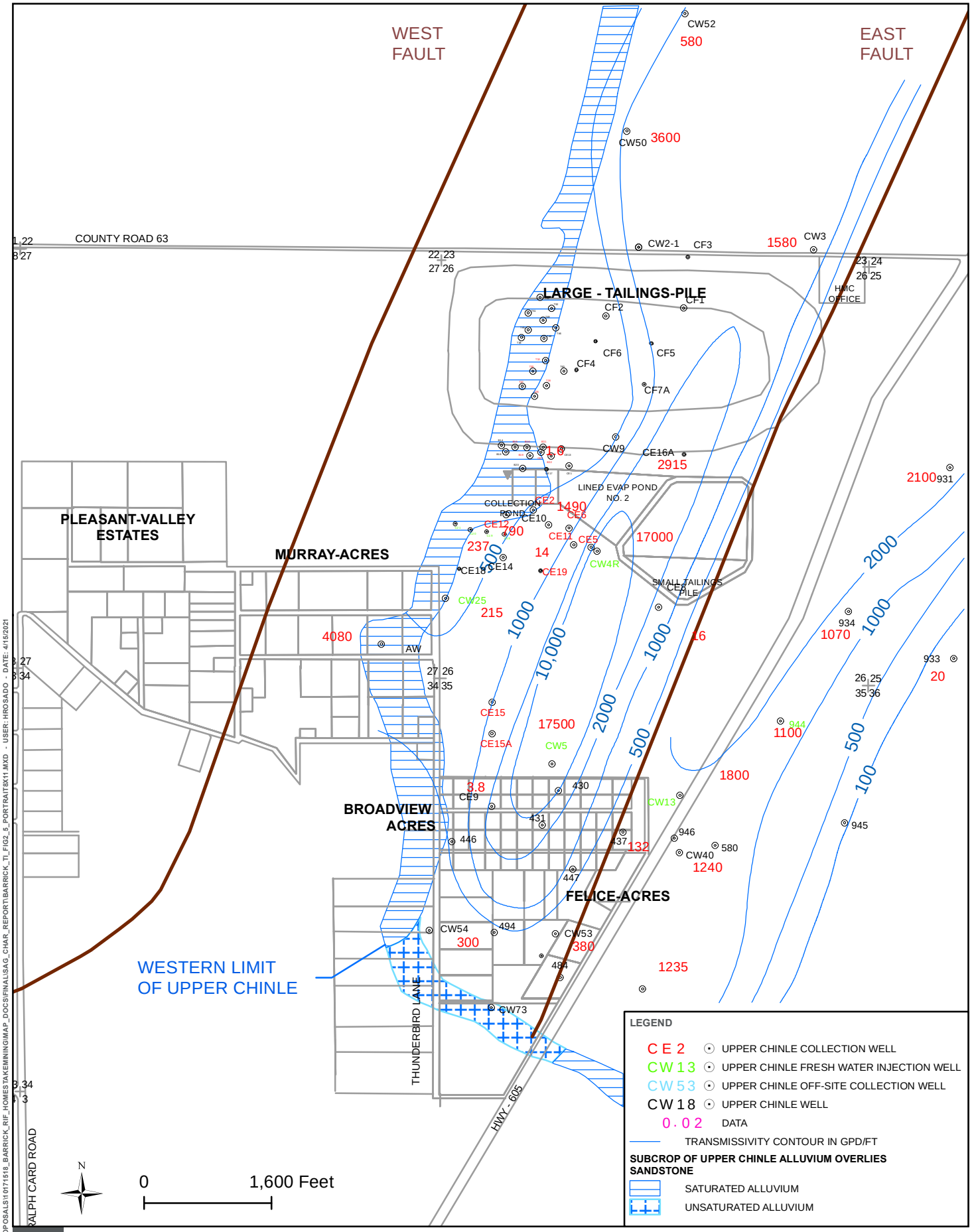

PATH: Z:\PROJECTS\PROPOSALS\10171518_BARRICK_RIF_HOMESTAKEMININGSMAP_DOCS\FINAL\SAG_CHAR_REPORT\BARRICK_TI_FIG2_5_PORTRAIT8X11.MXD - USER: HROSADO - DATE: 4/15/2021

UPPER CHINLE AQUIFER TRANSMISSIVITY

Source: 2018 Annual Monitoring Report/Performance Review, for Homestake's Grants Project Pursuant to NRC License, SUA1471 and Discharge Plan DP-200, HMC 2019

FIGURE 2-5

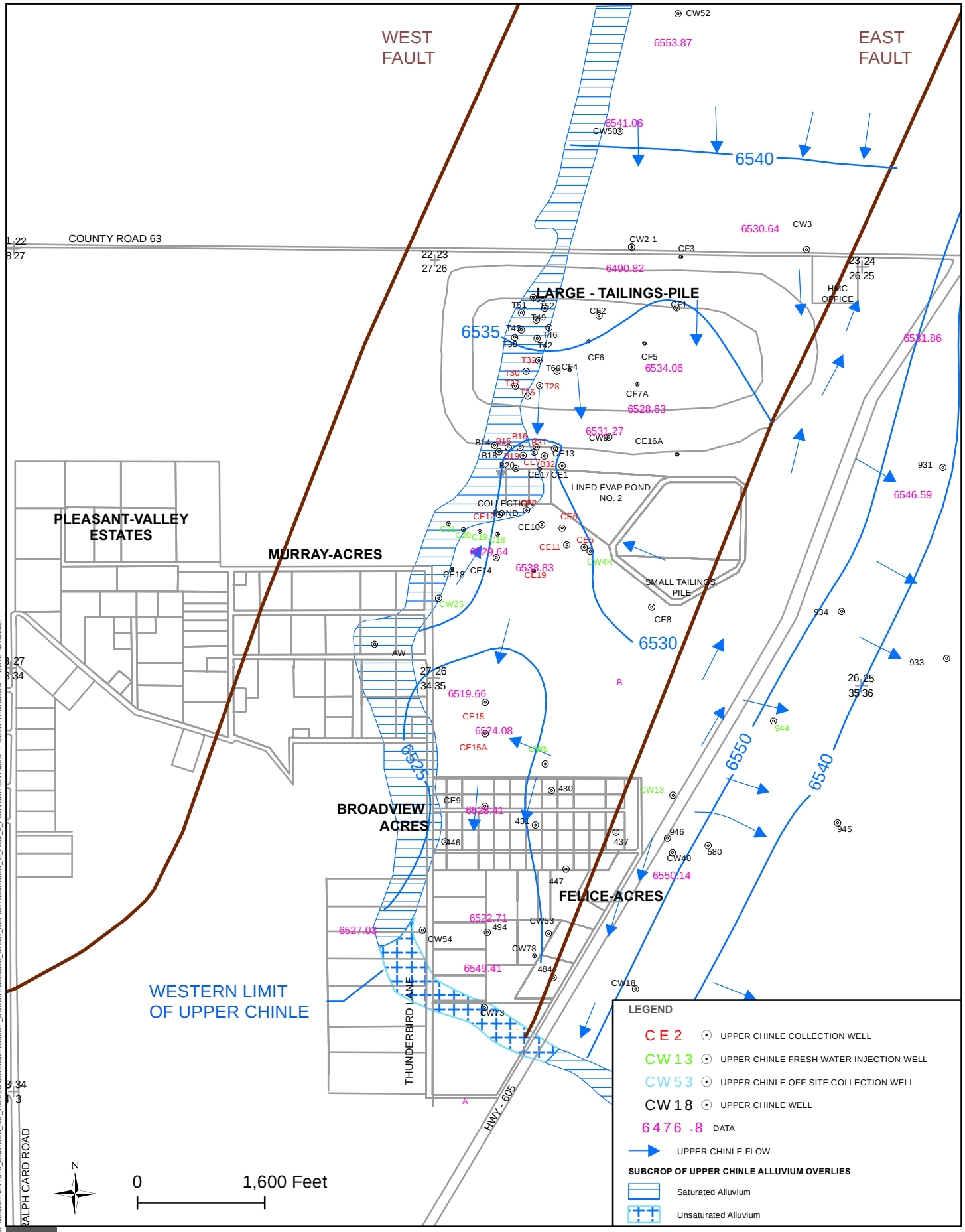

PATH: Z:\PROJECTS\PROPOSALS\10171518_BARRICK_RIF_HOMESTAKEMININGSMAP_DOCS\FINAL\SAG_CHAR_REPORT\BARRICK_TI_FIG2_6_PORTRAIT8X11.MXD - USER: HROSADO - DATE: 4/15/2021

UPPER CHINLE WATER ELEVATION & FLOW DIRECTION

FALL 2019

FIGURE 2-6

Source: 2018 Annual Monitoring Report/Performance Review, for Homestake's Grants Project Pursuant to NRC License, SUA1471 and Discharge Plan DP-200, HMC 2019

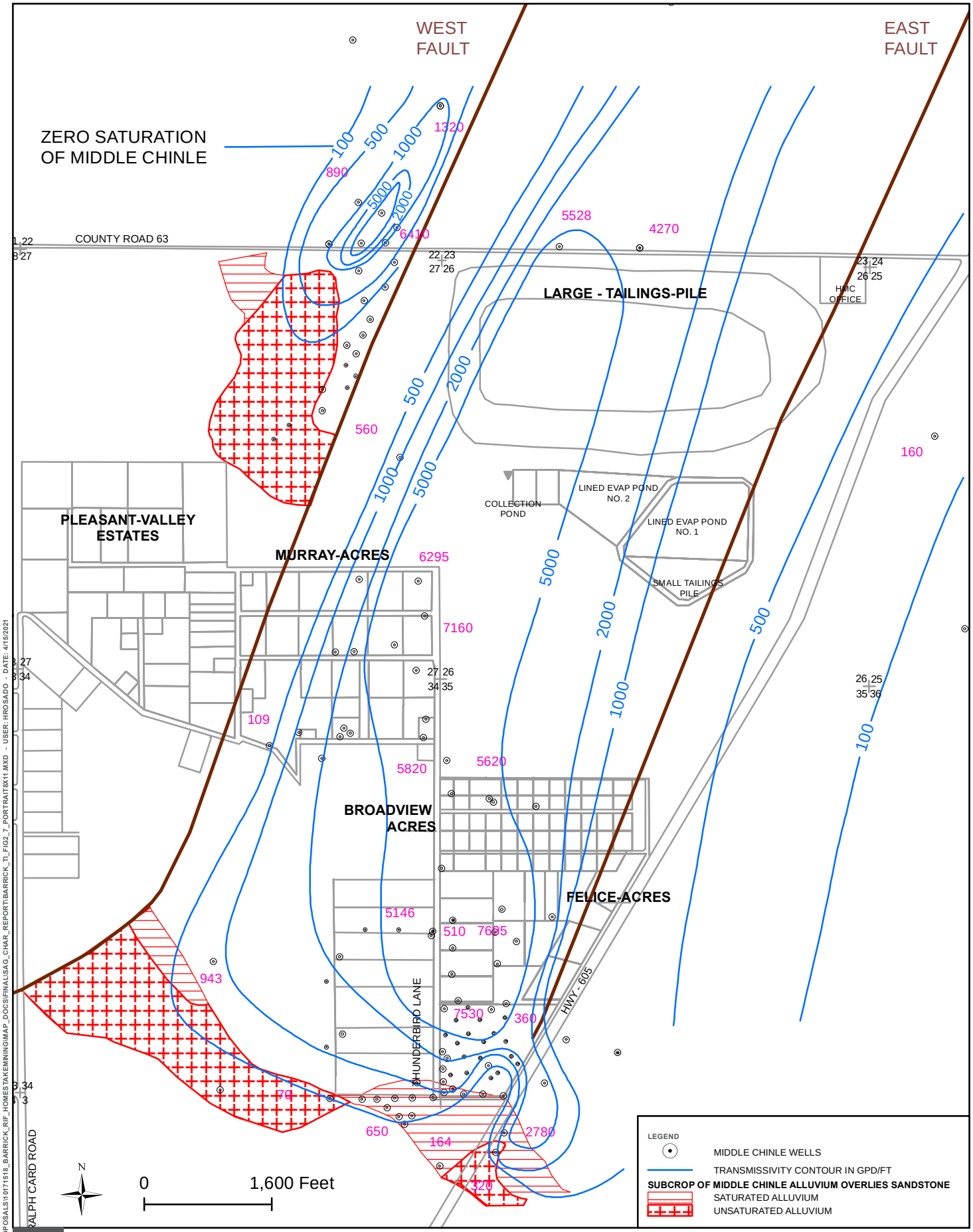

PATH: Z:\PROJECTS\PROPOSALS\10171518_BARRICK_RIF_HOMESTAKEMININGSMAP_DOCS\FINALISAG_CHAR_REPORT\BARRICK_TI_FIG2_7_PORTRAIT8X11.MXD - USER: HROSADO - DATE: 4/15/2021

HOMESTAKE

Source: 2018 Annual Monitoring Report/Performance Review, for Homestake's Grants Project Pursuant to NRC License, SUA1471 and Discharge Plan DP-200, HMC 2019

MIDDLE CHINLE TRANSMISSIVITY

FIGURE 2-7

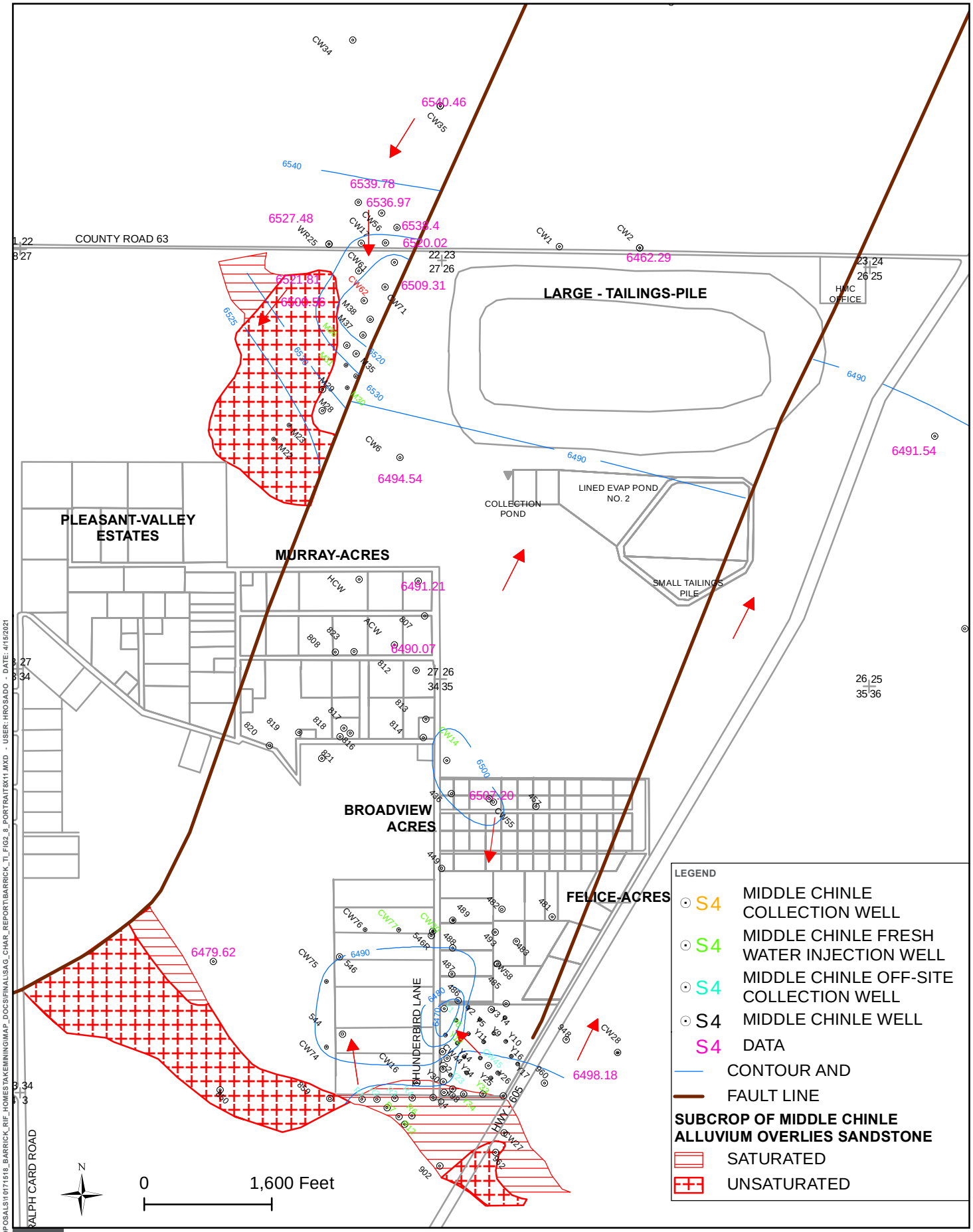

MIDDLE CHINLE WATER ELEVATION AND FLOW DIRECTION MAP

Source: 2018 Annual Monitoring Report/Performance Review, for Homestake's Grants Project Pursuant to NRC License, SUA1471 and Discharge Plan DP-200, HMC 2019

FALLS 2019

FIGURE 2-8

PATH: Z:\PROJECTS\PROPOSALS\1\0171518_BARRICK_RIF_HOMESTAKEMININGMAP_DOCS\FINALS\SAG_CHAR_REPORT\BARRICK_TI_FIG2_8_PORTRAIT8X11.MXD - USER: HROSADO - DATE: 4/15/2021

WEST FAULT

EAST FAULT

COUNTY ROAD 63

COUNTY ROAD 25

19 20 / 30 29

20 21 / 29 28

21 22 / 28 27

22 23 / 27 26

23 24 / 26 25

30 29 / 31 32

29 28 / 32 33

28 27 / 33 34

27 26 / 34 35

26 25 / 35 36

32 33 / 05 04

33 34 / 4 3

HMC OFFICE

LARGE - TAILINGS-PILE

COLLECTION POND

LINED EVAP POND NO. 2

SMALL TAILINGS PILE

PLEASANT-VALLEY ESTATES

MURRAY-ACRES

VALLE VERDE

BROADVIEW ACRES

FELICE-ACRES

THUNDERBIRD LANE

RALPH CARD ROAD

RAILROAD

HWY-122

HWY-605

100

20

21

840

104

50

655

1000

14500

32

1590

20

100

1000

1170

CW29

131

CW26

2300

1200

CW41

238

853

N

LEGEND

- Lower Chinle Wells
- Transmissivity Contour in GPD/FT
- Fault Line
- Saturated Alluvium
- Unsaturated Alluvium
- Lower Chinle

HOMESTAKE

Source: 2018 Annual Monitoring Report/Performance Review, for Homestake's Grants Project Pursuant to NRC License, SUA1471 and Discharge Plan DP-200, HMC 2019

0 1,500 Feet

LOWER CHINLE TRANSMISIVITY

FIGURE 2-9

WEST FAULT

EAST FAULT

COUNTY ROAD 63

COUNTY ROAD 25

19 20 / 30 29

20 21 / 29 28

21 22 / 28 27

22 23 / 27 26

23 24 / 26 25

30 29 / 31 32

29 28 / 32 33

26 25 / 35 36

27 26 / 34 35

32 33 / 05 04

33 34 / 4 3

HMC OFFICE

LARGE - TAILINGS-PILE

COLLECTION POND

LINED EVAP POND NO. 2

SMALL TAILINGS PILE

PLEASANT-VALLEY ESTATES

VALLE VERDE

MURRAY-ACRES

BROADVIEW ACRES

FELICE-ACRES

THUNDERBIRD LANE

RALPH CARR ROAD

RAILROAD

HWY-122

HWY-605

SOS MAP, SEE FIGURE 7.2-1A

1520'

CW32 6419.64

CW33 6468.75

CW31 6474.74

CW36 6474.05

CW38

CW43 6480.08

CW39

CW37 6488.87

CW29

CW26

CW41

536R

900

837

530

832

988

990

908

954

853

903

6465

6470

6475

6480

6485

6490

6450

6460

6455

6460

6465

6470

6475

6480

6470

LEGEND

- Lower Chinle Wells
- S4 Data
- Lower Chinle Flow
- Contour
- Fault Line
- Saturated Alluvium
- Unsaturated Alluvium

N

0 1,500 Feet

Source: 2018 Annual Monitoring Report/Performance Review, for Homestake's Grants Project Pursuant to NRC License, SUA1471 and Discharge Plan DP-200, HMC 2019

LOWER CHINLE WATER ELEVATION AND FLOW DIRECTION

FALL 2019

FIGURE 2-10

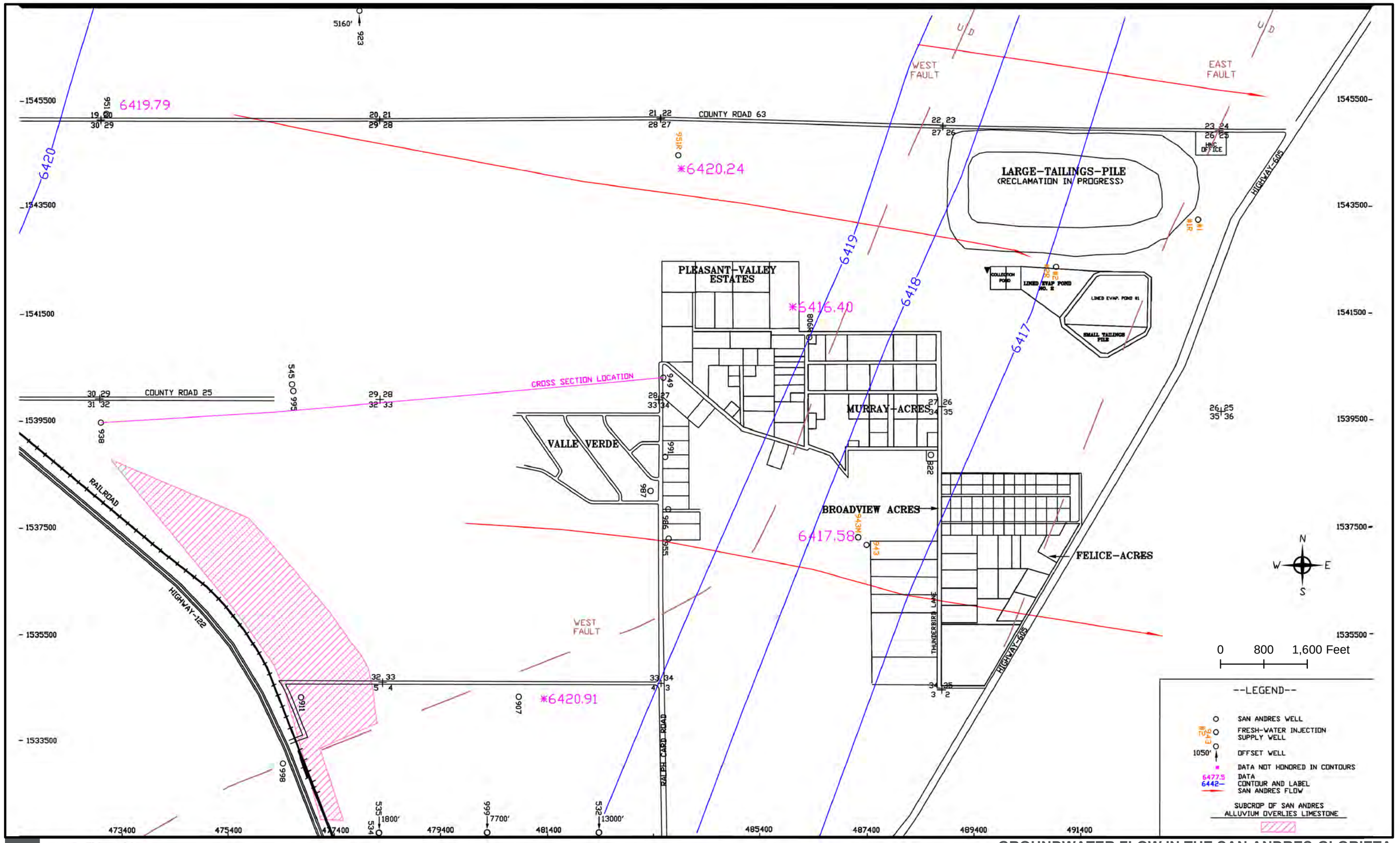

Source: 2018 Annual Monitoring Report/Performance Review, for Homestake's Grants Project Pursuant to NRC License, SUA1471 and Discharge Plan DP-200, HMC 2019

GROUNDWATER FLOW IN THE SAN ANDRES-GLORIETA

FALL 2019

FIGURE 2-11

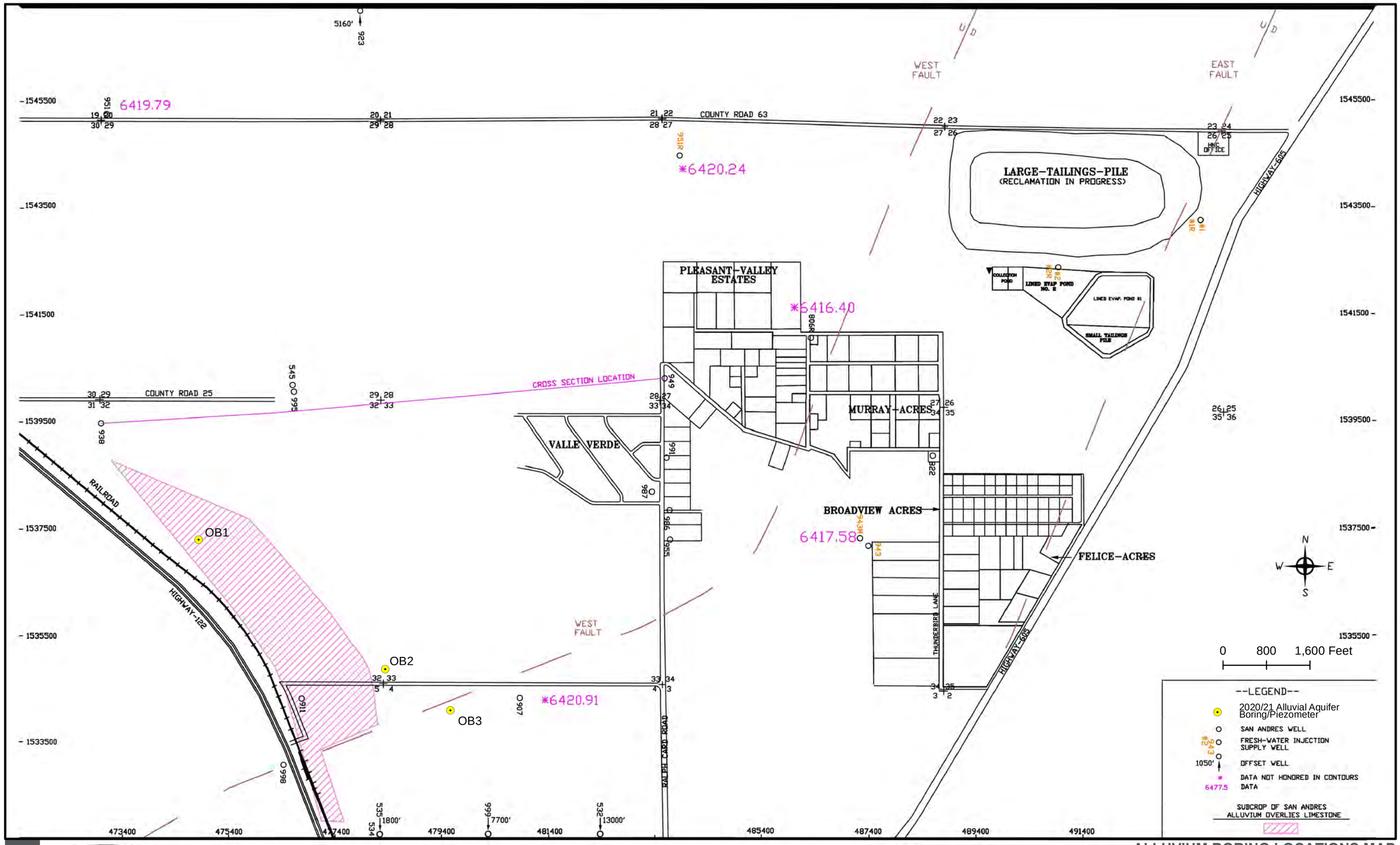

ALLUVIUM BORING LOCATIONS MAP

Source: 2018 Annual Monitoring Report/Performance Review, for Homestake's Grants Project Pursuant to NRC License, SUA1471 and Discharge Plan DP-200, HMC 2019

FIGURE 3-1

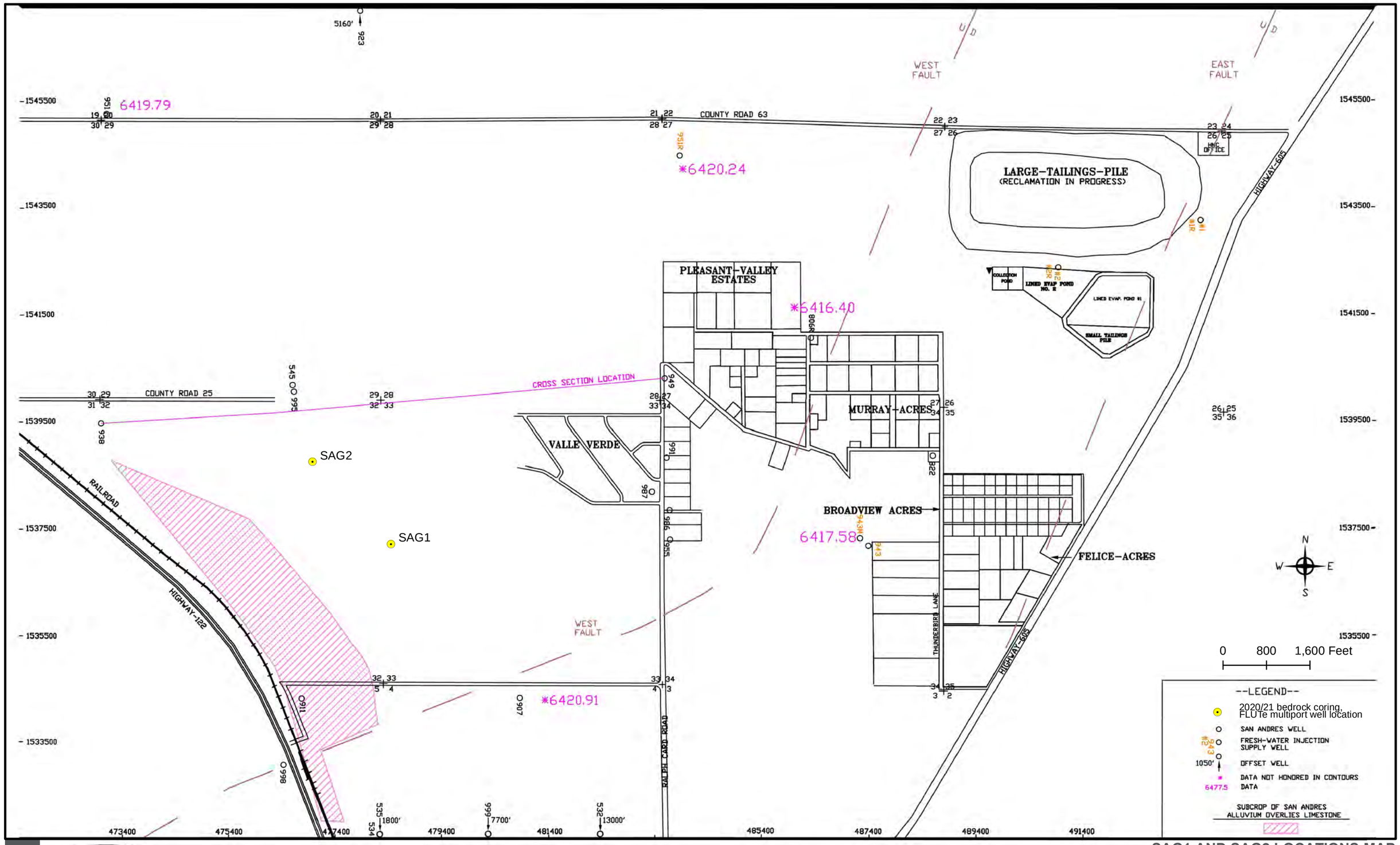

Source: 2018 Annual Monitoring Report/Performance Review, for Homestake's Grants Project Pursuant to NRC License, SUA1471 and Discharge Plan DP-200, HMC 2019

SAG1 AND SAG2 LOCATIONS MAP

FIGURE 3-2

Results of FLUTe profiling for hole
no. SAG1 for *HDR, Millan, NM*

Water Table depth	127	ft BGS
Hole depth	484.166	ft BGS
liner length	500	ft BGS
casing depth	260	ft BGS
hole diameter	5	inches
liner diameter	5.6	inches
date of measurement	2/1/2021	

The profile was measured to a depth of 482.46 ft
The flow rate per unit driving pressure was 0.036604 **gal/min/ft**
The transmissivity for the remainder of the hole is: 0.0757977 cm sq./sec
The average conductivity for the remaining 1.70585 ft of the hole is 1.46E-03 cm/sec
Total borehole transmissivity is 13.00448 cm2/s

Comments:

may be some inflow at 300 ft and 273 ft.
Extremely high flow at bottom portion of hole reduces the resolution to 360 ft
and the water addition rate exceeds the current pump capacity.
liner average velocity to 420 ft at 60 ft/min. (~60 gal/min.)

Contact for questions about data or reduction
carl Keller
Phone: 505-455-1300

Note: the flow rate curve is the liner velocity multiplied by the borehole cross section

A drop in flow rate is usually associated with loss into the hole wall.
The magnitude of the drop in velocity is a direct measure of the loss into the hole wall.
The agreement between the black monotonic fit and the yellow smoothed flow/velocity curve of the first graph is an indication of the data reliability.
The transmissivity curve of the second graph is calculated from the monotonic flow rate curve.

Monotonic curve (black over yellow) is corrected for the transient

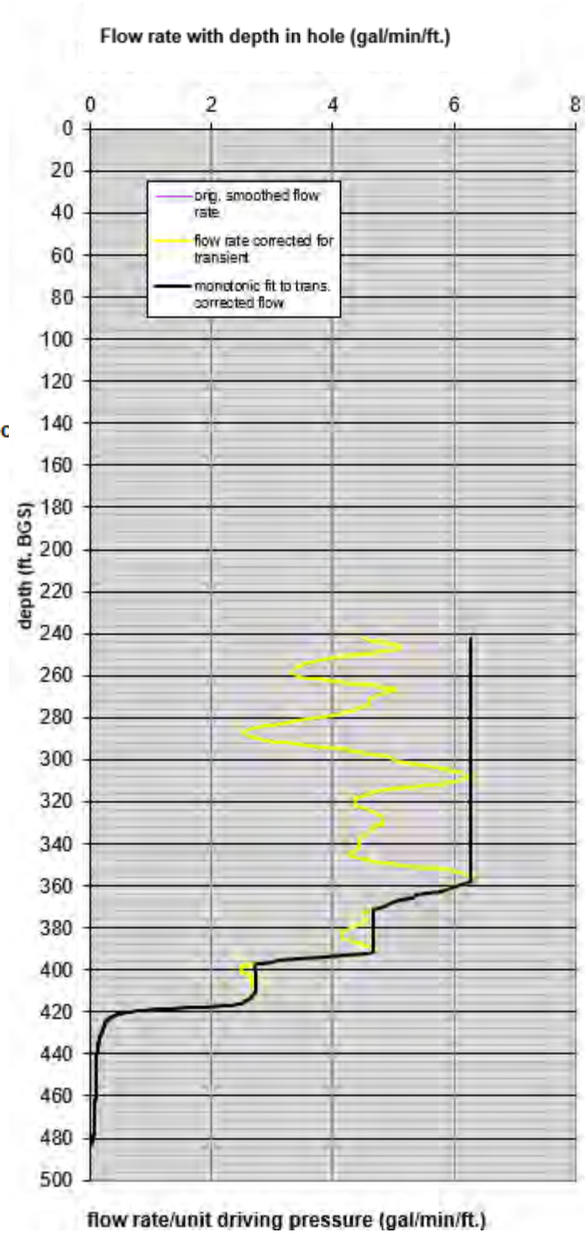

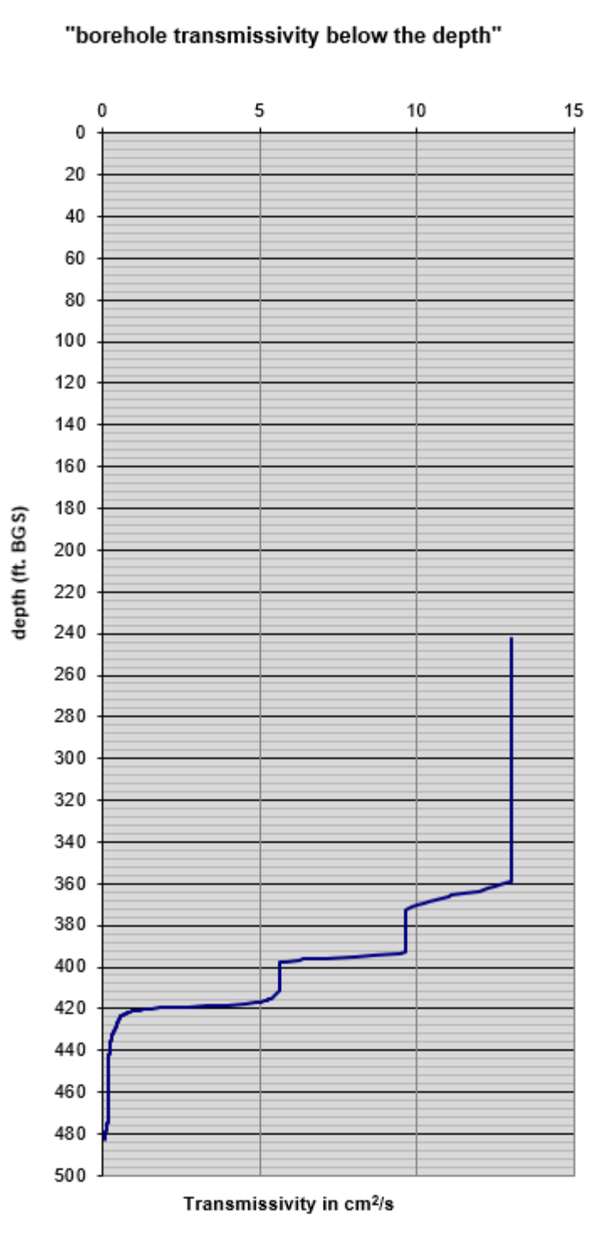

Results of FLUTe profiling for hole

no. SAG-2 for ***HDR, Grants, NM***

Water Table depth	131	ft BGS
Hole depth	376.25	ft BGS
liner length	500	ft BGS
casing depth	161	ft BGS
hole diameter	5	inches
liner diameter	5.6	inches
date of measurement	1/12/2021	

The profile was measured to a depth of 374.106 ft

The flow rate per unit driving pressure was 0.502606 **gal/min/ft**

The transmissivity for the remainder of the hole is: 1.0407572 cm sq./sec

The average conductivity for the remaining 2.14363 ft of the hole is 1.59E-02 cm/sec

Total borehole transmissivity is 16.8662 cm2/s

Comments:

Extremely fast flowing hole 120-60 gal/min.
Water table at the bottom of the borehole same at the beginning as when sealed to 377 ft. Suggesting head at and below 377 ft is dominant in the borehole with associated very high transmissivity
Highest head in the formation is at 98ft bgs as determined from changing of the water level in the liner until stable.
The lowest head in the formation may be lower, but of low transmissivity.
Reverse head profile yet to be reduced but dominated by head of 131 ft bgs.

Contact for questions about data or reduction
carl Keller
Phone: 505-455-1300

Note: the flow rate curve is the liner velocity multiplied by the borehole cross section

A drop in flow rate is usually associated with loss into the hole wall.
The magnitude of the drop in velocity is a direct measure of the loss into the hole wall.
The agreement between the black monotonic fit and the yellow smoothed flow/velocity curve of the first graph is an indication of the data reliability.
The transmissivity curve of the second graph is calculated from the monotonic flow rate curve.

Monotonic curve (black over yellow) is corrected for the transient

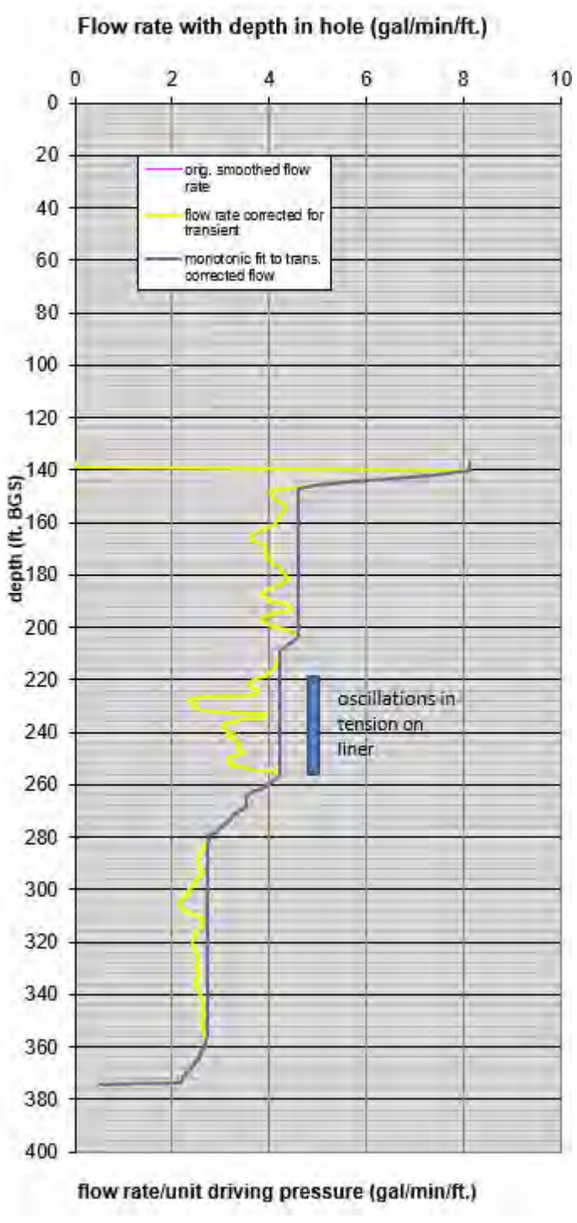

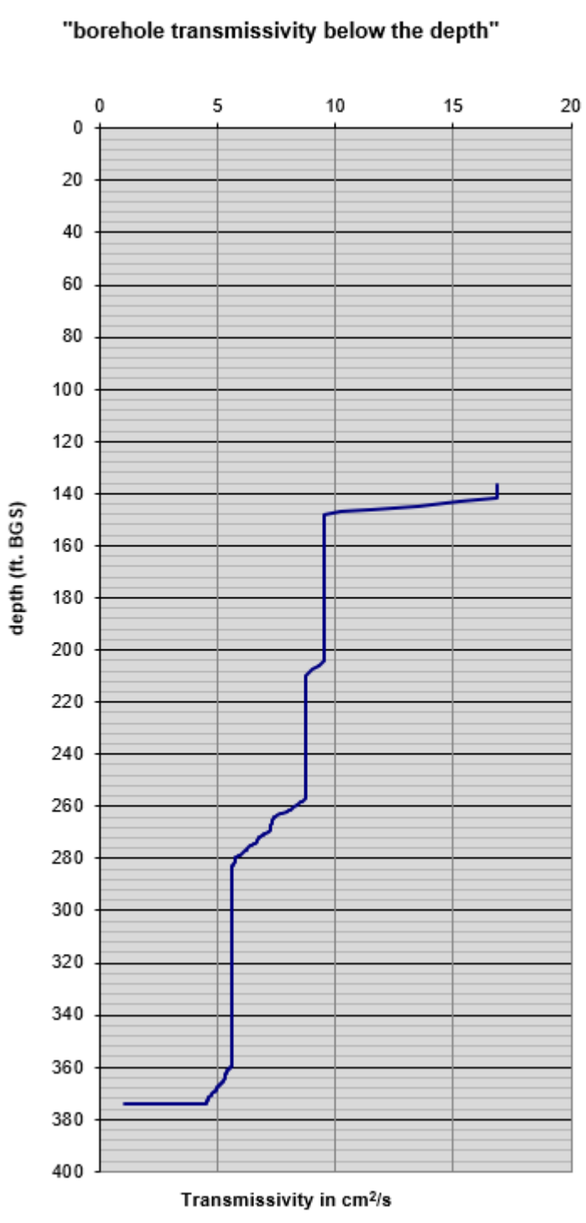

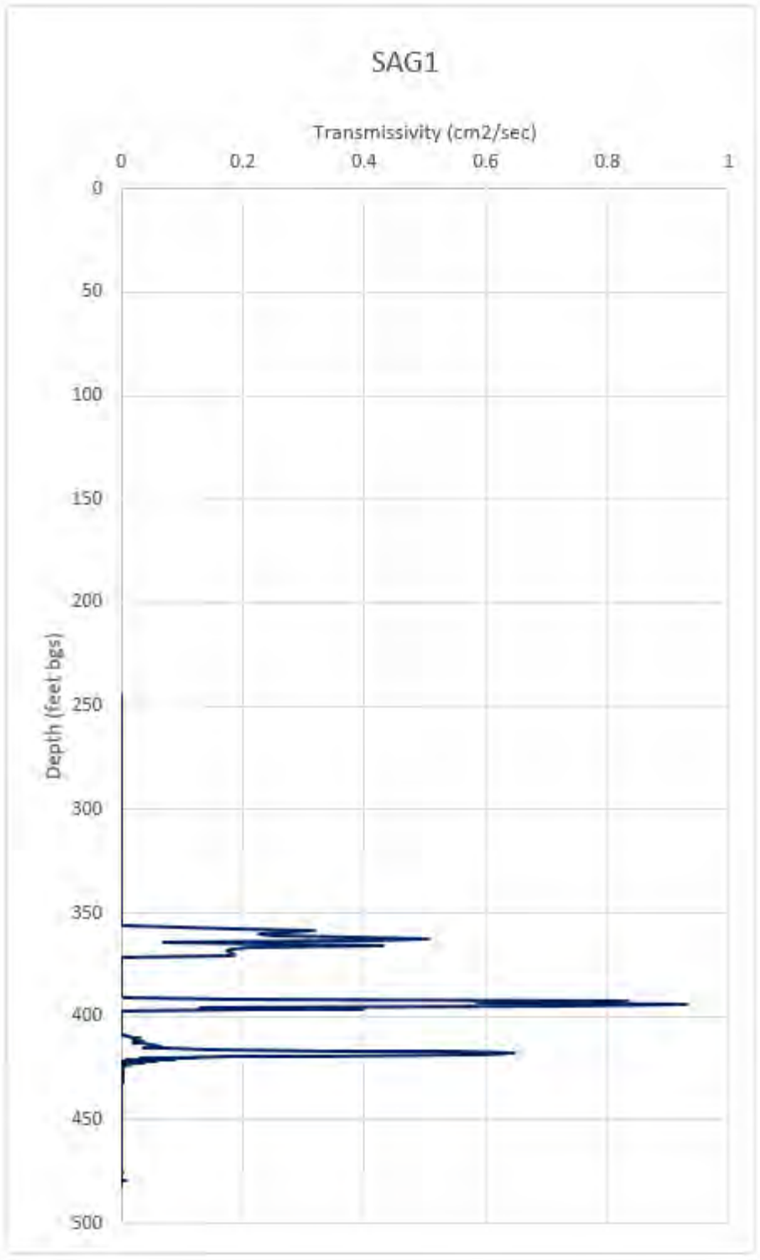

Constants			
Fluid Density	ρ	1000	kg/m3
Gravity	g	9.81	m/s2
Viscosity	μ	1.124E-03	kg/m s

Apature Frequency			
Range	Range	(number)	percent
1	100	418	87%
100	200	26	92%
200	300	19	96%
301	400	11	98%
401	500	8	100%
501	600	1	100%
	total	483	

Aperture Staistics		
max	504.1	microns
min	19.0	microns
geomean	58.5	microns
geomean	1.92E-04	feet
stdev	81.4	
Aperature (total)	36698	microns
Aperature (total)	0.1204	feet
Transmissivity (sum)	12.93	cm2/sec
Transmissivity (sum)	0.00129	m2/sec
Rock Thickness	240	feet
Rock Thickness	73.2	meters
Bulk K	1.77E-05	m/sec
Bulk K	5.01E+00	ft/day
#/fractures in borehole	483	
#/fractures/ft of borehole	2.0	
Fracture Porosity	0.00050	
Fracture Porosity	0.05%	

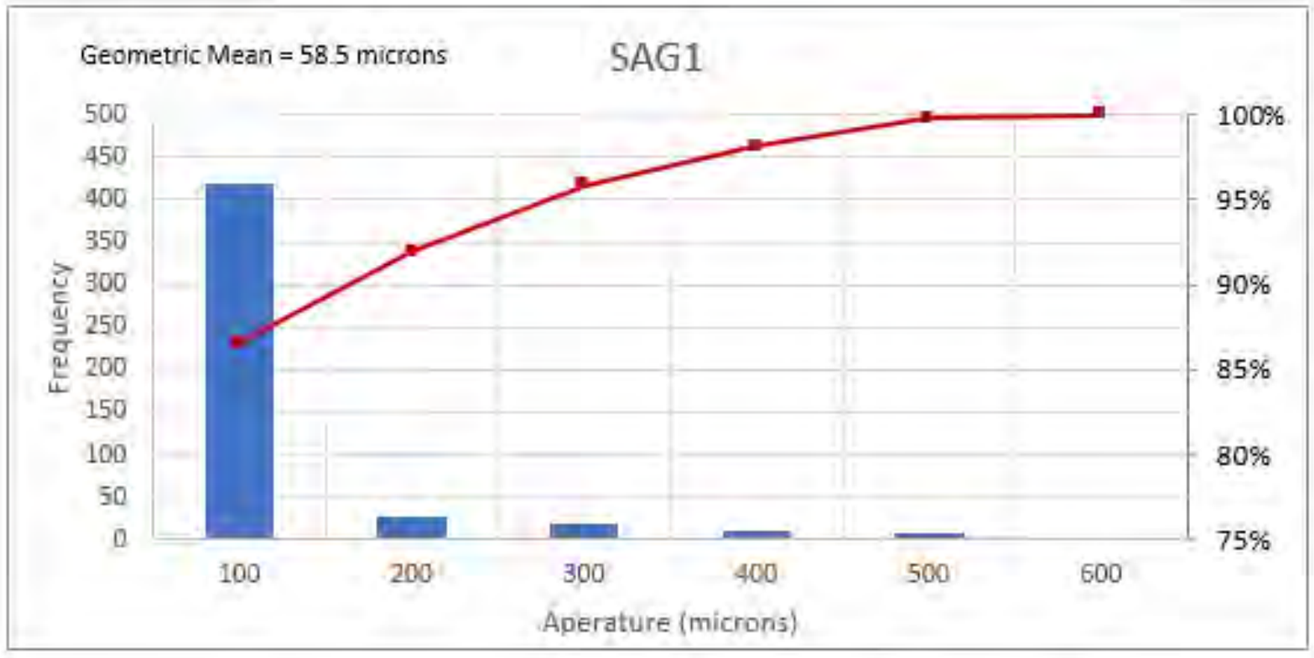

HOMESTAKE

SAG1 FLUTe™ APERTURE AND TRANSMISSIVITY STATISTICS

FIGURE 3-5

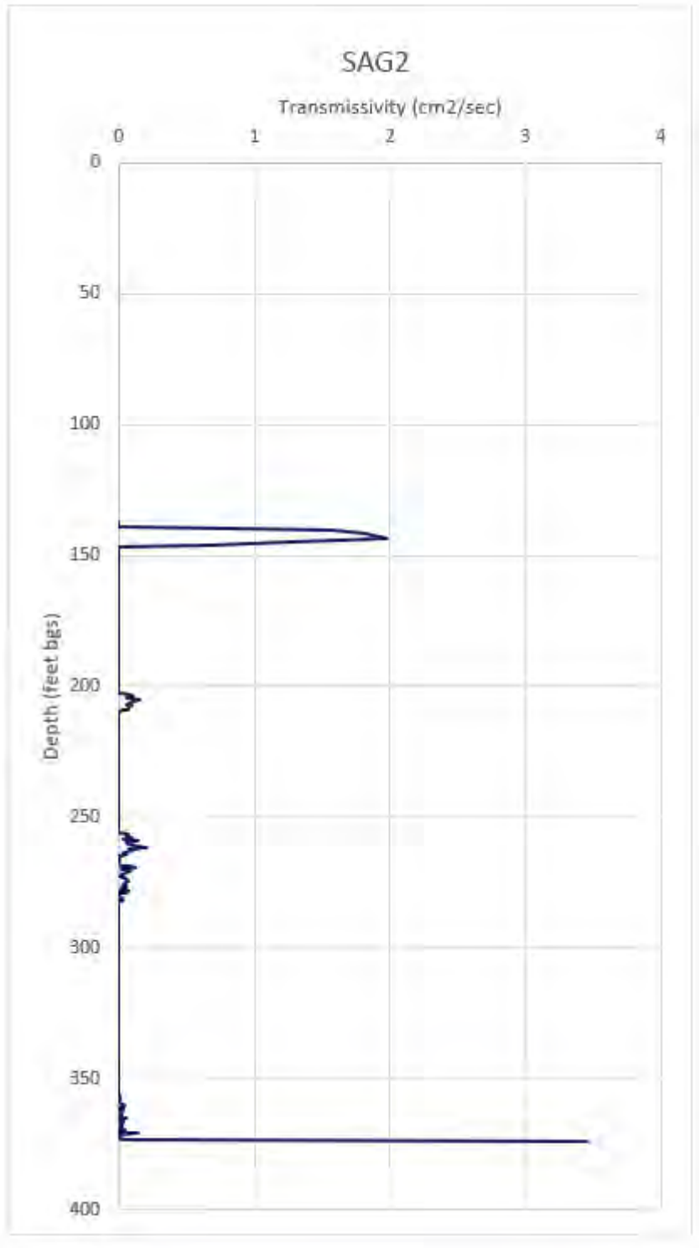

Constants			
Fluid Density	ρ	1000	kg/m3
Gravity	g	9.81	m/s2
Viscosity	μ	1.124E-03	kg/m s

Apature Frequency			
Range	Range	(number)	percent
1	100	15	12%
100	200	74	72%
200	300	33	98%
301	400	1	99%
401	500	0	99%
501	600	0	99%
601	700	0	99%
701	800	1	100%
801	900	0	100%
	total	124	

Aperture Staistics		
max	779.7	microns
min	12.7	microns
geomean	152.0	microns
geomean	4.99E-04	feet
stdev	77.4	
Aperature (total)	20695	microns
Aperature (total)	0.0679	feet
Transmissivity (sum)	8.50	cm2/sec
Transmissivity (sum)	0.00085	m2/sec
Rock Thickness	214	feet
Rock Thickness	65.1	meters
Bulk K	1.31E-05	m/sec
Bulk K	3.70E+00	ft/day
#/fractures in borehole	124	
#/fractures/ft of borehole	0.58	
Fracture Porosity	0.00032	
Fracture Porosity	0.03%	

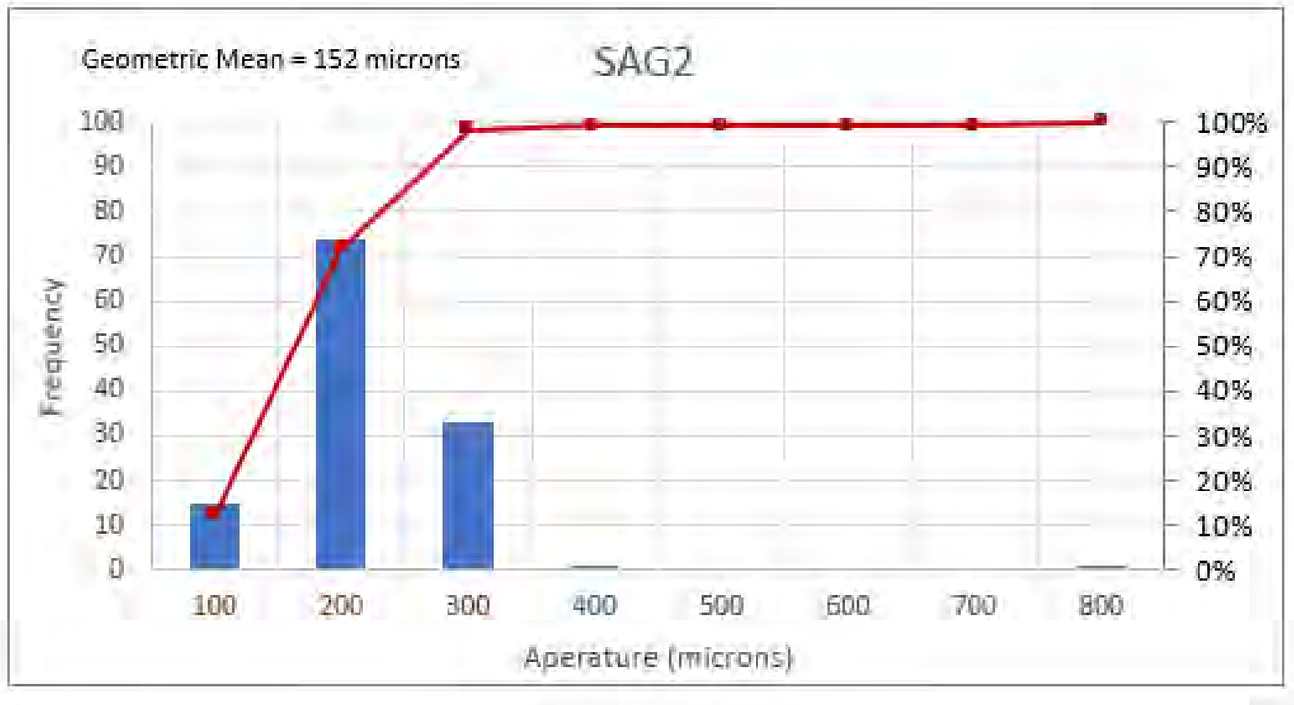

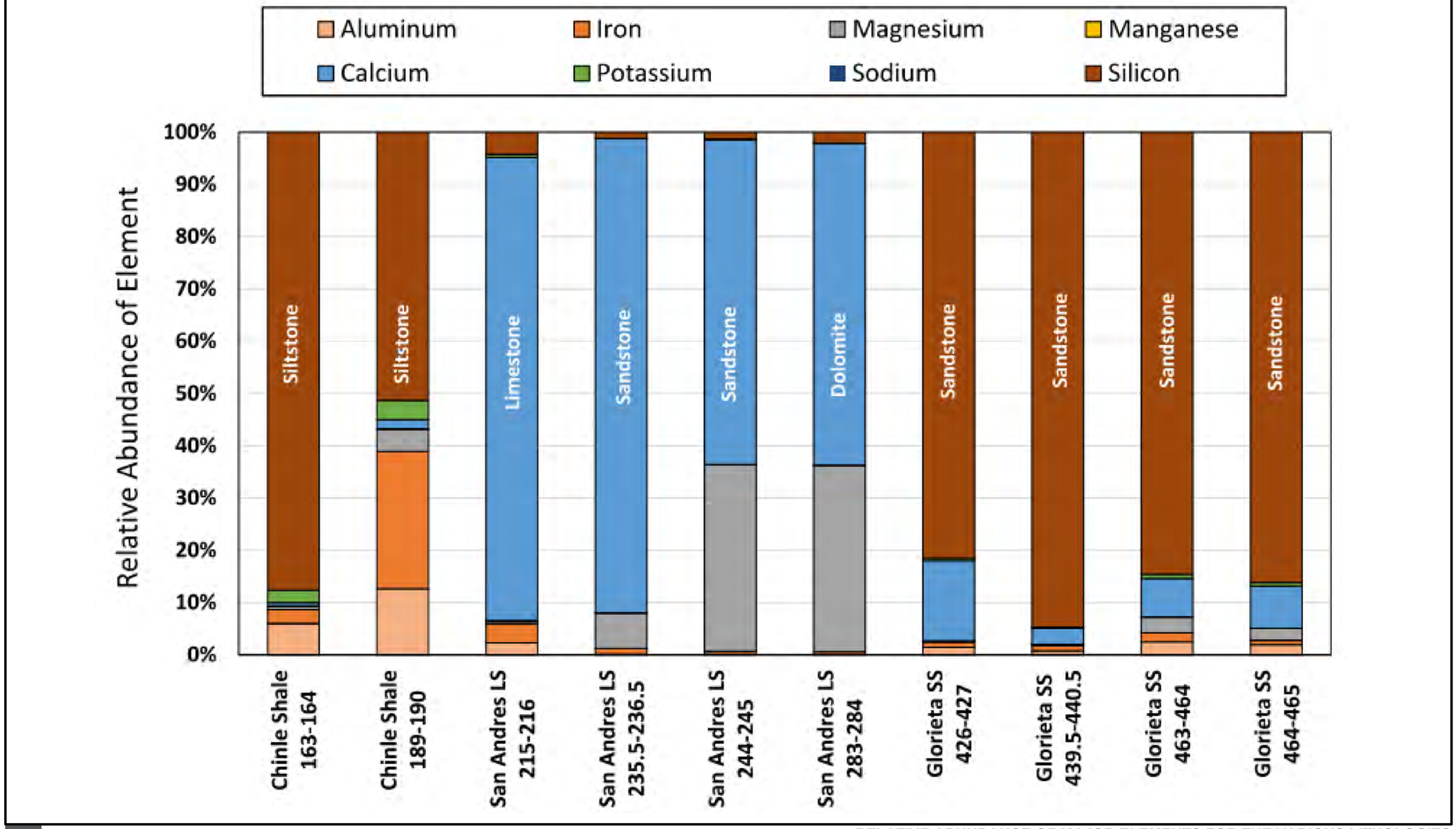

RELATIVE ABUNDANCE OF MAJOR ELEMENTS FOR THE VARIOUS LITHOLOGIES

FIGURE 3-7

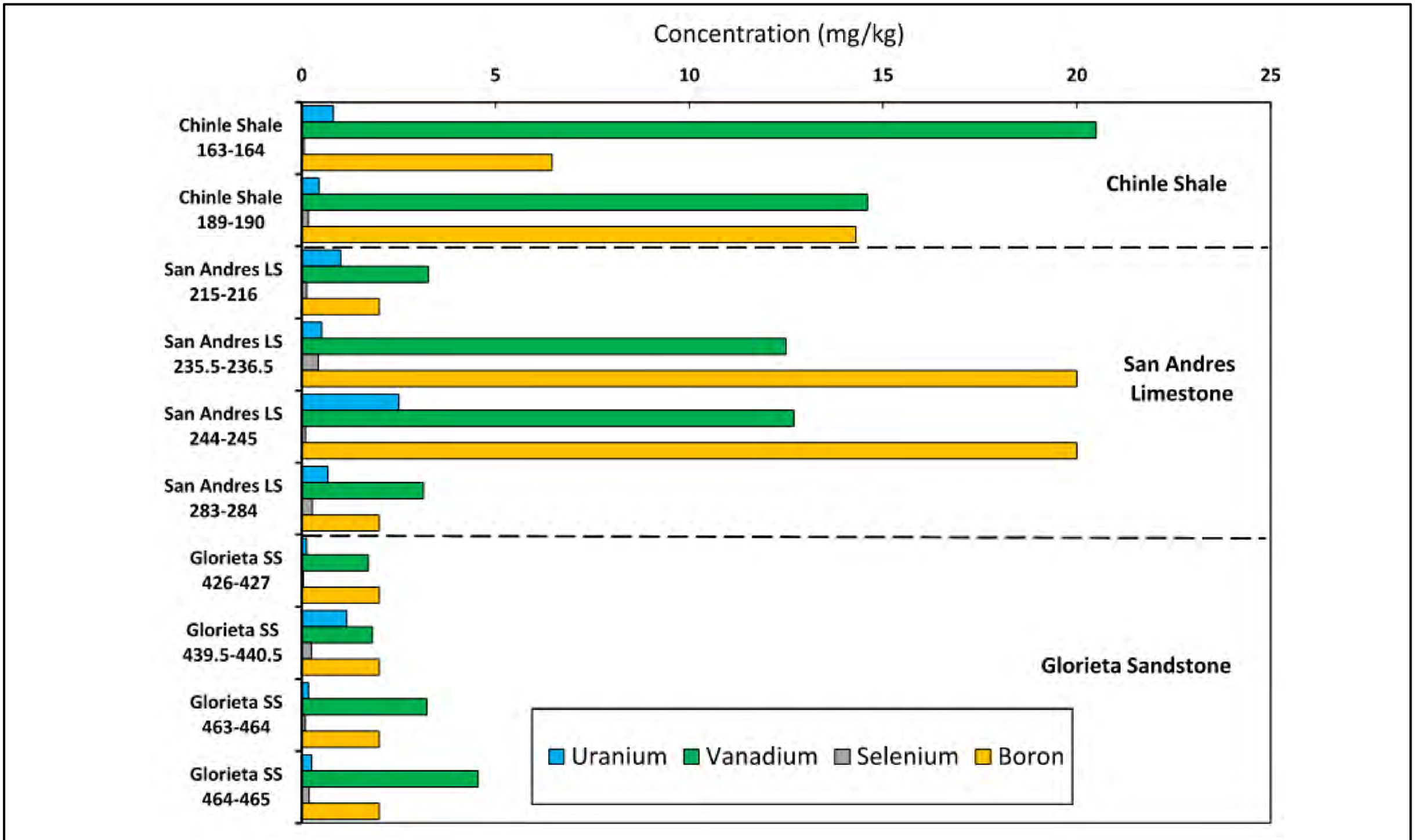

SELECTED TRACE ELEMENT CONCENTRATIONS FOR THE VARIOUS LITHOLOGIES

FIGURE 3-8

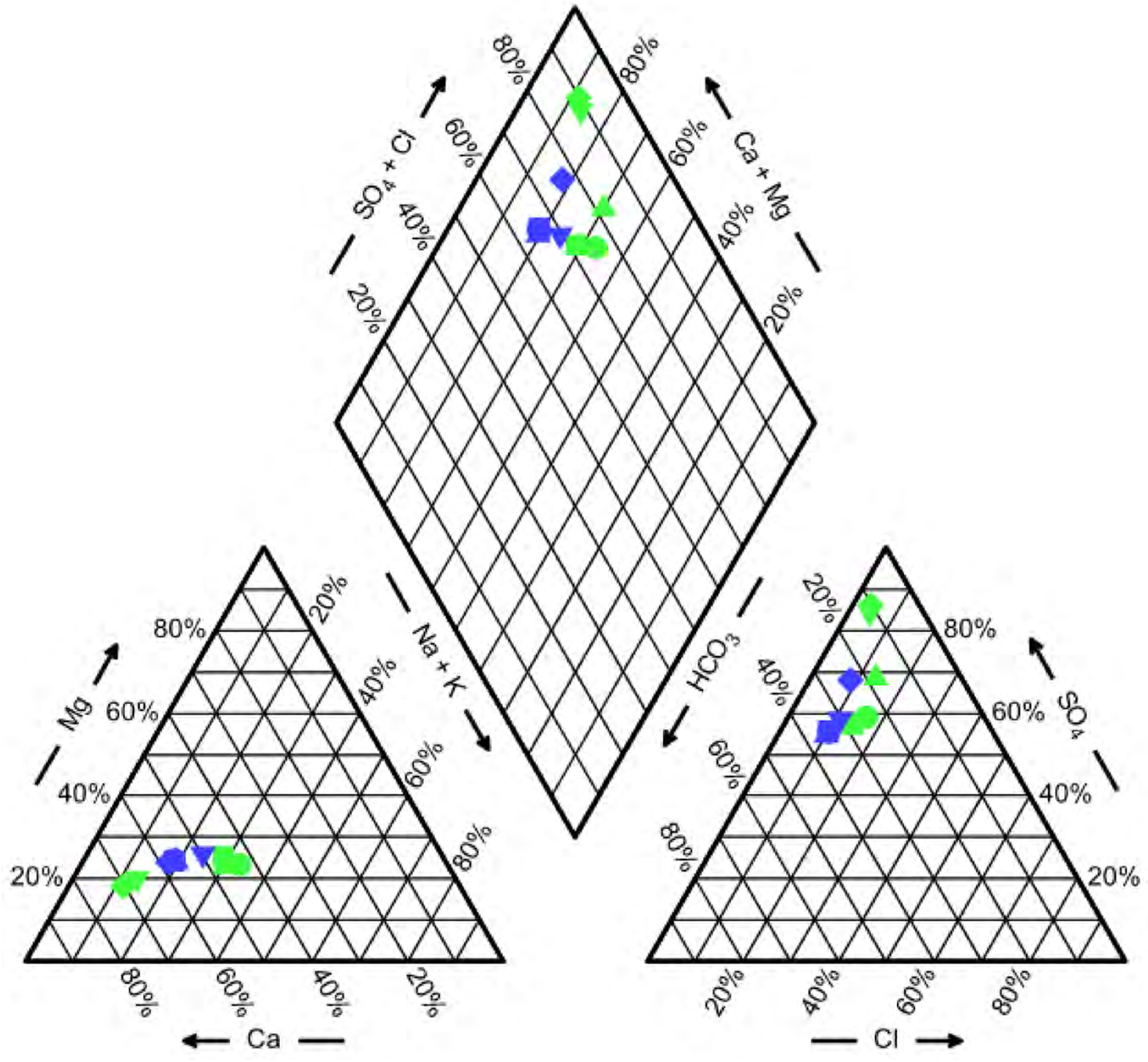

TRILINEAR DIAGRAM FOR THE SAG-1 AND SAG-2 GROUNDWATER SAMPLES

FIGURE 3-9

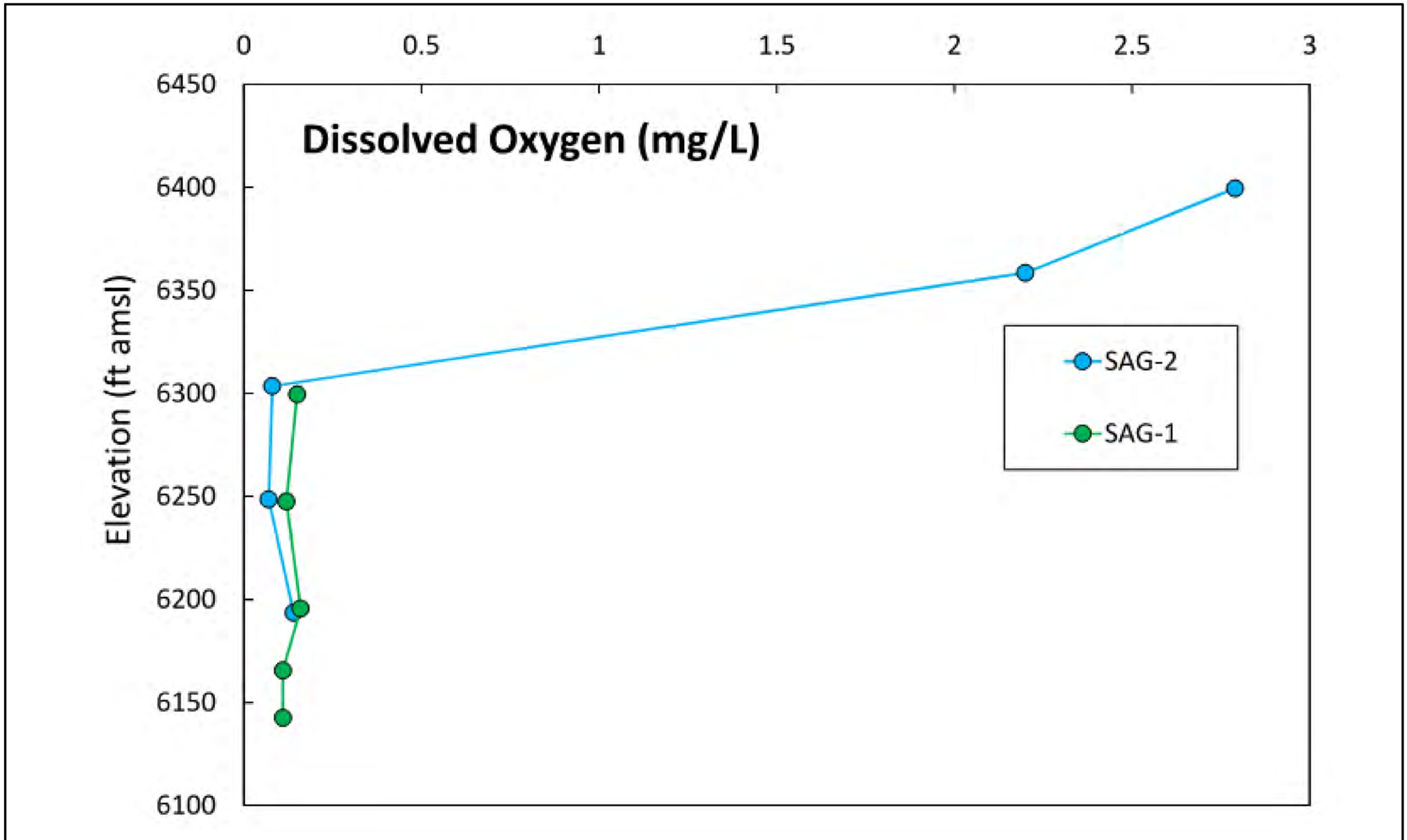

DISSOLVED OXYGEN PROFILE FOR SAG-1 AND SAG-2 GROUNDWATER

FIGURE 3-10

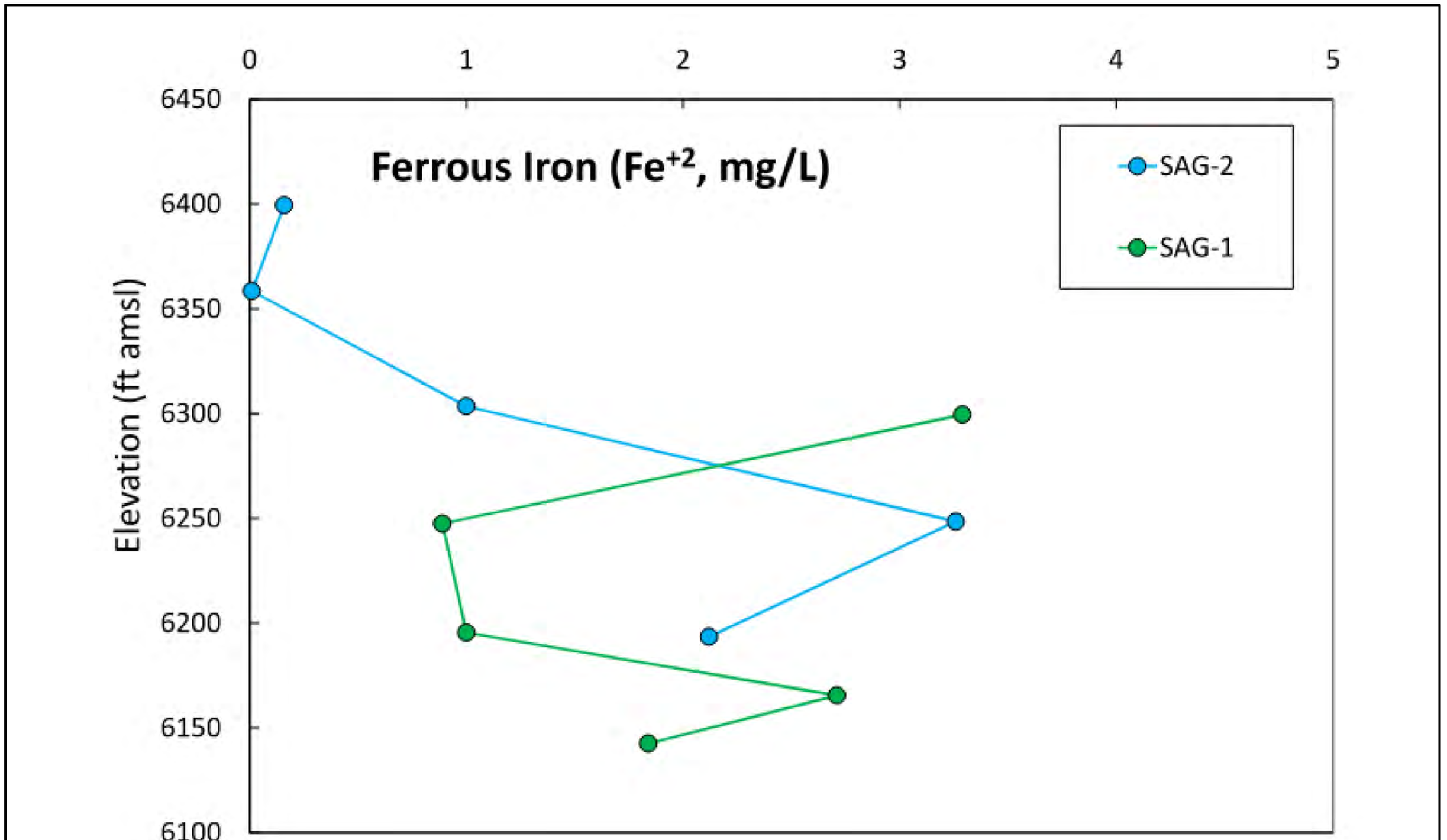

FERROUS FE PROFILE FOR SAG-1 AND SAG-2 GROUNDWATER

FIGURE 3-11

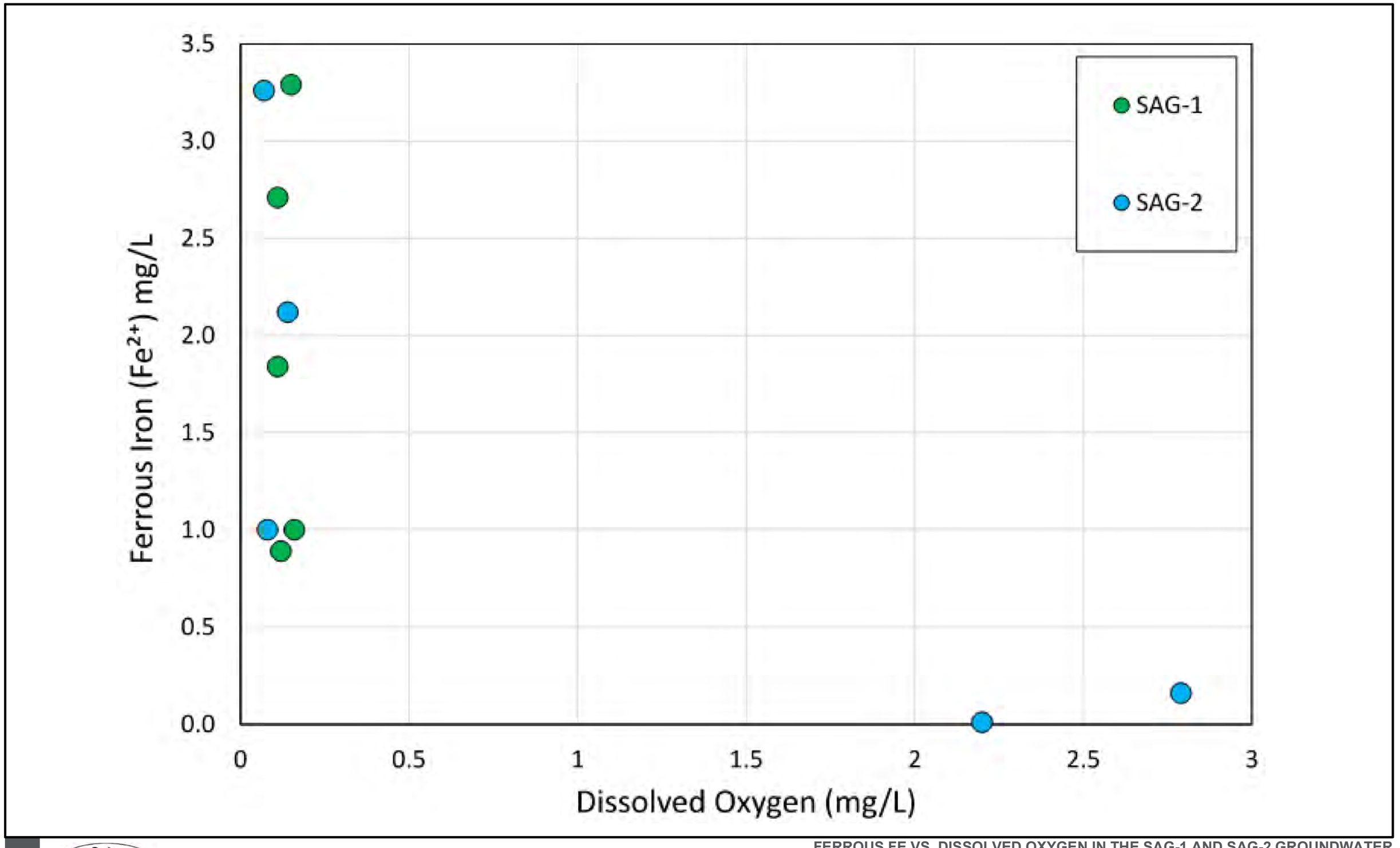

FERROUS FE VS. DISSOLVED OXYGEN IN THE SAG-1 AND SAG-2 GROUNDWATER

FIGURE 3-12

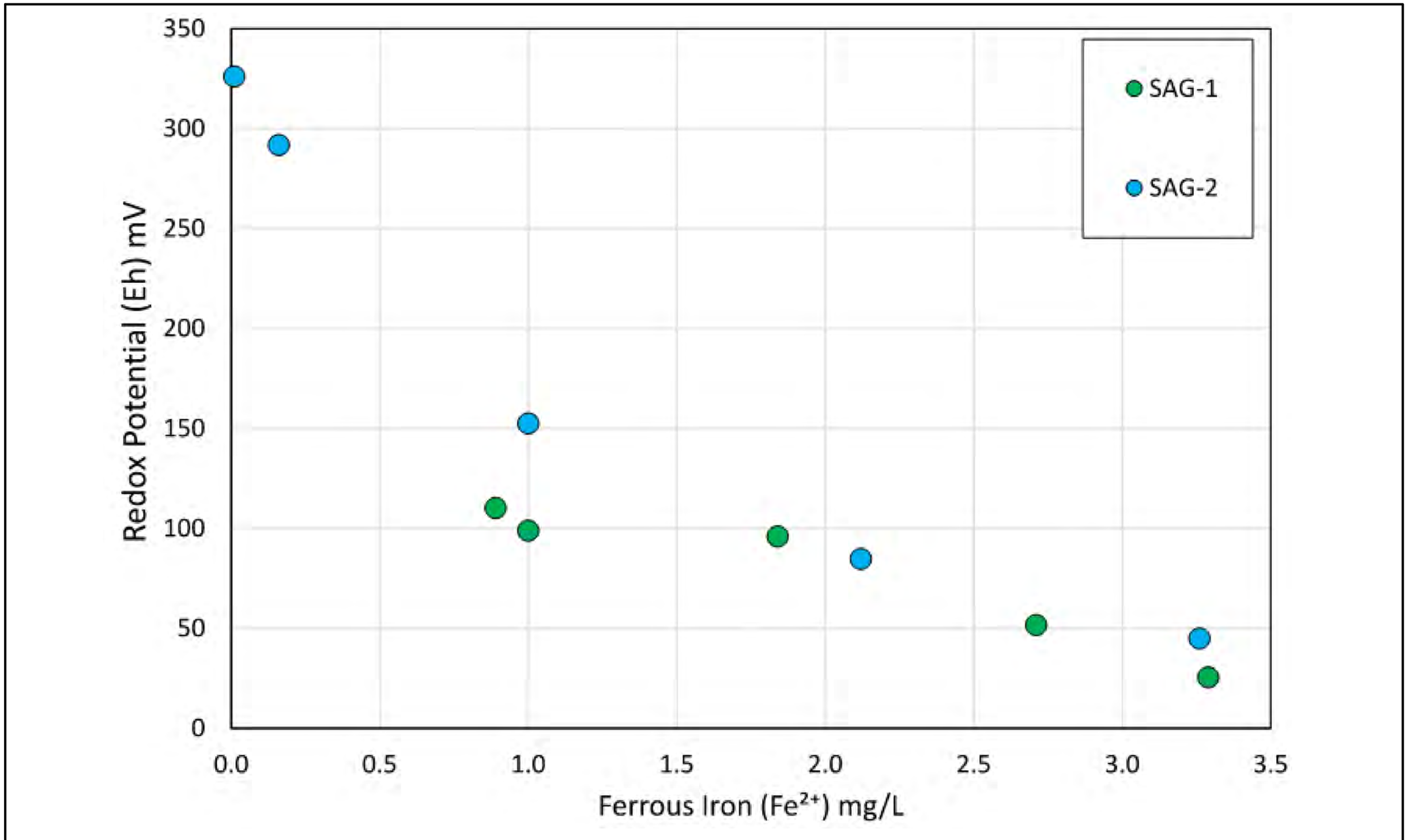

REDOX POTENTIAL (EH) VS. FERROUS FE IN THE SAG-1 AND SAG-2 GROUNDWATER

FIGURE 3-13

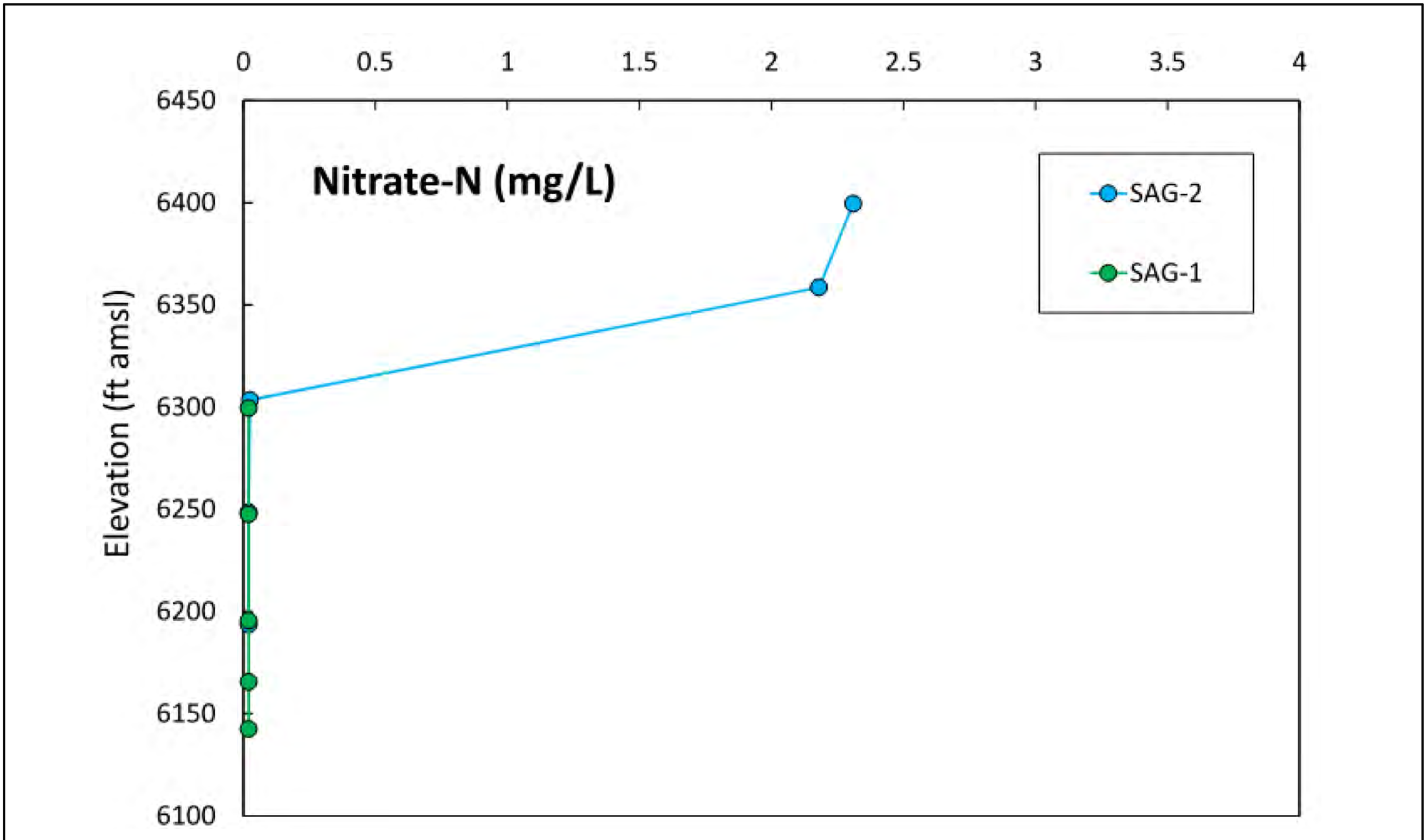

NITRATE-N PROFILES IN THE SAG-1 AND SAG-2 GROUNDWATER

FIGURE 3-14

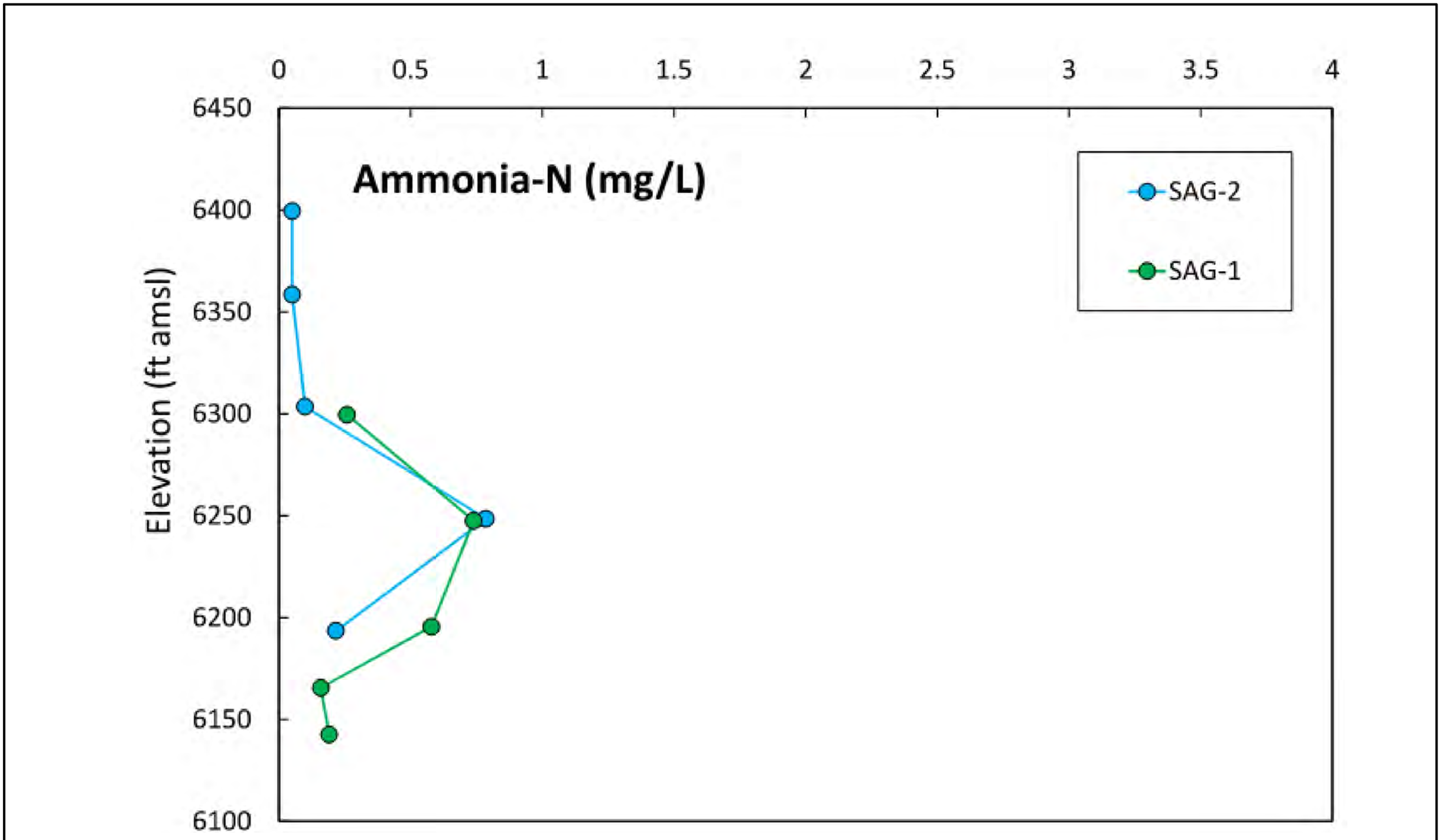

AMMONIA-N PROFILES IN THE SAG-1 AND SAG-2 GROUNDWATER

FIGURE 3-15

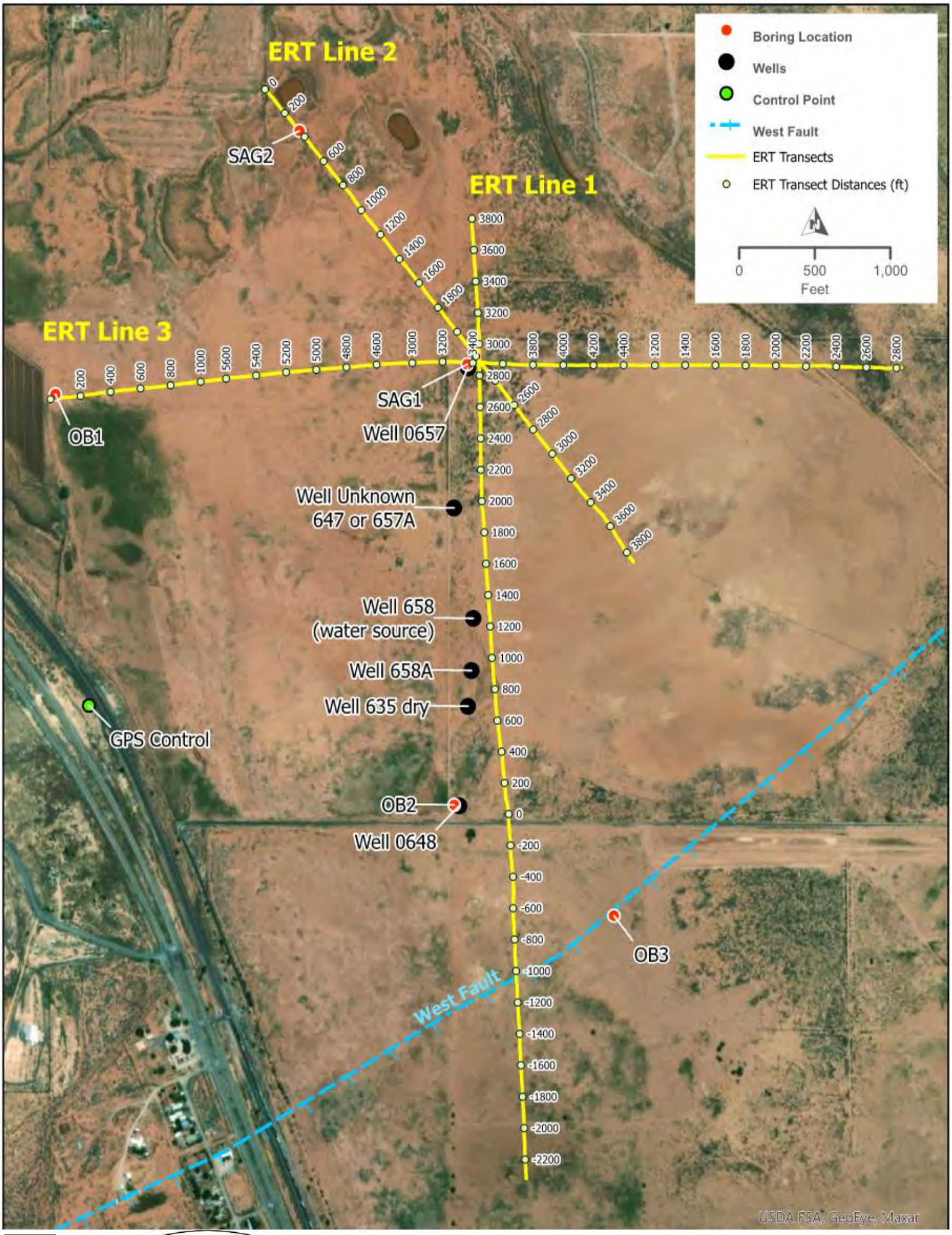

HOMESTAKE

ERT TRANSECT LOCATION MAP

FIGURE 3-16

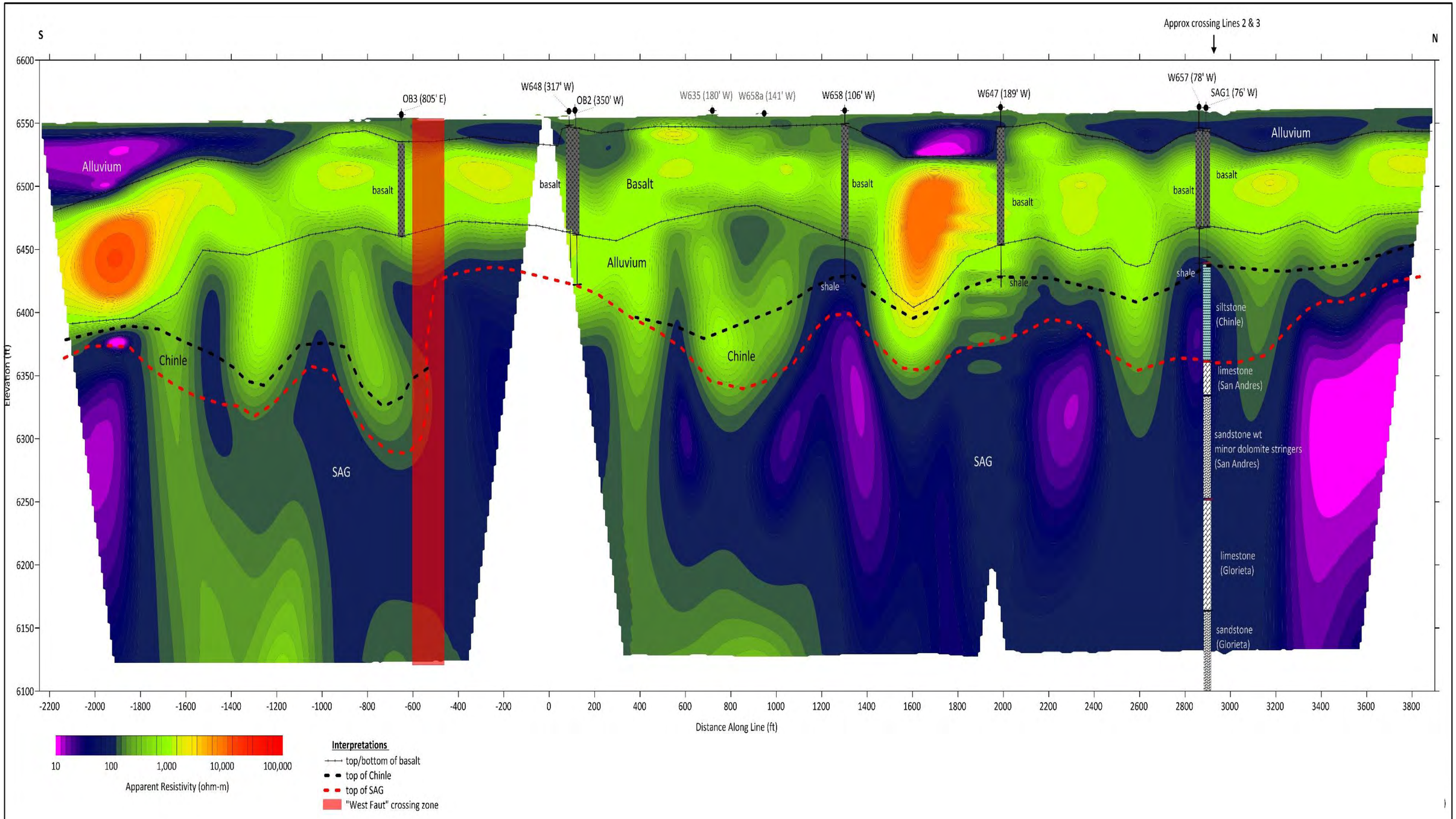

HOMESTAKE

ERT LINE 1 2D INVERSION MODEL

FIGURE 3-17

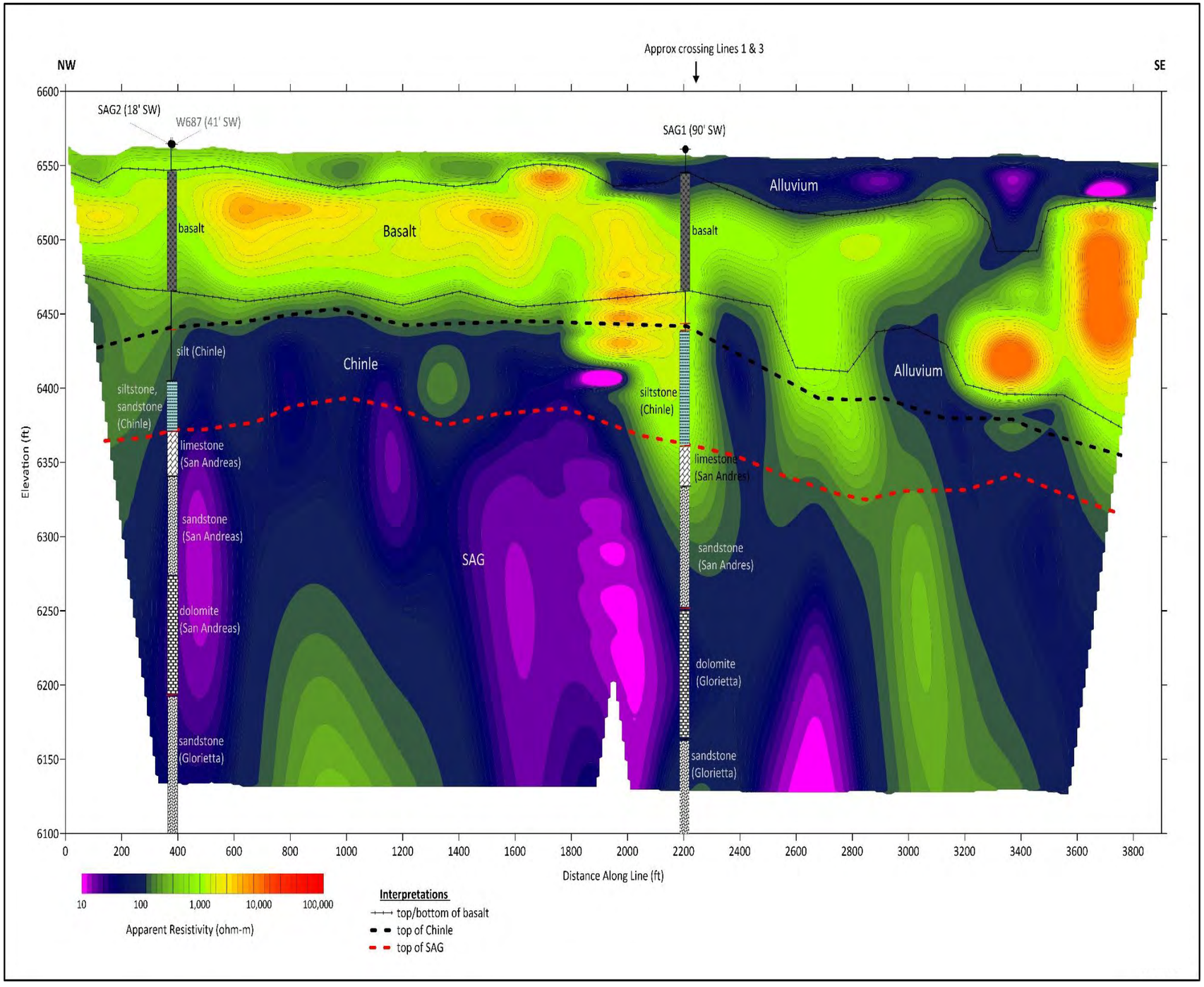

ERT LINE 2 2D INVERSION MODEL

FIGURE 3-18

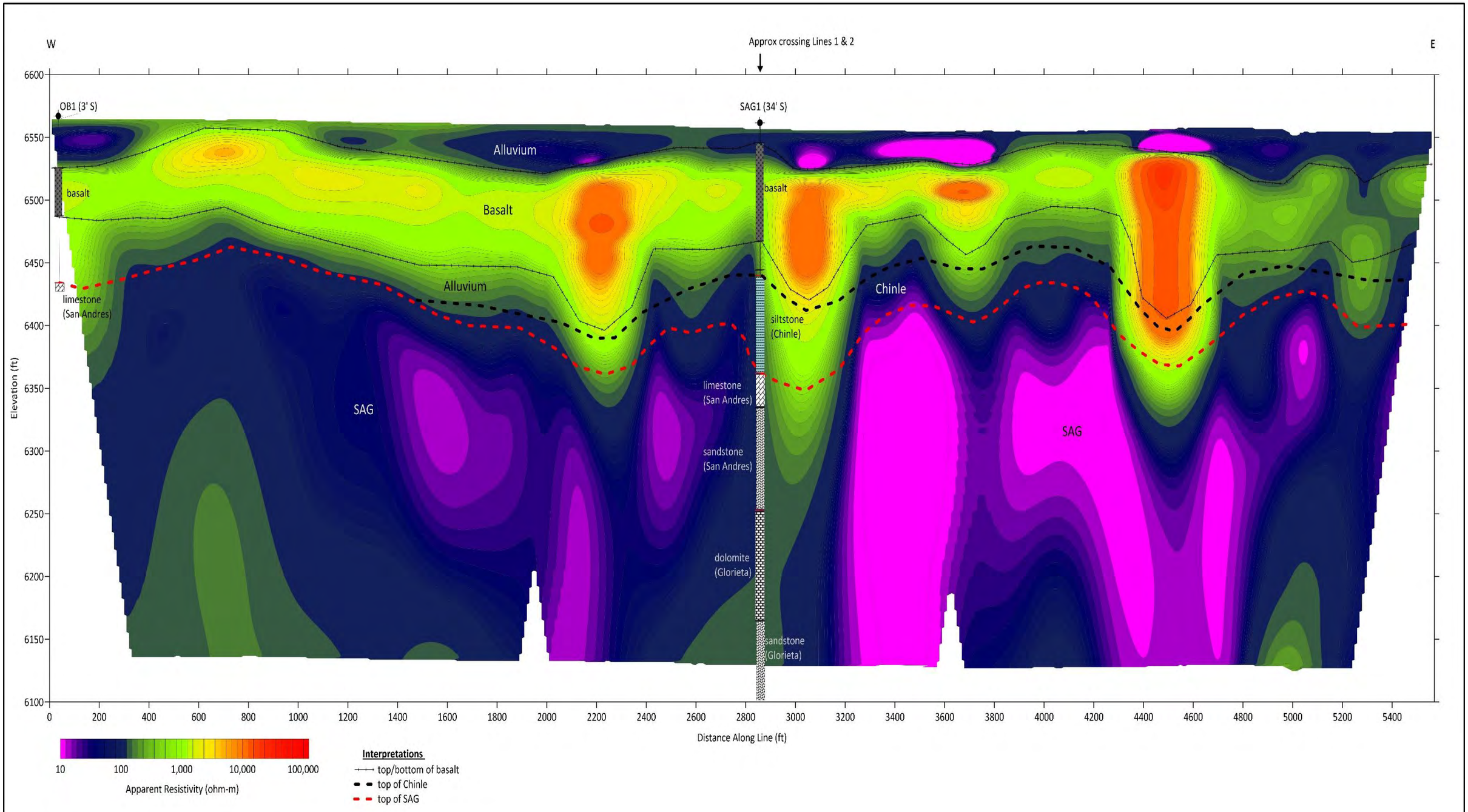

HOMESTAKE

ERT LINE 3 2D INVERSION MODEL

FIGURE 3-19

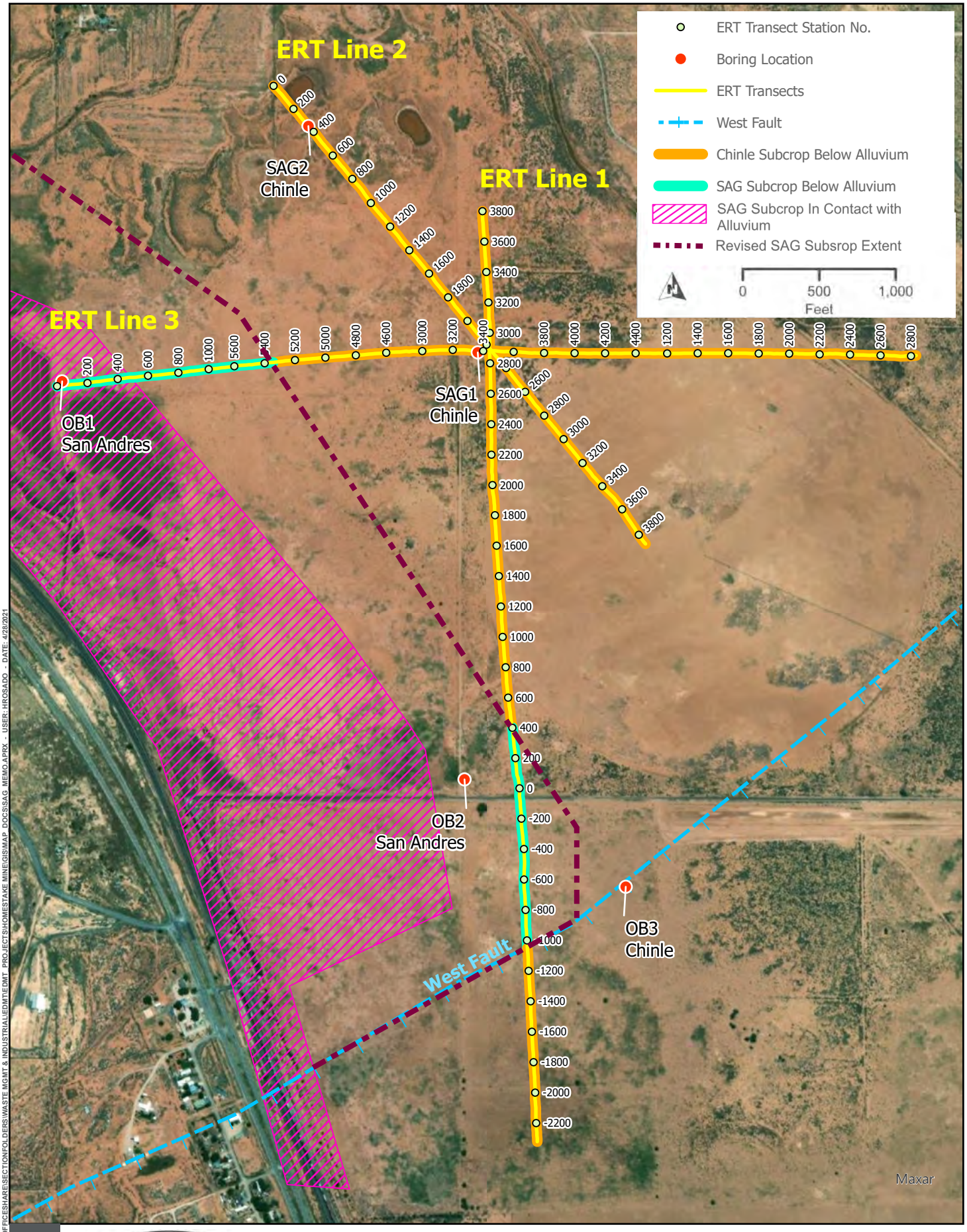

PATH: \\MAHPI-FILE01\OFFICESHARE\SECTIONFOLDERS\WASTE MGMT & INDUSTRIAL\EDMTE\DMT_PROJECTS\HOMESTAKE MINE\GIS\MAP_DOCS\SAG_MEMO.APRX - USER: HROSADO - DATE: 4/28/2021

HOMESTAKE

REVISED SAG SUBCROP

FIGURE 4-1